PLASMA BIOMARKERS IN MULTIPLE SCLEROSIS: A TREATMENT COMPARISON ANALYSIS OF HIGHLY EFFICACIOUS VERSUS MODERATELY EFFICACIOUS DISEASE MODIFYING THERAPIES

by © Shane Arsenault

A Thesis submitted to the School of Graduate Studies in partial fulfillment of the requirements for the degree of

Master of Science in Medicine, Department of Community Health and Humanities, Faculty of Medicine

Memorial University of Newfoundland

May 2024

St. John's Newfoundland and Labrador

Abstract

Multiple sclerosis (MS) is an immune-mediated demyelinating disease of the central nervous system. Clinicians may employ a “treat-to-target” (escalating disease modifying therapy (DMT) as needed) approach, or an “early intensive” (upfront treatment with highly efficacious medications at diagnosis) approach. Current evidence suggests that early aggressive control of relapsing activity results in less Central Nervous System (CNS) injury and a better long-term prognosis. Several biomarkers are used clinically to aid in the diagnosis of MS, and newly validated biomarkers such as cerebrospinal fluid (CSF) and serum neurofilament light chain (NfL) and glial fibrillary acidic protein (GFAP) are emerging as important diagnostic, prognostic, and therapeutic response biomarkers, especially in relapsing-remitting MS (RRMS). This study utilized a combined retrospective and prospective longitudinal active-comparator cohort study design to determine whether utilization of an “early-intensive” therapeutic approach resulted in significant differences in plasma NfL and GFAP concentrations. A total of 12 patients on high-efficacy DMT and 9 patients on moderately efficacious DMT were recruited for this analysis. Secondary outcomes included plasma C-X-C Motif Chemokine Ligand 13 (CXCL13), as well as relevant T and B immune cell subsets, including CD4+, CD8+, CD19+ immune cells, among others.

Keywords: Multiple Sclerosis, Neurofilament Light Chain, Glial Fibrillary Acidic Protein, Expanded Disability Status Scale, Annualized Relapse Rate, Disease Modifying Therapy, Magnetic Resonance Imaging, Gadolinium Enhancing Lesion

General Summary

Multiple sclerosis (MS) can cause serious problems and early death and affects nerves which run from our brain and spinal cord. Nerves are like electrical wires: they conduct impulses which allow our bodies to work and like electrical wires they are 'insulated'. This insulation (the myelin sheath) deteriorates in MS, causing the varied disease symptoms. Doctors can treat MS by using two main approaches. (1) They use medications that may be less effective but deemed to be safer (based on potential side effects) and escalate to more effective medications (with potentially more side effects) if the disease worsens. (2) Doctors may use the more effective medications first. Current large studies suggest that the second approach may result in better long-term outcomes.

It is thus important for doctors to be able to diagnose MS early and be able to decide which treatment regime would be best for each patient. Novel ways to do this involve the use of emerging biomarkers (biological substances which we can detect in bodily fluids). These include the neurofilament light chain (NfL), glial fibrillary acidic protein (GFAP) and CXCL13. Detecting these in high quantity in samples of spinal fluid and or blood reflect nerve breakdown.

This study aimed to determine whether moderate efficacy medications (approach 1) vs. higher efficacy medications (approach 2) resulted in significant differences in blood NfL, GFAP and CXCL13 concentrations.

Co-Authorship Statement

The author would like to acknowledge that Neva Fudge (Research Assistant in Dr. Craig Moore Neuroscience Laboratory) made major contributions to the methods section of this paper for sections 2.5 Peripheral PBMC Immune Phenotyping using Flow Cytometry, 2.6 Quantification of pro-inflammatory cytokines using Simoa® technology, and 2.7 Quantification of CXCL13 using ELISA. Aside from these contributions in the methods section, all written material is by Shane Arsenault.

Acknowledgements

I would first like to acknowledge Dr. Craig Moore (Canada Research Chair in Neuroscience and Brain Repair) in his role as my primary supervisor. Dr. Moore sparked my passion for multiple sclerosis research in my first year of neurology residency. It was through his guidance that I decided to undertake this master's and subsequent research, and it was his mentorship that allowed me to excel throughout my program. Moreover, Dr. Moore has been instrumental in advancing my knowledge and practical skill set within the field of neuroscience, including how to write successful grant proposals and appropriately review research articles, undoubtedly allowing me to further my career aspirations as a clinician-scientist. I would like to thank Neva Fudge, research assistant in the Moore laboratory, for completing all the peripheral blood mononuclear cell immune cell phenotyping and quantification of CXCL13 using enzyme linked immunosorbent assay (ELISA) on identified patient plasma samples. Without her collaboration this research would not have been possible. Additionally, Neva was a constant source of tutorship on practical neuroimmunology and provided invaluable advice regarding the statistical analysis of the data. I would also like to thank all other Moore laboratory personnel and fellow students, as without their work, many of the idea's sparked throughout this research project would not have occurred.

At the time that this research was completed, serum and plasma neurofilament light chain (NfL) could not be accurately quantified using ELISA, requiring the use of a Simoa® platform, unavailable in Newfoundland and Labrador. As such all patient plasma samples were shipped on dry ice for Simoa® platform analysis of NfL, in the laboratory of Dr. Raphael Schneider. As such, I would like to thank Dr. Schneider and his staff for the timely analysis of our samples.

Completing this master's thesis in conjunction with a neurology residency required the assistance of my neurology program director Dr. Fraser Clift. I would like to thank him for his endless mentorship and guidance on all clinical aspects of multiple sclerosis, and for his role in patent recruitment. Dr. Mark Stefanelli, who has been central to clinical MS research in Newfoundland and Labrador for many years, provided guidance and support throughout my master's, and was involved in patient recruitment for this study. Furthermore, I would like to thank the remaining members of my master's supervisory committee including Dr. Kathy Hodgkinson and Dr. Michelle Ploughman. Finally, I wish to thank all those patients living with MS in Newfoundland and Labrador who agreed to participate in this research.

This research was supported by grants from the Memorial University of Newfoundland Faculty of Medicine Dean of Medicine Collaborative Clinical and non-Clinical Research Grant ($30,000.00) and the Memorial University of Newfoundland Faculty of Medicine Medical Research Foundation Research Development Grant ($20,000.00). Dr. Craig Moore provided supplemental funding for this research through his grants with the Canadian Institute of Health Research (C.S.M: PJT155933), and the Multiple Sclerosis Society of Canada (C.S.M: EGID#3499).

Table of Contents

List of Tables

List of Figures

List of Appendices

CHAPTER 1

1. Introduction

1.1 Multiple Sclerosis Epidemiology

Multiple sclerosis (MS) is an immune-mediated demyelinating disease of the central nervous system (CNS) accompanied by chronic inflammation, neurodegeneration, and axonal loss. Currently, the exact etiology of MS is not fully elucidated, but it is most likely the result of complex interactions between environmental factors and genetic susceptibility, leading to an aberrant immune response and subsequent damage to the myelin sheath, oligodendrocytes, axons, and neurons (Compston 2008). MS is the most common cause of non-traumatic neurological disease in young adults, and Canada has one of the highest rates worldwide (Compston 2008). Approximately 85% of MS patients present initially with a clinically isolated syndrome (CIS), an event of focal neurological dysfunction such as optic neuritis or transverse myelitis. A majority of these patients would declare themselves as having clinically definite MS, and the majority convert to relapsing-remitting MS (RRMS), defined as periods of active disease followed by clinical remission (Compston 2008). Within 15-20 years most RRMS patients develop secondary progressive MS (SPMS), characterized by a continuous worsening with or without clinical relapses, while the other 10-15% of MS patients initially present with primary progressive MS (PPMS), characterized by gradual worsening of symptoms from disease onset without relapses (Compston 2008). Despite the differences in clinical presentation, basic science research is suggesting all MS disease subtypes are in fact on a spectrum of the same pathological process (Klineova 2018).

With approximately 90,000 individuals affected, the prevalence of MS in Canada is among the highest in the world, and the number is projected to reach 133,635 by 2031 (Amankwah 2017). MS preferentially affects females (3:1 ratio), with the majority (60%) of

adults diagnosed between the ages of 20 and 49 years old (Multiple Sclerosis International Federation, 2020). While less prevalent in males, several studies have suggested that male sex is associated with a poorer clinical outcome in relapsing MS, that male sex is associated with a faster time to progressive MS, and that male sex is associated with more rapid disability accumulation in those with PPMS (Ribbons 2015). Although much rarer, MS does occur in children, with a current pediatric prevalence in Canada of 5.4 cases per 100,000 population (Multiple Sclerosis International Federation, 2020).

In both relapsing and progressive forms of MS, axonal loss occurs throughout the CNS and correlates with the heterogeneous symptoms of motor/balance disturbances, sensory and visual impairments, and cognitive deficits (Compston 2008). An urgent unmet clinical need in the therapeutic management of MS remains the selection of initial treatment. Once patients have been diagnosed, clinical practices may employ a "treat-to-target" approach, which begins with moderately efficacious drugs and escalates to highly efficacious therapy such as the intravenous biologics (Appendix A), or even Hematopoietic Stem Cell Transplantation, if required (Thompson 2018; Cree 2019). In contrast, an "early intensive" approach offers aggressive upfront treatment with highly efficacious disease modifying therapies (DMTs) at the time of diagnosis. The theory and real-world evidence suggest that early aggressive control of relapsing activity will result in less CNS injury and a better long-term prognosis (Harding 2019; Brown 2019). Preliminary data from the ongoing prospective MS trials (TREAT-MS; DELIVER-MS) have demonstrated that "early intensive" therapy results in a longer duration of time to disability and a reduced rate of conversion from RRMS to SPMS, over a period of 36 months (Harding 2019; Brown 2019).

1.2 The Pathogenesis of Multiple Sclerosis

Over the past several decades, biomedical research has elucidated the molecular mechanisms through which MS affects the CNS. Different avenues of research, including experiments using the mouse model of MS (experimental autoimmune encephalomyelitis (EAE)), and the analysis of several validated and investigatory immunologic markers in the serum and cerebrospinal fluid (CSF) of MS patients, demonstrate an immune-mediated pathogenic mechanism for MS (Riley, 2016). CD4+ T cells have classically been viewed as the primary cellular drivers of MS (Carnero 2020; Compston 2008). When an antigen is presented to the adaptive immune system, antigen-presenting cells (APC's) provide the relevant antigen to CD4+ T cells (T helper (Th) cells) in the periphery. Subsequently, CD4+ T cells are activated, causing the downstream generation of autoreactive proinflammatory Th1 and Th17 subsets (Riley, 2016). It is noteworthy that the differentiation of Th17 cells in humans is different from the commonly used animal species (e. g. rodent) used in MS disease modeling (de Jong 2010). The Th1 and Th17 cells bind to adhesion molecules on the endothelial surface of CNS venules, and with the help of proteases (matrix metalloproteinases and chemokines), cross the disrupted blood-brain-barrier (BBB) with B cells and monocytes (Riley, 2016). The ability of some DMTs to decrease disease activity may relate to their ability to shift T cell differentiation from Th1 and Th17 to Th2 phenotypes, which have a less inflammatory profile (Riley, 2016).

After crossing into the CNS, specific target antigens are recognized and T cells are then reactivated, leading to an amplified immune response. The proinflammatory Th1 and Th17 cells proliferate, the B cells mature into antibody-secreting plasma cells, release cytokines, and serve as professional antigen presenting cells (APCs), while the monocytes develop into macrophages. The immune cells subsequently produce proinflammatory cytokines interleukin-12 (IL-12), IL-

23, interferon-γ, TNF-α, proteases, free radicals, antibodies, nitric oxide, glutamate, and other inflammatory mediators which ultimately damage the myelin sheath surrounding axons and the supporting oligodendrocytes (Riley, 2016). The production of the CD4+ Th17 cells are initiated by the proinflammatory cytokines IL-1, IL-6, and transforming growth factor-β, and subsequently maintained and enhanced by the cytokine IL-23 (Riley, 2016). Th17 cells produce the proinflammatory cytokine IL-17, TNF-α and granulocyte macrophage colony stimulating factor, which are crucial in the development of EAE (Riley, 2016).

Neuroimmunological research has recently demonstrated that microglia, the resident CNS macrophage, plays a complex role in the pathogenesis of MS. Microglia are present throughout the CNS, contribute to synaptic loss in MS, and have been detected in the slowly expanding lesions which have been linked to MS disease progression (Guerrero 2020). In the early stages of an MS lesion, transmembrane protein 119 (TMEM119) staining (specific for microglia) has demonstrated that approximately 40% of the initial portion of phagocytic cells are microglia, with the recruitment of peripheral macrophages found to increase as a lesion grows (Guerrero 2020). Through the detection of the purinergic receptor P2Y12 (ADP receptor specific for the ramified processes of microglia seen in their resting state), it has been demonstrated that almost none of the microglia in an active MS lesion are in their homeostatic state (Guerrero 2020). So called “activated” microglia are now thought to play a critical role in MS pathogenesis through the phagocytosis of myelin, antigen presentation to T cells and release of proinflammatory cytokines in active lesions (Guerrero 2020). In contrast to this, microglia in an “alternatively activated” state, play a crucial role in both clearing myelin debris and in remyelination (Guerrero 2020).). In the progressive stages of MS, the so called “activated” microglia and macrophages

may mediate neurodegeneration through excitotoxicity (cytokine and glutamate release) and oxidative injury (release of reactive oxygen/nitrogen species) (Kamma 2022).

MS is classically thought of as a T cell mediated disease. However, in the past decade, B cells have been shown to play a role in acute demyelination and contribute to disease progression (Dal Bianco 2008; Wootla 2011). Clinical trials that have examined the effects of rituximab and ocrelizumab, (anti-CD20 B cell depleting therapies), have strengthened this theory (Sospedra 2016; Hauser 2008; Kappos 2011). CD20 is a surface antigen with expression on pre-B and mature B cells. Studies investigating the efficacy of rituximab in MS patients have revealed that it may target antigen presentation by B cells and activation of T cells, thus influencing the production of proinflammatory and regulatory cytokines (Wootla 2011). One study has proposed that abnormal B-cell cytokine responses are responsible for MS relapses via activation of relevant proinflammatory T cells (Wootla 2011; Bar-2010). In addition to this, mouse model experiments that selectively depleted the cytokine IL-10 from B cells, subsequently aggravated EAE in those mice, and IL-10 secretion by B cells has been shown to be deficient in MS patients compared to healthy controls (Fillatreau 2002; Duddy 2007). Inflammatory B cell infiltrates have been found within the meninges of patients with MS, with a higher burden of these infiltrates correlating to the volume of cortical lesions, neurodegeneration, and clinical disability (Comi 2021; Magliozzi 2007).

MS, while primarily thought of as a white matter disease, has demonstrated extensive cortical and gray matter involvement through all subtypes of the disease, with greater cortical and gray matter disease associated with disability progression (Lucchinetti 2011; Eshaghi 2018; Calabrese 2012). In contrast to the relapsing forms of MS, progressive forms of the disease are thought to be driven primarily by intrinsic immune processes within the CNS (Lassmann 2012;

Correale 2017; Cree 2021). While active or enhancing lesions can occur in progressive forms of MS, the majority of lesions consist of slowly expanding (smoldering), inactive, and remyelinated shadow plaques and cortical lesions (Lassmann 2012). Neurodegeneration in progressive MS may also be generated by chronic microglial activation, impaired ion homeostasis, mitochondrial injury, and meningeal inflammation (Lassmann 2012; Correale 2017). In SPMS patients, B and T lymphocytes, macrophages, and plasma cells are concentrated in lymphoid follicles in the meninges and perivascular spaces, whereas in PPMS patients, there is more diffuse meningeal inflammation without follicles (Correale 2017). Furthermore, in progressive MS, spinal cord lesion load has been shown to be higher, and when analyzed with the level of spinal cord gray matter atrophy, is predictive of disability severity in progressive MS (Correale 2017; Kearney 2015; Schlaeger 2015).

1.3 Diagnosis of Multiple Sclerosis

MS is described as a chronic immune-mediated demyelinating disorder of the CNS with lesions disseminated in time and space. Prior to the advent of Magnetic Resonance Imaging (MRI), clinicians relied on the history and clinical examination in order to demonstrate these principles in order to make a diagnosis of MS. Currently, paraclinical tests, including MRI and CSF studies, are used in conjunction with the history and clinical examination in order to arrive at a diagnosis of MS. While seemingly straightforward, due to the transient nature of the symptoms, clinical heterogeneity of presenting symptoms, and subjectivity related to symptoms, arriving at a diagnosis of MS can be challenging.

1.3.1 Diagnosis of Clinically Isolated Syndrome or Relapsing-Remitting Multiple Sclerosis

The classic clinical features that are suggestive of a first clinical demyelinating relapse of MS include unilateral visual changes and eye pain (i.e., optic neuritis), unilateral sensory and/or

motor symptoms with or without bladder and/or bowel dysfunction, as well as infratentorial symptoms such as imbalance, incoordination, double vision, and/or vertigo (Oh 2022). Specifically, typical demyelinating relapses include acute unilateral optic neuritis; double vision due to internuclear ophthalmoplegia or sixth nerve palsy; facial sensory loss or trigeminal neuralgia; cerebellar ataxia and nystagmus; partial myelopathy; sensory symptoms in a central nervous system pattern; Lhermitte phenomenon (radiating shock/electric sensation down spine on neck flexion); asymmetric limb weakness; urge incontinence or erectile dysfunction (Oh 2022). These symptoms will typically progress over the course of days (last at least 24 hours), reach a nadir, then gradually decline over the course of days to weeks. Clinical signs are required on neurological examination for patients to meet clinical criteria, but as each patient will have a different threshold for experiencing and reporting symptoms, it can be ambiguous which symptoms meet these criteria (Appendix B). In addition to these confounding variables, well known symptoms of MS such as fatigue, cognitive dysfunction, and mood symptoms (depression, anxiety), while common as a dominant feature in relapses, are not considered in isolation to be either CIS or first presentation of MS (Brownlee 2017; Benedict 2020).

The McDonald criteria were first introduced in 2001 to aid in the rapid diagnosis of CIS or RRMS in those patients who presented with a typical (non-cognitive) demyelinating syndrome (Oh 2022). The McDonald criteria incorporated paraclinical factors so that the hallmark features of dissemination in space and time could be met by a combination of clinical and MRI characteristics (McDonald 2001). Since their inception, the McDonald criteria have undergone several iterations of revisions (2005, 2010, 2017), with the latest revisions leading to a higher sensitivity (McDonald 2001; Polman 2005; Polman 2010; Thompson 2018). When a patient presents with a typical clinical demyelinating syndrome with objective evidence of a

neurological deficit on clinical examination, dissemination in space and time can be met in several ways. If the patient has a medical history that is suggestive of a prior demyelinating attack with objective clinical findings, then they can be diagnosed with RRMS based solely on clinical features. With this said, even in those situations where patients can be diagnosed on clinical criteria alone, it is highly recommended to get an MRI of the brain and spinal cord. This imaging will help serve as a baseline for the patient and repeat or follow-up imaging may help determine if there is subclinical disease activity and the potential need to initiate or switch DMT.

In those patients without any history of a demyelinating event, dissemination in space can be demonstrated by evidence of T2-hyperintense MRI lesions in two of four typical MS-related white matter lesion locations (periventricular, juxtacortical/cortical, infratentorial, spinal cord) (Appendix B). The dissemination in time criteria may be demonstrated by the presence of both gadolinium-enhancing (Gd+) (active) and non-enhancing lesions, or by the presence of CSF-specific oligoclonal bands (OCBs) when patients meet dissemination in space criteria and present with a typical demyelinating attack (Appendix B). Importantly, the latest iteration of the McDonald criteria allows for Gd+ (active) and non-enhancing lesions to fulfill the dissemination in space or time criteria. The diagnostic criteria state that even in those patients who present with a typical demyelinating relapse, in order to satisfy a diagnosis of MS, the presentation should have no better explanation, necessitating a reasonable workup and differential diagnosis (MS mimics such as neuromyelitis optica spectrum disorder (NMOSD), myelin oligodendrocyte glycoprotein associated disorder (MOGAD), neurosarcoidosis, etc.). Furthermore, as the MRI portion of the McDonald criteria was not designed to differentiate between MS and other neurologic conditions, if any atypical clinical features are present on history or examination, additional testing (MRI entire neuraxis, serial MRI's, CSF testing, serum Anti-AQP4/MOG), and

longitudinal follow-up is necessary to ensure appropriate diagnosis and prevent improper treatment with immunomodulatory or immunosuppressive medications.

1.3.2 Diagnosis of Primary Progressive Multiple Sclerosis

The diagnosis of PPMS can be made in an individual with a one year history of steady disability progression, determined either retrospectively or prospectively, that is independent of clinical relapse with dissemination in space demonstrated by two or more of the following: one or more typical MS T2-hyperintense lesions in one or more of the periventricular, cortical/juxtacortical or infratentorial brain regions; two or more T2 spinal cord lesions; CSF-specific OCBs (Appendix B). The McDonald criteria for PPMS stress both the importance of an insidious neurological progression and the predominance of spinal cord lesions, which is known to be more common in progressive forms (Oh 2022). As is the case with diagnosing RRMS, the criteria can be difficult to practically apply early in the disease course when there is no functional decline and only minimal objective neurological signs, leaving the diagnosis of PPMS heavily dependent on the patient's perception of their deficits (Oh J 2022). Mood disorders (anxiety, depression), fatigue, and deconditioning can all affect perceptions of symptoms, confounding reports of neurological symptoms, and thereby delaying the diagnosis of PPMS.

In comparison to RRMS, patients diagnosed with PPMS tend to be older (roughly 10 years older), with approximately 5% presenting after 60 years of age, in a near 1:1 female: male ratio (Bermel 2010; Lublin 2014). The most common presentation in progressive MS (SPMS or PPMS) tends to be a progressive myelopathy, characterized by a slowly worsening spastic paraparesis generally without a discrete sensory level (Oh, 2022). It is important to exclude other potential causes of progressive myelopathy such as subacute combined degeneration associated

with vitamin B12 or copper deficiency, as well as adrenoleukodystrophy, mitochondrial inherited disorders, and progressive multifocal leukoencephalopathy. Less commonly, PPMS may consist of a progressive cerebellar ataxia or other brainstem or visual symptoms (Rice 2013).

While there are clear diagnostic guidelines widely available for the diagnosis of PPMS, none such guidelines exist to aid the neurologist in diagnosing SPMS. As such, the neurologist will, in many cases, diagnose progression in patients with RRMS retrospectively when the history supports a gradual worsening of disability over 6 months to 1 year (Kalincik 2015; Thompson 2018). Progression does not tend to be linear, with many patients experiencing periods of gradual progression that can be difficult to measure, and periods of relative stability. The traditionally used Expanded Disability Status Scale (EDSS) is sensitive for measuring pyramidal dysfunction but does not adequately address many other functional domains that are often affected in progressive disease (i.e., cognition). In an effort to amend this, functional scores have been added to the EDSS evaluation and the Multiple Sclerosis Functional Composite (MSFC) was developed to quantitatively assess leg, arm, and cognitive function (25-foot walk test, 9-hole peg test, and Paced Auditory Serial Addition Test now replaced by the Symbol Digit Modalities Test (SDMT), respectively), yet these are not able to accurately measure and diagnose progression (Fischer 1999).

A number of imaging biomarkers of progression are under investigation for their utility in detecting and monitoring MS progression, as there is only a weak correlation between MRI lesion load and clinical disability (Filippi 2020; Barkhof 2002). MRI features more closely associated with progressive MS, include a shift on MRI from active to inactive lesions (smoldering lesions) and progressive atrophy of both the gray and white matter of the brain and spinal cord (Bodini 2016; Bussas 2022). While not typically thought of as a disease affecting the

cortex, the volume of cortical lesions (≥ 7) and its change over time (4 years after disease onset), have proven useful in predicting conversion to SPMS (Scalfari 2018). Other advanced MRI techniques focus on examining axonal loss through measurement of gray matter, thalamic volume, and hippocampal volume, along with gray matter fraction, cortical lesion quantification and sodium imaging (Ontaneda 2015; Mahajan 2017).

1.4 Treatment of Multiple Sclerosis

Once a diagnosis of CIS or RRMS has been clarified, clinicians and patients may work together to institute a "treat-to-target" approach. Placing emphasis on patient safety, this approach begins with moderately efficacious drugs and escalates to highly efficacious therapy such as cladribine, ocrelizumab, or ofatumumab, if careful monitoring demonstrates signs of breakthrough disease activity (i.e., increase in EDSS, a breakthrough demyelinating relapse, new MRI T1-weighted enhancing lesions and/or new or enlarging T2-weighted lesions) (Cree 2019). In contrast to this approach, the initial use of high-efficacy DMTs, whether for treatment in RRMS or relapsing-SPMS, aims to gain rapid control of the inflammatory aspect of the disease. The current theory and real-world evidence suggest that early aggressive control of relapsing activity will result in less CNS injury and a better long-term prognosis (Harding 2019; Brown 2019).

Utilizing the data collected in the MSBase database, an international online registry of MS and other neuroimmunological conditions, it has been found that patients exposed to high-efficacy DMT within 2 years of an MS diagnosis, had better disability outcomes than those treated with these DMT's at a later stage in their disease (He 2020). Currently, two prospective MS trials, funded by the Patient-Centered Outcomes Research Institute (PCORI), TREAT-MS (TRaditional versus Early Aggressive Therapy for Multiple Sclerosis trial) and DELIVER-MS

(Determining the Effectiveness of earLy Intensive Versus Escalation Approaches for RR-MS) aim to address whether results such as these represent true early high-efficacy or rapid escalation for incomplete DMT efficacy (Harding 2019; Brown 2019). Transition to a different DMT is most often completed due to a lack of medication efficacy or patient tolerability issues. When a DMT transition is necessitated, previous research on disease outcomes generally supports the transition to a higher efficacy DMT (Hillert 2021; Kalincik 2015; Spelman 2015).

With the large-scale advances in targeted immunotherapies in the treatment of MS, there is now a plethora of DMTs (19 FDA approved DMTs) available for patients with MS (Table 1). Mirroring the development of these DMTs, various means for accurately assessing disease activity were established, leading to the current composite endpoint of NEDA-3 (no evidence of disease activity-3). NEDA-3 represents the absence of MRI disease activity (new/enlarging T2 lesions and/or T1 Gd+ lesions), relapses, and disability progression (measured via serial EDSS scores). Although not yet widely employed in clinical practice, the absence of accelerated brain volume loss (BVL), represents NEDA-4, an additional layer of monitoring for disease activity (Kappos 2016). The current milieu of DMTs comprise 10 different mechanisms of action, with all current approved therapies, with the exception of the interferon's beta and glatiramer acetate, considered to be immunosuppressive. Those patients taking any of the immunosuppressive medications require monitoring for infection, cannot begin DMT prior to treatment for any active infections, and generally should not receive live or live-attenuated vaccines (Kappos 2016). As there is no evidence-based method to choose the best DMT for an individual patient, the choice of DMT remains a joint decision between the patient and provider, resting on a balance between efficacy and potential adverse effects of the DMT, disease subtype, aggressiveness, along with any comorbid conditions of the patient and their preference.

Similar to the choice of DMT, the decision of DMT discontinuation depends upon a number of factors. As immune system function gradually declines with age, there is a concomitant decrease in MS inflammatory activity and an increase in the risk profile of immunosuppressive therapies. While there is no clear answer currently, evidence does suggest that those patients who have disease stability and discontinue their DMT after the age of 45 are more likely to have stable disease (Yano 2019). The randomized discontinuation of DMT in those 55 years and older with 5 years of disease stability is currently being investigated by the PCORI-funded Discontinuation of DMT in MS (DISCOMS) study (University of Colorado, 2022).

1.4.1 Interferon Beta

There are 5 separate versions of type I interferons (interferon beta-1b first approved) approved for use in patients with CIS, RRMS, and active SPMS, with all interferons being administered via subcutaneous (SC) or intramuscular injection (IM). While the mechanism of action is not known, proposed actions include upregulation of interleukin-10 (IL-10), VCAM-1, suppressor T-cell activity, along with reduced proinflammatory cytokine production and decreased antigen presentation to T cells (Rudick 1996; Calabresi 1997). As the first class of DMT approved for use in MS, they are now considered to be a lower efficacy medication, with reductions in the annualized relapse rate (ARR) ranging from 18% (interferon beta-1a at 30 μg/wk IM) to 32% (interferon beta-1a at 44 μg 3 times weekly) as compared to placebo (Panitch 2002). In addition to reductions in ARR, the interferons beta have shown up to 80% reduction in T1-weighted Gd+ lesions and disability progression up to 44% (Kalincik 2021).

When patients are counseled on the use of the interferons beta, they should be made aware that it is common to experience flu-like side effects for several hours after each dose,

which is lessened by acetaminophen or non-steroidal anti-inflammatory drugs (NSAIDs). As they can rarely cause hepatotoxicity, leukopenia, thrombocytopenia, patients should have a complete blood count (CBC) and liver transaminases monitored at least yearly. Importantly, as the interferons beta are considered non-teratogenic, they are safe for use during pregnancy and breastfeeding. The interferons are immunomodulatory, not immunosuppressive, do not increase the risk for opportunistic infections and do not significantly negatively affect immune responses to vaccines (Ciotti 2020).

1.4.2 Glatiramer Acetate

Glatiramer acetate, a mixture of synthetic polypeptides composed of four amino acids resembling myelin basic protein (MBP), is approved for use in patients with CIS, RRMS, and active SPMS and is delivered via subcutaneous (SC) injection (20 mg daily versus 40 mg 3 times weekly) (Schrempf 2007). Similar to the beta interferon's, the mechanism of action of glatiramer acetate is not fully elucidated, with proposed actions including alteration of Th1 and Th17 proinflammatory subsets to the less inflammatory Th2 subtype (Schrempf 2007). Glatiramer acetate has been shown to reduce annualized relapse rate (ARR) between 29% (20 mg daily) and 45% (40 mg 3 times weekly), and T1-weighted Gd+ lesions by 35% when compared to placebo (Johnson 1995; Comi 2010; Khan 2013).

The major benefits of glatiramer acetate include the lack of blood monitoring, the absence of any drug interactions, and no increased risk of opportunistic infections. When patients are counseled on the use of glatiramer acetate, they should be made aware that they can experience an immediate post-injection reaction that is self-limited and is benign (flushing, chest pain, palpitations, tachycardia, anxiety, dyspnea, constriction of the throat, and urticaria) and they can develop lipodystrophy at injection sites over time. As is the case with the beta

interferon's, glatiramer acetate is non-teratogenic, and considered safe for use during pregnancy and breastfeeding (Sandberg-Wollheim 2018). Furthermore, it does not increase the risk for opportunistic infections, and while reduced responses have been noted to the seasonal flu vaccination, they are generally still considered to be protective (Ciotti 2020).

1.4.3 Teriflunomide

Teriflunomide, the active metabolite of leflunomide, is approved for use in patients with CIS, RRMS and SPMS, and is taken as a once daily oral medication (Oh 2014). Teriflunomide selectively and reversibly inhibits dihydroorotate dehydrogenase, leading to reduced pyrimidine synthesis, and subsequently reducing activated T and B lymphocytes and their migration into the CNS (Bar-Or 2014). Clinical trial data from several large, randomized phase III studies including TEMSO, TOWER, TENERE, TERACLES, and TOPIC and have shown that teriflunomide (14 mg daily dose), when compared to placebo, reduced ARR between 31% to 36%, 12-week confirmed disability by 30%, and T1-weighted Gd+ lesions by 80% (Oh 2014; O'Connor 2011).

When patients are counseled on the use of teriflunomide they should know that it can cause nausea, headaches, transient hair thinning, elevated blood pressure, diarrhea and arthralgia, and peripheral neuropathy (Oh J 2014). As teriflunomide is an immunosuppressant, patients must be screened for latent tuberculosis, and as it can cause elevations in alanine transaminase (ALT), monthly liver function tests must be completed for the first 6 months (Oh 2014). While extremely rare, cases of progressive multifocal leukoencephalopathy (PML), a potentially fatal condition that is caused by lytic infection of glial cells by the Jackson Cunningham (JC) virus, have been reported with the use of teriflunomide (Oh J 2014). As it is teratogenic, teriflunomide cannot be used in males or females not using effective contraception,

and accelerated removal can be completed with cholestyramine or activated charcoal in the event of pregnancy or serious adverse effects (Oh J 2014).

1.4.4 Fumarates

Dimethyl fumarate is approved for use in patients with CIS, RRMS, and active SPMS and is taken as a twice daily oral medication (240 mg PO BID) (Mills 2018). The main mechanism of action for all approved fumarates (dimethyl fumarate, diroximel fumarate, monomethyl fumarate) is the activation of nuclear factor (erythroid-derived 2)-like 2 (Nrf2) pathways in humans, a key factor in the cellular response to oxidative stress (Mills 2018). Two large, randomized placebo-controlled phase III clinical trials, DEFINE and CONFIRM, demonstrated that dimethyl fumarate reduced ARR by 53% and 44%, respectively (Mills 2018). In addition to this, patients in the DEFINE and CONFIRM studies administered the 240 mg PO BID dosing regimen demonstrated 38% and 21% reductions in confirmed 12-week disability progression, along with a 90% and 74% reduction in T1-weighted Gd+ lesions (Mills 2018). The other two fumarates, diroximel fumarate and monomethyl fumarate, have the same active metabolite as dimethyl fumarate, but are much less commonly used in clinical practice (Mills 2018).

When patients are counseled on the use of dimethyl fumarate, they should know that it can cause flushing (treated with aspirin taken 30 minutes prior to dose), and gastrointestinal upset that generally improves with time. Diroximel fumarate has an improved gastrointestinal tolerability profile compared to dimethyl fumarate (Naismith 2020). As is the case with teriflunomide, there have been cases of PML reported with dimethyl fumarate when patients have experienced prolonged lymphopenia (Mills 2018). Other potential adverse events include hepatotoxicity, and opportunistic infections with nocardia, listeria monocytogenes, mycobacterium tuberculosis, and aspergillus. As such, 6 monthly CBC and liver function tests

are recommended. Furthermore, women should not become pregnant while taking any of the fumarate medications, breastfeeding is not recommended, and the limited available evidence with vaccinations suggests vaccine efficacy (von Hehn 2017).

1.4.5 Sphingosine-1-phosphate Receptor Modulators

Fingolimod was the first oral DMT approved for use in MS, the only DMT approved for use in pediatric RRMS, and is now clinically indicated in patients 10 years of age and older with CIS, RRMS, and active SPMS (Barry 2019). As a sphingosine-1-phosphate (S1P) receptor modulator of receptors 1,3,4 and 5, fingolimod decreases the trafficking of autoreactive lymphocytes into the CNS by blocking S1P1-dependent egress of lymphocytes out of lymph nodes (Barry 2019). The main effect of this is a decrease in both the peripheral blood lymphocyte and neutrophil counts that return to normal after treatment cessation. Importantly, fingolimod, along with all other S1P modulators, cross the blood brain barrier (BBB), where they have been shown to affect neurogenesis, cellular function, and migration (Barry 2019). The TRANSFORMS and FREEDOMS were two large multicenter randomized clinical trials that compared fingolimod against interferon beta-1a and placebo, respectively (Cohen 2010; Kappos 2010). FREEDOMS demonstrated a reduction in ARR by 50%, confirmed disability progression and rate of brain volume reduction by 30%, and 37.8% more patients on fingolimod than placebo had no T1-weighted Gd+ lesions by the end of the study (Kappos 2010). In comparison, in the TRANSFORMS study, patients on fingolimod had ARR reduced by 52%, 30% reduction in the rate of brain volume loss, and no difference in confirmed disability progression (Cohen 2010). In addition to these two pinnacle trials, the PARADIGMS study examined the efficacy of fingolimod versus interferon beta-1a in pediatric patients with MS (ages 10-17 years), and it was shown to reduce ARR by 82% and T1-weighted Gd+ lesions by 66% (Chitnis 2018a).

Siponimod was the second SIP receptor modulator approved for use in patients with CIS, RRMS, and active SPMS, and though it has the same proposed mechanism of action as fingolimod, it selectively modulates S1P receptors 1 and 5 (Scott 2021). Importantly, prior to dosing the CYP2C9 genotype of patients must be determined, as those with a CYP2C9*1/*3 or *2/*3 genotype require the dose to be reduced from 2 mg daily to 1 mg daily, and those with a CYP2C9 3*/3* genotype cannot receive this DMT (Scott 2021). The pivotal EXPAND trial was a randomized, double-blind, placebo-controlled phase 3 clinical trial in patients with SPMS who had an EDSS between 3.0-6.5, EDSS progression in the previous 2 years, and no evidence of relapse in the previous 3 months (Scott 2021). Siponimod reduced the time to 3-month confirmed disability progression in those with active SPMS (1 point increase if baseline EDSS 3.0-5.0- or 0.5-point increase if baseline EDSS 5.5-6.5) by 21% when compared to placebo, and in non-relapsing SPMS patients by 14-20% when compared with placebo. In addition to this, siponimod resulted in lower percentage decreases in whole brain volume from baseline at 12 and 24 months, as well as cortical grey matter and thalamic volume loss (Scott 2021).

In addition to siponimod, ozanimod is another S1P receptor modulator approved for use in CIS, RRMS, and active SPMS, which also selectively modulates S1P receptors 1 and 5. Following an initial one week up-titration, ozanimod is taken as a 0.92 mg once daily oral medication (Cohen 2019). Ozanimod was initially studied in the two large multicenter, randomized, double-blind, phase 3 clinical trials RADIANCE and SUNBEAM, against interferon beta-1a (Cohen 2019; Comi 2019). While ozanimod was found to decrease the ARR by 38% and 48%, T1-weighted Gd+ lesions by 53% and 63% in the two trials, there was no significant difference seen in either 3 or 6-month confirmed disability progression. Ponesimod is the most highly selective S1P receptor modulator, acting only on the S1P1 receptor. It is

approved for use in patients with CIS, RRMS, and active SPMS, and similar to siponimod and ozanimod, it requires an initial up-titration, but if more than 4 consecutive doses are missed, it requires re-titration. Ponesimod was evaluated against teriflunomide (14 mg daily) in the phase 3 OPTIMUM trial, the first phase 3 study comparing 2 oral DMT's in RRMS (Kappos 2021). While ponesimod was found to reduce ARR by 30.5% and the number of T1-weighted Gd+ lesions by 58.5% compared to teriflunomide, there was no statistically significant difference in confirmed disability progression between the treatment groups.

Those patients taking any of the S1P modulators need to have an ECG completed prior to initiation, and they are all contraindicated in individuals with known cardiac abnormalities (myocardial infarction, unstable angina, stroke, transient ischemic attack, decompensated heart failure requiring hospitalization, class III/IV heart failure, Mobitz type II second-degree or third-degree atrioventricular block, or sick sinus syndrome without a functioning pacemaker) (Kappos 2010). Fingolimod specifically requires cardiac monitoring of the first dose, as the risk of bradycardia or arrhythmia are higher with this DMT (Subei 2015). The clinical trial safety data demonstrated an increased risk of infections with all S1P modulators. Thus, all patients taking an S1P modulator should have evidence of prior varicella-zoster virus (VZV) infection or be vaccinated against this virus and should have continuous monitoring for infections including PML (Subei 2015). Furthermore, S1P receptor modulators pose an increased risk of macular edema, especially for patients with diabetes mellitus or uveitis, necessitating ophthalmology referral and follow-up (Subei 2015). Pregnancy and live attenuated vaccinations are contraindicated when taking any of the S1P modulators, there is a risk of severe rebound disease on discontinuation, and there is a potential increased risk of posterior reversible encephalopathy syndrome (PRES) and malignancies such as lymphoma (Subei 2015). As there is no currently available vaccination data available for ozanimod and ponesimod, all vaccination recommendations for S1P receptor modulators come from studies of fingolimod and siponimod. Patients taking fingolimod were found to have reduced seroprotection rates (reduced 22% to

50%) to the administration of the seasonal flu and tetanus toxoid booster vaccinations, and dramatically reduced rates of seroprotection (3.8% versus 100%) from the administration of the BNT162b2 COVID-19 mRNA vaccine (Kappos 2015; Achiron 2021). In a study of interrupted (stopping 7-10 days prior to vaccination and restarting 14 days after vaccination) versus uninterrupted siponimod administration, responses to the seasonal influenza A/B vaccine were found to be better in the interrupted siponimod group, with no relevant antibody effect on the pneumococcal polysaccharide vaccine (Ufer 2017).

1.4.6 Cladribine

Cladribine (a purine nucleoside analogue) oral cytotoxic therapy for patients with RRMS or active SPMS, is given as 3.5mg/kg cumulative dose over 2 years (1.75mg/kg per course), with each course spaced at least 43 weeks apart and divided into two cycles that are separated 23 to 27 days (Cross 2022). The initial efficacy of oral cladribine tablets was evaluated in the CLARITY study (96-week placebo-controlled trial), which assessed two cumulative dosing regimens (3.75 mg/kg versus 5.35mg/kg), compared to placebo (Giovannoni 2010). This study found that the 3.25mg/kg dose led to a significant reduction in ARR, median number of Gd+ lesions and the median number of active T2 lesions (Giovannoni 2010). The CLARITY extension trial demonstrated a continued relapse-free status in years 3 and 4 for the majority of those patients initially treated with cladribine (Giovannoni 2018). Cladribine tablets have gained marketing authorization in more than 75 countries for the treatment of patients with various forms of relapsing MS. There has since been a large body of clinical trial and real-world evidence indicating the efficacy of cladribine in the treatment of relapsing forms of MS.

As an immune reconstitution therapy (IRT), cladribine produces long-term effects on the immune system through cytotoxic effects on B and T cells, and it penetrates the BBB (AlSharoqi 2020). Whereas the risk of adverse events increases with cumulative dose exposure

with continuous maintenance DMTs, the risk of adverse events with IRTs is greatest during the initial post-treatment period (Boyko 2018). There are three immune phases associated with cladribine therapy: reduction, repopulation, and reconstitution. With full effector function regained, the reconstituted immune system is now both quantitatively and qualitatively different than it was prior to therapy, potentially explaining the long-term efficacy seen with cladribine and alemtuzumab therapy (Giovannoni 2022). The co-administration of further immunosuppressive and/or myelosuppressive therapies is contraindicated, and while corticosteroids could reduce the efficacy of cladribine, it can in practice be co-administered if clinically necessary. Moreover, effective contraception should be instituted until at least 6 months after the last dose in each treatment course in both women and men of reproductive potential (Mavenclad (Cladribine) [package insert]. Rockland, MA: EMD Serono, Inc.; 2019).

Those patients taking cladribine should have a full blood count, liver function tests, urea/electrolytes, and serum immunoglobulins checked, along with an infection screen that includes hepatitis B/C; tuberculosis (QuantiFERON); human immunodeficiency virus (HIV) 1&2; syphilis; VZV; vaginal human papillomavirus (HPV) or cervical smear testing; and screening for cutaneous warts (Klotz 2019). Furthermore, while vaccinations can be delayed and given after immune reconstitution, in the era of the COVID-19 pandemic, COVID-19 vaccinations can be administered during active treatment, as recent research has confirmed that patients treated with cladribine produce antibodies to the SARS-CoV-2 mRNA vaccine (Klotz 2019). In addition to the aforementioned workup for cladribine institution, patients will require a baseline MRI Head (+/- spine if indicated), followed by 3 and 7-month post-treatment complete blood counts to assess total lymphocyte counts (nadir and rebound) (Giovannoni 2022).

1.4.7 Natalizumab

Natalizumab is a monoclonal antibody (mAb) approved for use in patients with CIS, RRMS, and active SPMS, that is administered as 300 mg intravenous (IV) infusion every 4 weeks (Polman 2006). Natalizumab reduces inflammation through binding to the α4 subunit of α4β1 and α4β7 integrins, subsequently blocking the binding of these integrins to their endothelial receptors (VCAM-1 and mucosal addressin-cell adhesion molecule 1) in B and T cells. This prevents these cells from binding to activated CNS endothelium, and the subsequent migration of leukocytes across the BBB (Polman 2006). In addition to this, natalizumab is thought to further reduce inflammation through inhibition of α4-positive leukocytes binding with fibronectin and osteopontin, subsequently blocking the movement of these cells through tissues (Polman 2006). Two large trials investigated the utility of natalizumab against placebo, and as an add-on therapy to interferon beta-1a, demonstrating ARR reduction by 67% and 56%, respectively (Polman 2006; Rudick 2006). In addition to reduced ARR, natalizumab resulted in a 92% reduction in the mean number of T1-weighted Gd+ lesions versus placebo.

Natalizumab is widely known to increase the risk of PML, but this is nearly always limited to those patients with antibodies to the JC virus (Ryerson 2019). Specific risk factors for those with JC virus positivity include level of anti-JCV antibodies in serum (anti-JCV antibody index > 0.9), use of immunosuppressant therapy before natalizumab initiation, and greater than 2 years of natalizumab treatment (Ryerson 2019). Employing an extended interval dosing schedule, where patients receive infusions every 6 weeks as opposed to every 4 weeks, has shown benefit in reducing the risk of developing PML (Ryerson 2019). In addition to the risk of PML, there is also an associated risk of herpetic infections (meningitis/encephalitis), JC virus infection of cerebellar granule cells, rare cases of lung infections with pneumocystis jirovecii, mycobacterium avium-intracellulare, aspergillus, and burkholderia cepacia, and very rarely severe hepatotoxicity (Morrow 2022). The RESTORE trial identified that patients discontinuing natalizumab should begin another DMT within 4-6 weeks, due to the risk of rebound MS relapse activity (Fox 2015).

With regard to pregnancy data, fetal malformation and pregnancy loss do not seem to occur, but third trimester exposure may cause reversible hematologic alterations (Haghikia 2014; Friend 2016). There is also data to suggest that treatment with natalizumab in pregnant patients with highly active disease in the first trimester reduces the risk of MS disease activation, when compared to abrupt discontinuation at conception (Demortiere 2021). Women should be counseled not to breastfeed, as natalizumab can be detected in breastmilk, and vaccination data have revealed inadequate humoral responses to seasonal flu vaccines (Metze 2019).

1.4.8 Ocrelizumab and Ofatumumab

Ocrelizumab and ofatumumab are both anti-CD20 cytolytic monoclonal antibodies approved for use in patients with CIS, RRMS, active SPMS, and in the case of ocrelizumab, PPMS (Hauser 2017; Hauser 2020). Ocrelizumab is administered as 600 mg IV infusion every 6 months, whereas ofatumumab is administered as a 20 mg SC injection every month. While the mechanism of action of these anti-CD20 lytic monoclonal antibodies are not fully elucidated, it most likely relates to the roles of B lymphocytes in T-cell activation and the production of proinflammatory cytokines and chemokines, and as a B-cell therapy, they do not cross the BBB (Hauser 2017). Importantly, these anti-CD20 lytic therapies do not deplete stem cells (pro-B cells), many plasmablasts, and the antibody-producing plasma cells (B cells that do not express CD20) (Greenfield 2015). In the pivotal OPERA I and II trials, ocrelizumab was found to reduce ARR by 46% and 47% compared to interferon beta-1a, Gd+ lesions by 94% and 95%, and reduce 12-week confirmed disability progression by 40% (Hauser 2017). In addition to this, the ORATORIO study enrolled patients with PPMS, and ocrelizumab was found to reduce EDSS progression by 24% and worsening of the 25-foot walk test by 25%, when compared to placebo (Montalban 2017). Ofatumumab was studied in two large randomized controlled trials, ASCLEPIOS I and II, and revealed a reduction in ARR by 51% and 59% respectively, when

compared to teriflunomide 14 mg daily (Hauser 2020). Additionally, ofatumumab reduced Gd+ lesions by 98% and 94% in the two trials, and pooled confirmed disability progression by 34.4% (Hauser 2020).

When counseling patients about the anti-CD20 therapies, they should know that there is an increased risk of upper and lower respiratory infections, reactivation of hepatitis B, infection with herpes viruses, very rare cases of PML, and a potential increase in the risk of breast cancer, although this has been contested (Hauser 2017). The risks associated with pregnancy are not fully known, but ocrelizumab and ofatumumab are both IgG1 subtype immunoglobulins that can cross the placental barrier and have been shown to cause transient peripheral B-cell depletion in infants exposed in utero. The VELOCE study demonstrated that ocrelizumab reduced humoral responses to the influenza and pneumococcal vaccinations, and only 22.7% of patients on ocrelizumab receiving the BNT162b2 COVID-19 mRNA vaccine achieved a protective humoral antibody response (Bar-Or A 2020). As such, required live or live-attenuated vaccinations must be completed 4 weeks or more prior to treatment initiation.

1.4.9 Alemtuzumab

Alemtuzumab, like cladribine, is an immune reconstitution therapy, and it is approved only for use in patients with RRMS and active SPMS who have failed two or more DMT's. It is an anti-CD52 cytolytic monoclonal antibody delivered as an IV infusion in a 5-day course in year 1, and as an IV infusion in a 3-day IV course 1 year later (Cohen 2012). Alemtuzumab is thought to destroy circulating CD4+ and CD8+ T cells, B cells, natural killer cells, and monocytes/macrophages (Cohen 2012). As seen with cladribine, the immune cell subsets gradually return, with the immune system now becoming quantitatively and qualitatively different than it was prior to treatment. The CARE-MS I and II single blinded studies compared alemtuzumab (12 mg daily IV) to interferon beta-1a (44 µg SC 3 times weekly), with alemtuzumab reducing ARR by 49% and 55% in each trial, respectively (Cohen 2012; Coles

2012). Interestingly, while there was a statistically significant reduction in 6-month confirmed disability progression in CARE-MS II, this was not observed in CARE-MS I (Guarnera 2017).

Alemtuzumab carries a significant adverse event profile including a potentially life-threatening infusion reaction, increases the risk of melanoma, thyroid cancer, and lymphoproliferative cancers, and it may cause fetal harm. Upper and lower respiratory infections, herpes virus related infections, thyroid disease (Grave's, hypothyroidism, thyroiditis), and secondary autoimmune conditions such as immune thrombocytopenia (ITP) and anti-glomerular basement membrane disease, which are thought to occur through lymphocyte reconstitution, are all relevant risks with alemtuzumab treatment (Guarnera 2017). As such, patients receiving alemtuzumab must be given anti-herpes prophylaxis from the first day of the initial 5-day dosing until 2 months after the 5-day treatment or until the CD4+ lymphocyte count is ≥ 200 cells/mL (Guarnera 2017). Given these potential adverse events, patients receiving alemtuzumab should have a CBC with differential, serum creatinine, and urinalysis with cell counts completed monthly, along with thyroid function tests every 3 months until 4 years after their last dose (Guarnera 2017). Furthermore, similar to other DMT's, live viral vaccinations should be avoided while taking alemtuzumab, and as vaccine responses are blunted during treatment, any necessary vaccinations should be given 2-4 weeks prior to treatment initiation (McCarthy 2013).

1.4.10 Mitoxantrone

Mitoxantrone is an antineoplastic anthracenedione that was approved for use in aggressive RRMS, SPMS, and progressive-relapsing multiple sclerosis (Marriott 2010). Mitoxantrone reduces lymphocyte proliferation through intercalation into DNA strands, inducing strand breakage and inhibition of the DNA repair enzyme topoisomerase II. Despite three clinical trials demonstrating the benefit of mitoxantrone in reducing ARR, MRI activity, and confirmed disability progression, mitoxantrone carries serious and potentially life-threatening risks that include dose-limiting cardiotoxicity (lifetime dose 140 mg/m^2), and

potentially fatal secondary leukemia, making it a rarely used DMT for MS in the current treatment landscape (Millefiorini 1997; Hartung 2002; Edan 1997).

1.4.11 Bruton Tyrosine Kinase Inhibitors

Bruton Tyrosine Kinase (BTK) is a non-receptor tec kinase that is found within the cytoplasm of hematopoietic cells (Yang 2015). While BTK is predominantly found in B cells, it is selectively downregulated in T cells and plasma cells through mRNA expression analysis (Smith 1994). The highly selective irreversible BTK inhibitors evobrutinib, tolebrutinib, and orelabrutinib, and the reversible BTK inhibitor fenebrutinib, all target B-cell activation and aspects of innate immunity, including macrophage and microglia biology (Arsenault 2022). There are many phase 3 clinical trials investigating the utility of the oral BTK inhibitors in RRMS, active SPMS, non-active SPMS and PPMS.

The Evolution RMS 1 & 2 trials are double-blind, double-dummy, active-controlled phase 3 studies comparing evobrutinib twice daily versus IM injection of interferon β−1a once weekly, with promising phase 2 trial data for the reduction in T1-weighted Gd+ lesions. (Arsenault 2022). Another BTK inhibitor, tolebrutinib may be the first B-cell depleting therapy that inhibits the peripheral immune system and crosses the BBB to suppress immune cells that have migrated into the brain and modulates the activity of CNS microglial cells. There are currently 4 separate safety and efficacy phase 3 trials in patients with RRMS, SPMS and PPMS. The GEMINI 1 & 2 trials are comparing daily tolebrutinib against teriflunomide (14 mg daily) in those patients with RRMS, while the PERSEUS and HERCULES trials will assess safety and efficacy of daily tolebrutinib against placebo, in those patients with PPMS and non-relapsing SPMS (Arsenault 2022). In addition to this, the FENhance and FENtrepid studies will study the safety and efficacy of fenebrutinib compared to teriflunomide in RRMS patients, and

ocrelizumab in PPMS patients, respectively. Orelabrutinib, an irreversible CNS penetrant BTK inhibitor, is currently being investigated for its efficacy in patients with RRMS in a phase 2 study, while remibrutinib, a highly selective oral BTK inhibitor is currently being investigated in the REMODEL I and II phase 3 trials in RRMS and active SPMS patients against teriflunomide (14 mg daily) (Arsenault 2022).

1.5 Radiological biomarkers in Multiple Sclerosis

MRI is a paraclinical tool that is paramount in the diagnosis and monitoring of disease activity in MS. As previously mentioned, in patients without any history of a demyelinating event, dissemination in space can be demonstrated by evidence of T2-hyperintense MRI lesions in two of the four typical MS-related white matter lesion locations (periventricular, juxtacortical/cortical, infratentorial, spinal cord). MRI can be utilized to ensure patients meet the dissemination in time criteria if both gadolinium-enhancing (Gd+) (active) and non-enhancing lesions are present, in those with a history of demyelinating relapse. Furthermore, most clinical trials institute T1-weighted Gd+ lesions and T2-weighted lesion load as either primary or secondary endpoints to measure the efficacy of a DMT. Imaging biomarker research has elucidated several candidates for both the diagnosis of MS, and as a marker of disease progression.

The central vein sign (CVS) is one such imaging biomarker that has demonstrated utility in differentiating microangiopathic white matter disease from MS-related demyelinating lesions and is now undergoing validation in large prospective clinical trials (Mistry 2016; Sati 2014; Sati 2016). The CVS is thought to be representative of lesions that formed due to perivenular inflammation and demyelination, a characteristic that is pathognomonic of MS-related lesions, and these can be visualized on MRI when the appropriate susceptibility weighted imaging (SWI)

protocol is employed. The North American Imaging in Multiple Sclerosis (NAIMS) cooperative detailed several characteristics of the CVS in T2 imaging that include: appears as a thin hypointense line or small hypointense dot; visualized in at least two perpendicular MRI planes, and appears as a thin line in at least one plane; has a small apparent diameter (<2 mm); runs partially or entirely through the lesion; is positioned centrally in the lesion (that is, located approximately equidistant from the lesion's edges and passing through the edge at no more than two places), regardless of the lesion's shape (Sati 2016). While there is no agreed upon ideal criteria regarding the CVS for clinical use, the most employed criterion is the 40% rule, whereby if ≥ 40% of lesions contain the CVS, then it is highly likely that this is representative of MS (Tallantyre 2011). As this technique requires examination of every single lesion for the CVS, this is time and labor intensive, limiting its utility in clinical practice. As such, less time, and labor-intensive techniques such as the "select 3" and "6-lesion rule" have been proposed (Solomon 2018; Mistry 2016). Additionally, the capability of the CVS as a prognostic imaging biomarker in RIS and early RRMS is also being evaluated (Suthiphosuwan 2019).

In the last several years, a few imaging biomarkers of disease progression have been proposed, as accumulated evidence suggests that there is only a weak correlation between MRI lesion load and clinical disability (Filippi 2020; Barkhof 2002). Some of the MRI features shown to be more closely associated with progressive MS include a shift on MRI from active to inactive lesions, known as smoldering lesions, along with progressive atrophy of both the gray and white matter of the brain and spinal cord (Bodini 2016; Bussas 2022). While MS is not typically thought of as a disease affecting the cortex, imaging biomarker research has demonstrated that the volume of cortical lesions (≥ 7) and its change over time (4 years after disease onset), are useful in predicting conversion to SPMS (Scalfari 2018). Other investigation MRI techniques

focus on examining axonal loss through measurement of gray matter, thalamic volume, and hippocampal volume, along with gray matter fraction, cortical lesion quantification and sodium imaging (Ontaneda 2015; Mahajan 2017). In addition to these, another imaging biomarker in development to aid clinicians in accurately assessing for disease progression in MS is the paramagnetic rim sign, which is thought to be representative of chronically active, smoldering lesions (Absinta 2016; Absinta 2018). Paramagnetic rims can be identified around some non-enhancing chronic lesions on susceptibility-based MRI sequences and have been shown through MRI-pathological correlation to contain iron-enriched microglia, making them a potential imaging surrogate for chronic smoldering lesions and marker of disease progression (Gill 2023). With this said, as the paramagnetic rim sign can be seen in lesions in patients with radiologically isolated syndrome (RIS) or early RRMS, specific thresholds will need to be further developed for the paramagnetic rim sign to be considered diagnostically and clinically viable as an imaging biomarker for disease progression (Suthiphosuwan 2020; Absinta 2019).

1.6 Biofluid Biomarkers

Elevated intrathecal production of oligoclonal immunoglobulins (IgG/M/A/D) is the most consistent laboratory abnormality seen in patients with MS and is believed to represent immune cell activation within the CNS (Cross 2006). While not specific for MS, elevated intrathecal immunoglobulin (Ig) remains an important biomarker for the diagnosis of MS (Cross 2006). Several studies have correlated elevated levels of IgG, higher numbers of oligoclonal bands (OCBs), and an elevated IgG index with a worse prognosis (Cross 2006). MS diagnostic guidelines currently refer to two different methods to satisfy a diagnosis: quantitatively elevated IgG (IgG index) and the detection of OCBs by isoelectric focusing (Deisenhammer 2019; McDonald 2001). CSF OCB number and IgG index can be followed over time to monitor drug

response, however this is not done in routine practice. While a few studies have examined OCB number and IgG antibody (Ab) levels pre- and post-treatment to individual DMTs such as natalizumab and rituximab, no studies have compared these biological markers pre- and post-treatment across different drugs (Cross 2006; Stüve 2009; Villar 2015). In addition to the aforementioned biomarkers, other soluble molecules are being investigated for their role as predictive, diagnostic, disease activity, and/or treatment-response biomarkers. These are categorized into exploratory and validated biomarkers (i.e., biomarkers with high likelihood of clinical utility) (Comabella 2014; Rotstein 2019).

1.6.1 Neurofilament Light Chain (NfL)

With regards to emerging biomarkers, NfL has become the frontrunner for potential employment in clinical practice. Neurofilaments are cytoskeletal components of neurons that provide structural support and maintain the size, shape, and integrity of axons (Varhaug 2019). Neurofilament subunits are released into the CSF during neuroinflammatory and neurodegenerative processes. While not specific to MS, CSF neurofilament levels provide an indication of axonal and neuronal death, and can subsequently be used as a diagnostic, disease activity, and treatment response biomarker in MS. Importantly, the levels of CSF NfL increase naturally as we age, primarily thought to be due to age-related neuronal degeneration, so CSF NfL measurements are compared against standardized age-matched healthy controls (Varhaug 2019). Retrospective analyses have shown that CSF NfL can be used as a predictor of patients with CIS that will eventually develop clinically definite MS up to six years prior to clinical diagnosis (Varhaug 2019). Patients with RRMS or SPMS have demonstrated higher baseline levels of CSF NfL than healthy controls; these levels increase when patients experience a relapse and are correlated to magnetic resonance imaging (MRI) lesion load and disability

scores (i.e., expanded disability status scale (EDSS)) in MS (Varhaug 2019). Furthermore, CSF NfL levels decrease in response to MS treatments such as fingolimod or natalizumab, suggesting a role of NfL as a surrogate endpoint for treatment efficacy (Comabella 2014).

The seminal meta-analysis on CSF NfL by Martin et al. 2019 summarized the results of five studies comparing CSF NfL concentration in RRMS patients versus the CSF NfL concentration in non-inflammatory neurological disease controls (Martin 2019). This analysis demonstrated statistically significant higher CSF NfL concentrations in four of the five included studies, with overall forest plot significance ($p<0.0001$) (Martin 2019). Additionally, this meta-analysis illustrated that CSF NfL levels were higher in all subtypes of MS compared with both healthy and neurological disease controls and that CSF NfL levels correlate most closely with inflammatory disease activity (i.e., levels higher in RRMS patients experiencing an acute relapse versus those in remission). This analysis proved that treatment with a high efficacy DMT such as natalizumab was associated with significant reductions in CSF NfL concentrations post-treatment, irrespective of clinical course and relapse rate (Martin 2019). Despite the significance of this work, this analysis was not able to compare CSF NfL concentrations in RRMS patients across different DMT categories.

A key characteristic for a practical biomarker includes how accessible it is. As a lumbar puncture (LP) is an invasive procedure, serial CSF NfL measurements are not practical for most patients with MS or their care providers. Recognizing this limitation, NfL is present at several times lower concentration (pg/ml versus ng/ml) in the peripheral blood compared to the CSF, as a result of leakage or diffusion through the blood-brain barrier (BBB). Using the single molecule array technology (Simoa®), NfL can be measured in the blood at a sensitivity one-hundred twenty-six times that of traditional enzyme-linked immunosorbent assays (ELISAs) in

both serum and plasma samples (approximately 10% lower concentration in plasma samples as compared to serum) (Varhaug 2019). Several studies have confirmed that serum and plasma NfL levels correlate well with CSF NfL across baseline, disease progression, and treatment response parameters (Disanto 2017; Mattsson 2017; Preische 2019).

Serum NfL levels have been shown to be significantly higher in MS patients as compared to healthy controls, and these levels in patients with MS correlate with radiological and clinical markers of disease activity (i.e., MRI T1-weighted enhancing lesions and T2-weighted lesion load in brain and spinal cord; annualized relapse rate and EDSS) (Disanto 2017; Kuhle 2016). Specifically, there is a clear association between serum NfL concentrations and focal active inflammatory (enhancing) T1-weighted MRI lesions. Those patients with CIS or RRMS who have experienced a recent relapse or disease progression (as evidenced by increase in EDSS) have also shown higher serum NfL levels than healthy controls and those MS patients in remission, and these same patients are also more likely to develop a further relapse or EDSS progression within the following year (Disanto 2017; Disanto 2016; Varhaug 2018). This indicates the utility of serum NfL as a surrogate marker of recent neuronal damage, and the potential clinical use in the early identification of disease activity in the absence of clinical and radiological evidence. The increase in CSF NfL levels as we age is similarly seen in serum NfL levels in healthy controls and patients with all MS subtypes, highlighting the utility of serum NfL as a surrogate for CSF NfL measurements (Thebault 2022). Other studies examining serum NfL concentrations in neurological disorders such as amyotrophic lateral sclerosis (ALS) and Alzheimer's disease have demonstrated a close association between increased serum NfL concentrations and disease activity, suggesting that serum NfL reflects ongoing neuronal damage, regardless of the underlying disease pathogenesis (Disanto 2017; Thebault 2020).

Similar to the decrease in CSF NfL seen in response to fingolimod or natalizumab, serum NfL levels have been shown to decrease in response to DMT, supporting the role of serum NfL as a biomarker for DMT responsiveness (Comabella 2014; Varhaug 2018; Piehl 2017).

Serum NfL levels that have been collected within five years of MS disease onset have been shown to correlate well with long-term (10 years) radiological markers (T2-weighted lesion volume and whole brain atrophy) (Chitnis 2018b). Separate prospective analysis further demonstrated that serum NfL levels were positively associated with EDSS values and transition to SPMS (Thebault 2020). In this study, baseline values greater than 7.62 pg/mL predicted development of EDSS $\geq$ 4.0 and whether a patient would develop progressive MS over the fifteen-year follow-up period (Thebault 2020). The EDSS value of 4.0 was chosen in this study, as previous research has demonstrated that once patients reach an EDSS of 4.0, regardless of prior relapses and previous rate of disability progression, further disability progression occurs in a relatively uniform fashion (Confavreux 2000). Specifically, patients with levels < 7.62 pg/mL were 4.2 times less likely to develop an EDSS score of $\geq$ 4 and 7.1 times less likely to be clinically noted to have developed progressive MS (Thebault 2020). This value is similar to the < 8 pg/mL value that was identified by another group when examining MS patients for "No Evidence of Disease Activity" (NEDA-3) following alemtuzumab (anti-CD52 DMT) induction therapy (Banwell 2013). NEDA-3 is the most commonly used iteration of NEDA, and this iteration includes no evidence of clinical relapse activity, disability progression (increase in EDSS), or new and/or enlarging T2 and/or T1 gadolinium-enhancing lesions measured over the first 1-2 years on DMT (Rotstein 2022). Thus, serum NfL could be utilized in practice as a sensitive predictive measure of those patients least likely to progress in the long-term, as well as a potential disease worsening and treatment response biomarker.

1.6.2 Glial Fibrillary Acidic Protein

Glial fibrillary acid protein (GFAP), expressed only in mature astrocytes in the CNS, is an intermediate monomer filament protein (approximately 8-9 nm in length), which represents reactive hyperplasia (astrocytosis) of astrocytes following CNS tissue injury and aging (Madeddu 2013). In recent years, GFAP has emerged as a potential CSF biomarker for several neurodegenerative conditions, including MS, due to its release into the CSF and serum following axonal degeneration and astrogliosis (Storoni 2012). In MS, demyelination and subsequent axonal degeneration and death is caused by a complex interaction of immune cell infiltration into the CNS (CD4+/CD8+ T cells, B cells, macrophages), microglia activation, iron accumulation and mitochondrial dysfunction (Huss 2020). GFAP concentrations have been shown to be elevated in the CSF of MS patients when compared to healthy controls, and this increase has been linked to disability progression and irreversible axonal damage (Petzold 2002; Rosengren 1995). As attaining CSF samples via LP is an invasive procedure, further studies have investigated the utility of measuring GFAP in the serum of MS patients as a potential biomarker of disease progression and have found significant elevations in GFAP levels in those with MS compared to healthy controls (Abdelhak 2018). As serum GFAP has been suggested as a marker of disease progression in MS, subsequent analysis have related serum GFAP levels with EDSS scores and have utilized this to differentiate inflammatory (CIS/RRMS/relapsing-SPMS) from progressive forms (non-relapsing SPMS/PPMS) of MS (Ayrignac 2020). Therefore, serum GFAP is another easily accessible potential biomarker for early detection of disease progression in MS.

In a meta-analysis of CSF and serum GFAP studies in MS, CSF, and blood GFAP were found to be higher in patients with all subtypes of MS than in healthy and disease controls (Sun

2021). In this study, CSF GFAP levels were significantly different between RRMS patients and healthy controls, as well as those RRMS patients in remission and experiencing a relapse (Sun 2021). Importantly, this study demonstrated a significant difference in the CSF GFAP concentrations between progressive MS patients and healthy controls, and between those patients with RRMS and those in the progressive phase of the disease (Sun 2021). As repeat CSF sampling is invasive, this meta-analysis also reviewed studies that examined serum GFAP levels to determine if the differences seen in CSF GFAP were mirrored by serum GFAP concentrations in these same groups.

While the results of this meta-analysis demonstrated a significantly higher concentration of GFAP in the serum of MS patients (all subtypes) compared to healthy controls, there was no significant difference seen between patients with RRMS specifically, and healthy controls (Sun 2021). Additionally, the levels of serum GFAP were significantly higher in those patients with PPMS versus those with RRMS, indicating that CSF and serum GFAP can potentially accurately differentiate MS subtypes (Sun 2021). CSF and serum GFAP have thus been proposed as a biomarker to identify present disease progression and to prognosticate progression independent of relapse activity (PIRA), an important unmet need as disability worsening often continues despite near complete suppression of acute disease activity under current high-efficacy therapies (Sun 2021; Sellebjerg 2009). In the near future, serum NfL and GFAP may be combined and implemented in routine clinical practice as a means of monitoring acute/relapsing disease activity and PIRA. This could potentially offer MS clinicians and neurologists a means for prognostication, early detection of relapse activity in MS patients that appear to have "quiescent" disease, monitor for potential signs of disease progression (i.e., switch from RRMS to SPMS), and another means to assess DMT responsiveness.

In addition to CSF and serum NfL and GFAP, several other proteins have been found to be present at increased concentrations in the CSF of MS patients with active disease, including: lymphoid chemokine CXC Motif Chemokine Ligand 13 (CXCL13), Myelin Basic Protein (MBP) and Secreted Phosphoprotein 1 (SPP1) (Khademi 2011; Lamers 1998; Comabella 2005). Additionally, the glycoside hydrolase protein Chitinase 3-like 1 (CHI3L1) is elevated in the CSF of patients with CIS who later go on to develop RRMS, as compared to those patients who do not convert (Comabella 2010).

1.6.3 CXC Motif Chemokine Ligand 13

CXCL13, originally identified as a B-cell chemoattractant, has important functions in lymphoid neogenesis, and has been implicated in the pathogenesis of MS (DiSano 2020). CSF analysis of MS patients has demonstrated increased concentrations of CXCL13 intrathecally, with these values providing useful diagnostic and prognostic information. Furthermore, in healthy and non-inflammatory neurological disease (NIND) controls, CXCL13 is produced in the periphery, but not intrathecally (DiSano 2020). In a seminal analysis by DiSano and colleagues (2020), they quantified intrathecal synthesis of CXCL13 and produced the CXCL13 index (I_{CXCL13}), similar to how IgG index is assessed and corrects for differences in serum and blood-CSF barrier integrity between MS patients (DiSano 2020). In this study, serum, and CSF CXCL13 concentrations, as well as Q_{CXCL13} (CSF/serum ratio) values, were significantly elevated in MS patients compared to NIND controls. Importantly, the I_{CXCL13} was calculated to correct for albumin variability between MS patients, and this was shown to be significantly elevated in MS patients when compared to NIND controls as well, demonstrating that CXCL13 is intrathecally produced in MS patients (DiSano 2020). I_{CXCL13} was shown to be the best predictor of future disease activity, with higher specificity and sensitivity than OCBs and CSF

NfL, in both CIS and clinically definite MS patients. With this said, the highest values for sensitivity, specificity, positive and negative predictive values, were seen when I_{CXCL13} was combined with CSF NfL concentrations (DiSano 2020).

1.6.4 Chitinase 3-Like 1

Chitinase 3-like 1 (CHI3L1) is a member of the chitin glycoside hydrolase 18 family of proteins produced by macrophages and astrocytes (Floro 2022). In a recent systematic review and meta-analysis on the role of CHI3L1 protein as a biomarker in MS, CSF CHI3L1 concentrations were found to be statistically significantly higher in patients with clinically definite MS versus healthy controls, even when accounting for the differences in age between the MS and healthy control groups (Floro 2022). In this analysis, CSF CHI3L1 levels were significantly higher in CIS patients who later converted to clinically definite MS compared to those who did not, and while concentrations were significantly higher in PPMS patients versus those with RRMS, this difference was not seen in SPMS patients (Floro 2022). This finding further suggests that the increased CSF concentrations of CHI3L1 seen in MS patients may be due to predominant intrathecal production of CHI3L1 in the more chronic, progressive phase of the disease, that while present in early stages of MS pathogenesis, predominates in the PPMS subtype (Floro 2022).

1.6.5 Myelin Basic Protein and Secreted Phosphoprotein 1

Myelin basic protein (MBP) is the second most abundant protein in myelin, making up approximately 30% of all myelin protein, and its detection in the CSF is a marker of myelin degeneration (Martinsen 2022). Previous research on antibody production against MBP did not demarcate a clear association between anti-MBP antibodies and progression to clinically definite MS (Kuhle 2007). Further, while MBP and its components have shown increased concentrations

in the CSF of MS patients experiencing an acute relapse, there currently appears to be little diagnostic value.

Osteopontin, also known as early T cell-activation gene 1 or secreted phosphoprotein 1 (SPP1), acts a proinflammatory cytokine in neuromyelitis optica spectrum disorder (NMOSD) and MS (Orsi 2021). SPP1 has been implicated in the neuroinflammatory and neurodegenerative components of MS pathogenesis. It is produced by T and B cells, macrophages, dendritic cells, and natural killer cells, and has been shown to induce the proinflammatory Th17 cell subset that is implicated in MS pathogenesis (Orsi 2021). Regarding the neurodegenerative component of MS pathogenesis, SPP1 is secreted into the extracellular matrix by microglia, activating and recruiting macrophages and other cells that assist in modulating an inflammatory response (Orsi 2021). SPP1 has thus been examined as a potential biomarker in MS, with a recent meta-analysis demonstrating statistically significant elevations in the CSF and serum of MS patients (relatively higher in CSF) when compared to controls, with the highest CSF concentrations seen in RRMS patients experiencing an acute relapse (Agah 2018).

1.7 Chemokines and Chemokine Receptors

Chemokines, cytokines and their receptors have critical roles in the induction, maintenance, and resolution of inflammatory processes throughout the body (Blandford 2023; Raman 2011). Classification of chemokines is completed via their function and expression, or via the cysteine residues of their ligands, (CC, CXC, C, and CX3C), with the CXC family of chemokines having one additional amino acid between the first two cysteine residues (Nomiyama 2011). Chemokines and their respective receptors are key mediators in the recruitment of immune cells (CD4+, CD8+, CD14+, CD19+, CD56+) to inflammatory sites (Maghazachi 2003). Chemokines and chemokine receptors play an important role in the

pathophysiological processes underpinning MS, and are expressed by neurons, astrocytes, and oligodendrocytes (Cui 2020). In MS it has been shown that there is shift to a proinflammatory milieu of chemokine/chemokine receptors in T cells, which have the capability of recruiting inflammatory cells into the CNS, leading to inflammation and degeneration (Cui 2020; Karpus 2020).

The CXCR3 chemokine receptor is expressed on lymphocytes is a crucial mediator of T cell migration and function (Dhaiban 2020). CXCR3 binds gamma interferon-inducible chemokines including CXCL9, CXCL10, and CXCL11 (Dhaiban 2020). CXCR3 expression has been shown to be upregulated on peripheral CD4+ lymphocytes in MS patients during an acute demyelinating relapse (Balashov 1999). Several studies have quantified the expression of CXCR3 on peripheral and CSF T cells using flow cytometry, albeit with conflicting results (Teleshova 2002; Sørensen 2002; Matsui 2005). One study found higher concentrations of CXCR3+ T cells in peripheral and CSF T cells compared to non-inflammatory neurological disease (NIND) controls, with a higher proportion of CXCR3+ T cells in the CSF compared to the peripheral compartment (Teleshova 2002). This finding suggests that CXCR3, and its ligand CXCL10, are an important mediators of T cell trafficking into the CNS (Teleshova 2002; Blandford 2023). In another analysis, while the proportion of CD4+ and CD8+ T cells expressing CXCR3 in the CSF was found to be higher than in blood, no difference was seen in the concentrations of CXCR3+ T cells between patients with MS and NIND controls (Sørensen 2002; Blandford 2023). Furthermore, another study did document a significantly elevated percentage of CD4+CXCR3+ cells in the blood of patient with active relapsing MS (Matsui 2005).

1.8 Purpose

The primary purpose of this combined retrospective and prospective, longitudinal comparative cohort study was to determine if plasma NfL, GFAP, and CXCL13 levels are viable indicators of RRMS disease activity and disease progression and to determine their association with relevant plasma immune cell subsets.

1.9 Research Question and Hypotheses

In adults (18 years and older) in NL, Canada, with clinically definite RRMS (Revised 2017 McDonald criteria (Appendix B), does the implementation of an "early-intensive" therapeutic approach with highly efficacious DMTs result in (1) lower plasma NfL concentrations; (2) lower plasma GFAP concentrations; and (3) lower plasma CXCL13 concentrations compared to treatment with a "treat-to-target" approach with moderately efficacious DMTs?

The central hypothesis of this study is that adult NL patients with RRMS who receive an "early intensive" therapeutic approach with highly efficacious DMTs will have significantly lower plasma NfL and CXCL13 concentrations than those adult RRMS patients receiving the "treat-to-target" therapeutic approach with moderately efficacious DMTs. Furthermore, this study hypothesizes that there will be no statistically significant difference in plasma GFAP concentrations between RRMS patient cohorts. Given that serum GFAP has been suggested as a marker of disease progression in MS, we would not expect the one-year follow-up period to capture clinical disease progression in our cohort. In addition to the plasma biomarker concentrations, we posit that the concentrations (normalized values to total PBMC's) of the immune cell subsets: 1.CD45+ 2.CD3+ 3.CD4+ 4.CD8+ 5.CD14+ 6.CD19+ 7.CD56+ 8.CD4+CXCR3+ 9.CD8+CXCR3+ 10.CD14+CXCR3+ 11. CD19+CXCR3+ 12.

CD56+CXCR3+ will be significantly lower in patients with RRMS who receive the "early intensive" therapeutic approach with highly efficacious DMTs compared to those RRMS patients who receive moderate efficacy DMT.

1.10 Outcome Measurements

The primary outcome to be compared among the "early intensive" highly efficacious treatment group and the "treat-to-target" moderately efficacious treatment group will be the plasma concentrations of NfL and GFAP. NfL is present at lower concentrations in the peripheral blood as a result of leakage or diffusion through the BBB. Using the Simoa® assay, NfL can be measured in the plasma at a much higher sensitivity than with traditional ELISA. Plasma NfL samples were shipped on dry ice out of NL to the research laboratory of Dr. Raphael Schneider to be analyzed via the Simoa® assay machine. Secondary outcomes for this research include CXCL13 and plasma concentrations; change in concentrations of the immune cell subsets: 1.CD45+ 2.CD3+ 3.CD4+ 4.CD8+ 5.CD14+ 6.CD19+ 7.CD56+ 8.CD4+CXCR3+ 9.CD8+CXCR3+ 10.CD14+CXCR3+ 11.CD19+CXCR3+ 12. CD56+CXCR3+.

CHAPTER 2

2. Methods

2.1 Co-Authorship Statement

The author would like to acknowledge that Neva Fudge (Research Assistant in Dr. Craig Moore Neuroscience Laboratory) made major contributions to the methods section of this paper for sections 2.5 Peripheral PBMC Immune Phenotyping using Flow Cytometry, 2.6 Quantification of pro-inflammatory cytokines using Simoa® technology, and 2.7 Quantification of CXCL13 using ELISA.

2.2 Eligibility Criteria and Study Design

The population of interest in this study were adults aged 18 years and older in Newfoundland and Labrador, Canada, with clinically definite RRMS, as defined by the revised 2017 McDonald diagnostic criteria (Appendix B). This study was a single center combined retrospective and prospective, longitudinal comparative cohort study that took place at the Health Sciences Centre in St. John's, NL from September 2020 to December 2022. Inclusion criteria for this study required participants to have a baseline EDSS score of 0-5.5, a diagnosis of RRMS in accordance with the revised 2017 McDonald Criteria, and the ability to perform the Timed 25-Foot Walk Test (T25FWT) (Appendix D). Specific exclusion criteria included a diagnosis of PPMS or SPMS at screening, a known diagnosis of HIV, hepatitis B/C, active or latent tuberculosis, progressive multifocal leukoencephalopathy, severe renal or hepatic disease, or significantly impaired bone marrow function or significant anemia, leukopenia, neutropenia, or thrombocytopenia. Furthermore, participants with any comorbid disease requiring chronic treatment with systemic corticosteroids/immunosuppressants during the study period were excluded, as well as those with any previous treatment with immunosuppressive medication

without an appropriate washout period prior to study enrollment. Every effort was made to match the participants in each group by age, sex, EDSS, time from last clinical demyelinating relapse, and MRI activity. This was an active-comparator group study, so those participants in the control group were treated with moderately efficacious DMT's including teriflunomide (n=6), glatiramer acetate (n=1), and dimethyl fumarate (n=2). These patients constituted the "treat-to-target" therapeutic approach cohort. Study participants in the intervention group were all on highly efficacious DMT's including cladribine (n=4), ofatumumab (n=6), natalizumab (n=1), and ocrelizumab (n=1). These patients constituted the "early intensive" therapeutic approach cohort. The primary outcomes of interest for this study were the plasma concentrations of NfL and GFAP. The secondary outcomes consisted of the plasma concentrations of CXCL13 and the change in concentrations of the immune cell subsets.

2.3 Sample Size Calculation

A power analysis was utilized to estimate the sample size needed to test for the difference in concentration of plasma NfL (primary outcome) in RRMS patients who receive the "treat-to- target" therapeutic approach with moderately efficacious DMTs or the "early intensive" therapeutic approach with highly efficacious DMTs. According to the seminal meta-analysis on serum NfL by Disanto et al. 2017, the median serum NfL concentration was 35.9 pg/mL in the Lugano cohort, and this was approximately 42 times lower than the CSF NfL concentrations (1,521.1pg/mL) for the MS patients (Disanto 2017). In this portion of the study, most of the MS cohort consisted of patients with CIS or RRMS (11.3% PPMS; 2.1% SPMS; 9.1% RIS). There was a strong positive association between CSF NfL and serum NfL levels, with a 10% increase in CSF leading to concomitant 5.9% increase in serum NfL. Furthermore, an additional MS cohort, the Swiss Multiple Sclerosis Cohort (SMSC) had a median serum

NfL level of 29.4 pg/ml (Disanto 2017). As was the case for the Lugano cohort analysis, the serum NfL levels were positively associated with age, there was no sex association, and storage time was not significantly associated with serum NfL levels once corrected for age. In addition to this, the disease duration was significantly associated with serum NfL, and this association disappeared once corrected for age, suggesting that disease duration could be utilized as a proxy for age (Disanto 2017). In the SMSC cohort, the median value for serum NfL for both CIS/RRMS was 27.2 pg/mL with an interquartile range (IQR) of 19.2–57.2 pg/ml. In this cohort, the median value for serum NfL for both SPMS/PPMS was 41.4 pg/mL with an interquartile range (IQR) of 32.1–57.2 pg/mL.

In 2017, Disanto and colleagues produced a distribution of serum NfL across different ages with 80th, 90th, 95th, 97.5th, and 99th serum NfL percentiles for each age group (30-70 years in 5-year increments) for healthy controls, allowing for age-matched stratifications. The 80th percentile for healthy controls at ages 40 and 45 were 26.0 pg/mL and 29.1 pg/mL, respectively. In our patient cohort the median age for the “treat-to-target” DMT group was 44.2 years, and 40.3 years for the “early intensive” DMT group. Other studies have examined the correlation between serum and plasma NfL, finding a high concordance between the two, albeit with plasma NfL approximately 23% lower than that seen in serum (Sejbaek 2019).

Further prior analysis of serum NfL have found that baseline serum NfL concentrations are associated with long term clinical disease progression, and that it may serve as a biomarker of subsequent poor clinical outcomes (Thebault 2020). In this cohort, median serum NfL concentrations in all (recent relapse and no recent relapse) RRMS patient baseline samples were 10.06 pg/mL, with an interquartile range (IQR) of 7.61 pg/mL (Thebault 2022). These values were 8.5% higher than the median levels in healthy controls (7.26 pg/mL w/ IQR of

4.62 pg/mL) (Thebault 2020). As our study had an active comparator group to examine changes in plasma NfL in response to DMT over time, we used the median and IQR values of baseline RRMS patients, along with the 38.5% relative difference seen with controls by Thebault 2020, to calculate our sample size. Median and IQR were used in sample size prediction, as these data are not normally distributed. Implementing a power of 90% and increasing the value of percent difference to 40%, a sample size of n=17 was calculated at α=0.05. In other words, with a total of 17 patients between the two groups, there would be a 90% chance of detecting a statistically significant difference in plasma NfL levels between RRMS patients on moderate versus high efficacy DMT.

2.4 Sampling Plan and Recruitment

Every potential RRMS patient meeting the inclusion criteria was eligible to participate in the study (n=21). All potential study participants were provided a detailed explanation of the study including the significance and future implications of the research. RRMS patients were recruited into this research study through two pathways:

2.4.1 Pathway A

RRMS patients meeting the research study eligibility criteria who were previously enrolled into the neurology clinic research database for MS research, were contacted by phone (these patients already provided consent to be contacted in the future) and asked if they could return for repeat blood draw. These patients were identified through linking de-identified data in our study database, with personal participant information provided via their consent forms kept in storage in the neuroimmunology laboratory. Many patients, for the purposes of our study, were identified in this retrospective manner, as having clinically definite RRMS. It was through this retrospective analysis that all patient data such as clinic notes, EDSS, and specific

DMT, was garnered. All attempts were made to recruit only those RRMS patients who were approximately one-year post-initiation of their respective DMT. It should be noted that participants recruited this pathway who were initially on moderately efficacious DMT but were then switched to highly efficacious DMT were still eligible (baseline samples provided without any drug on board) if an appropriate washout time interval between the medication change was followed (patients verified as having recovered their lymphocyte counts) prior to beginning treatment with the drug of interest. Furthermore, in those study participants who switched DMT category, the one-year timeline for follow-up plasma samples was based upon the DMT category into which they switched (one year from start of new medication).

2.4.2 Pathway B

RRMS patients meeting the research study eligibility criteria who were not previously enrolled into the neurology clinic research database for MS research, were recruited directly at their clinic appointments. A thorough history and clinical neurological examination is conducted on a patient's first visit to these clinics and the neurologist then orders appropriate bloodwork, including MS mimic studies (diseases that can mimic the clinical picture of MS include NMOSD and MOGAD). Further to this, the neurologist will typically order a T1/T2-weighted MRI of a patient's brain (MRI Head with Gd), and when clinically indicated, of their spine (MRI spine with Gd). If this information is equivocal, then a patient requires a LP to assess the CSF IgG index level and whether OCBs are present in the CSF. It was during these clinic visits for patients with a suspect diagnosis of RRMS, that dissemination of the research study information occurred. As a result of this temporal relationship, it was inevitable that some potential study participants were subsequently excluded, as they were diagnosed with a different pathology based upon their CSF analysis. As was the case with participants recruited

via pathway A, and as the principal investigator (PI) was not involved in recruiting all patients in pathway B directly, these patients were identified through linking de-identified data in our study database, with personal participant information provided via their consent forms kept in storage in the neuroimmunology laboratory. Several patients recruited in this pathway were identified in this retrospective manner as having clinically definite RRMS. Once these patients were identified, either directly by the PI through the clinic or retrospectively, all patient data such as clinic notes, EDSS, and specific DMT was analyzed.

2.5 Blood Collection

Approximately 20mL of blood was collected in EDTA tubes by nursing staff at pre-and post-treatment clinic visits. This blood was processed, plasma analyzed for NfL, CXCL13 concentrations, and Peripheral Blood Mononuclear Cells (PBMCs) were cryopreserved. Plasma samples were shipped on dry ice out of province to a research laboratory equipped with a Simoa® assay machine to perform plasma NfL and GFAP analysis.

2.6 Peripheral PBMC Immune Phenotyping using Flow Cytometry

500,000 PBMCs were centrifuged at 300g for 10 minutes and the supernatant decanted. The cells were resuspended in 100uL of flow buffer (1% bovine albumin serum, 2mM EDTA, 2mM sodium azide in PBS). The PBMC cell suspension was added to a DURAclone IM Phenotyping BASIC tube (Beckman Coulter, B53309), mixed and incubated at 4°C for 30 minutes. The cells were washed with 4mL flow buffer, centrifuged at 300g for 10 minutes, decanted and resuspended in 100micolitres 2% paraformaldehyde. The data was acquired using the Cytoflex flow cytometer (Beckman Coulter). CD45+, CD3+, CD4+, CD8+, CD56+, CD14+, CD19+, CD4+CXCR3+, CD8+CXCR3+, CD14+CXCR3+,

CD19+CXCR3+, and CD56+CXCR3+ immune cells were quantified using FlowJo software (Figure 2.1).

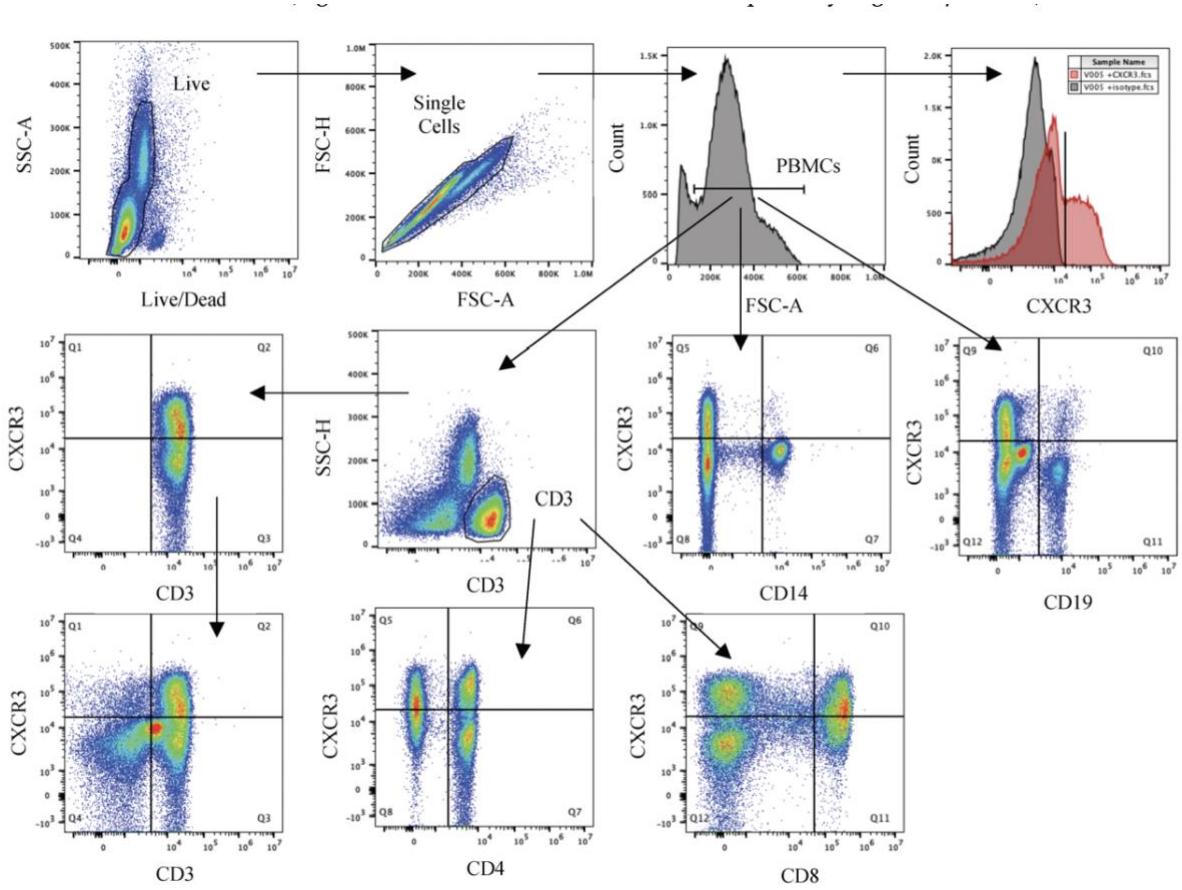

Figure 2.1. Peripheral PBMC gating strategy. Live cells were selected based on staining with a Live/Dead stain, then single cells based on FSC grouping. PBMCs were gated from the background using FSC-A. From the PBMC population, CXCR3 positive staining was identified using a cut-off based on comparing antibody staining (red) to its isotype (grey). CD3+ cells were selected from the PBMC population by gating using CD3 and SSC—H, and then split into CD4+ and CD8+ subpopulations. CD14+ monocytes and CD19+ B cells were gated from the whole PBMC populations using positive staining.

2.7 Quantification of Plasma NfL and GFAP using Simoa® technology

Human plasma was shipped to the Schneider laboratory at the Li Ka Shing Knowledge Institute affiliated with St. Michael's Hospital, the Keenan Research Centre for Biomedical Science, and the University of Toronto, to quantify NfL and GFAP using the Simoa® bead technology. This technology utilizes ultra-specific magnetic beads to isolate single copies of the protein of interest, label them with fluorescent tags and quantify them in your sample.

2.8 Quantification of CXCL13 using ELISA

A CXCL13 Solid Phase sandwich ELISA kit (R&D systems) was used to quantify CXCL13 in undiluted human plasma as per manufacturer's instructions. In brief, 96 well plates were coated with CXCL13-specific antibodies. Plasma samples and known standards were incubated on the plate and the CXCL13 proteins were captured/HRP tagged. The absorbance and subsequent CXCL13 levels were detected/quantified using a BioTek Cytation 5 imaging system and Gen5 software.

2.9 Quantification of CSF NfL

CSF NfL was measured in the laboratory of Dr. Craig Moore at Memorial University of Newfoundland by a commercially available ELISA (Quanterix Corporation) according to manufacturer's instructions.

2.10 EDSS

EDSS (Appendix C) pre-treatment scores were calculated by clinical neurologists. Those patients recruited into this research study from prior enrollment in either the Innate and Adaptive Immune Cell Mechanisms in Multiple Sclerosis Study or the HITMS study (Pathway

A), had baseline EDSS scores already calculated. The PI gained access to these EDSS scores through retrospective analysis of the patient's electronic medical record (MediTech). Patients enrolled via pathway A continued to follow-up with their own neurologist, who subsequently calculated their follow-up EDSS scores. Patients enrolled via Pathway B (newly diagnosed RRMS patients not previously enrolled in either research study) had their baseline EDSS scores calculated by their own neurologist.

2.11 Statistical Analysis

Statistical analyses were conducted using Prism 10 (GraphPad Software Inc, Boston, MA, USA). The Mann-Whitney U test was implemented as a non-parametric test to measure the difference in baseline CSF and plasma NfL between moderate and high-efficacy groups. The Mann-Whitney U test was also used to assess for any significant differences in baseline plasma GFAP and CXCL13 levels between the moderate and high-efficacy groups. A non-parametric two-sided Spearman rank correlation was used to assess the correlation between baseline plasma and CSF NfL, as well as to assess the correlation between baseline plasma NfL and plasma GFAP and CXCL13. Furthermore, non-parametric Spearman correlation was implemented to assess the baseline (no DMT onboard) relationship between plasma NfL and all immune cell subsets (CD45+, CD3+, CD4+, CD8+, CD14+, CD19+, CD56+, CD4+CXCR3+, CD8+CXCR3+, CD14+CXCR3+, CD19+CXCR3+, and CD56+CXCR3+). Further baseline analysis included examination of the relationship between time from last clinical demyelinating relapse and both plasma biomarkers and immune cell subsets using non-parametric spearman correlation. One patient within this cohort represented an outlier (i.e., time from relapse of 37 months), and given the potential significant confounding effects on the data, this patient was

removed from this analysis, as well as from subsequent analysis of time from relapse versus baseline normalized plasma immune cell subset concentration.

The Wilcoxon matched pairs signed rank test was performed for each immune cell subset for both the moderate-efficacy DMT and high-efficacy DMT groups, to assess for significant changes in these individual immune cells in response to DMT. The Mann-Whitney U test was then be used to determine if there are any significant differences in the changes in the measured plasma immune cell subsets and plasma biomarkers (NfL, GFAP, CXCL13) between the moderate and high-efficacy DMT groups. Furthermore, to assess for any significant correlations between the change (i.e., delta) in plasma biomarkers and change in immune cell subsets in response to DMT, a two-sided spearman rank correlation was conducted for every delta immune cell subset against each delta plasma biomarker. Lastly, ANCOVA analysis of the relationship between delta plasma biomarkers and immune cell subsets between groups was conducted to determine if DMT influenced plasma concentrations of these biomarkers, immune cell subsets, and their relationship to one another.

Given that the number of patients in each group were low and there were multiple comparisons made, it was necessary to conduct a Bonferroni correction for each statistical test. The Bonferroni correction was only necessary when analyzing and comparing plasma biomarker concentrations to plasma immune cell subsets, as this was an exploratory analysis. There were 39 comparisons when employing the Mann-Whitney U test and Wilcoxon matched pairs rank test so the Bonferroni correction would be $p=0.05/(39-1)=0.0013$. As there were 165 correlations conducted, for any Spearman correlation calculations, the Bonferroni correction would be $p=0.05/(165-1)=0.0003$.

2.12 Ethical Considerations

Informed consent for inclusion in this research study was appropriately attained for all study participants. The MS research nurse (Lillian McGrath) disseminated the details of the research study to patients and the author reviewed the information in the handout with the patients during their clinic visits. It was explained to patients that this research study is a part of the larger "Innate & Adaptive Immune Cell Mechanisms in Multiple Sclerosis" study (Appendix F). In addition to this, either the MS research nurse, author or staff neurologists indicated to eligible patients that their agreement or refusal to participate in the study would not have an impact on their care. It was emphasized that all study participants would receive the same level of care that other patients with MS who were not enrolled in the study were receiving. No monetary incentives were offered to patients for participating in this study.

2.13 Data Collection, Protection, and Storage

Once patients provided written informed consent to participate in the study, their consent form was immediately transferred to the research office of Dr. Craig Moore. These forms contain the patient's name and signature and were kept in an appropriately marked binder in a locked filing cabinet, to which only Dr. Craig Moore, the PI, and relevant laboratory staff had access. Each study participant was assigned a number corresponding to their temporal addition into the study (i.e., the first individual to be recruited into the study was identified as patient 1). Dr. Craig Moore created the Innate & Adaptive Immune Cell Mechanisms in Multiple Sclerosis study and HITMS study database, from which this research study drew some of its participants. As this research study used baseline CSF and blood samples provided by patients already enrolled in these databases, it was necessary to create a separate encrypted database to eliminate any crossover contamination of information. As such, only the PI, Dr.

Craig Moore and relevant laboratory staff had access to the information in this database. This database was accessible only on the password protected computer in the research laboratory of Dr. Craig Moore. All data, including baseline demographics, concentrations of CSF and plasma biomarkers, and clinical parameters such as EDSS, were entered into this database manually by the PI. At the end of this research study, all patient data will be securely stored for a minimum of five years by the PI and Dr. Craig Moore.

CHAPTER 3

3. Results

3.1 Baseline Demographics

In total, the patient cohort (n=21) included 9 patients in the low-moderate efficacy DMT group and 12 patients in the high-efficacy DMT group. Patients age and sex were matched between the two groups. The mean age for the low-moderate efficacy DMT group is 43.8 years versus 40.3 years for the high-efficacy DMT group (Table 1). In the low-moderate efficacy DMT group, females constitute 77.8% (n=7) and males constitute 22.2% (n=2), and in the high-efficacy DMT group, females constitute 83.3% (n=10) and males constitute 16.7% (n=2) of the cohort. The baseline EDSS in the low-moderate efficacy DMT group was 2.0 with a range of 0 to 2.0 and a standard deviation of 1.05 versus a baseline EDSS of 1.0 with a range of 0 to 2.5 and a standard deviation of 0.73 in the high-efficacy DMT group. In the low-moderate efficacy DMT group 6 patients were ultimately prescribed teriflunomide (n=6; 66.7%), with 1 patient being prescribed glatiramer acetate (n=1; 11.1%) and 2 patients dimethyl fumarate (DMF) (n=2; 22.2%). In the high-efficacy DMT group 4 patients were prescribed cladribine (n=4; 33.3%), 6 patients ofatumumab (n=6; 50%), and 1 patient each natalizumab (n=1; 8.3%) and ocrelizumab (n=1; 8.3%).

It should be noted here that as natalizumab is not an immune cell depleting DMT, like the other DMT's in this group, the results for this patient were removed from immune cell subset analysis and regression analysis between immune cells and biomarkers. With this said, the results for this patient were included in the baseline (pre-DMT) analysis of plasma biomarkers only. Furthermore, each group were matched in terms of relapse activity and MRI activity (defined as any new or enlarging lesions) in the year prior to treatment. In the low-moderate efficacy group, 7 patients (77.8%) had a clinical relapse and MRI activity in the year prior to

initiation of their current DMT. In the high-efficacy group, 9 patients (75%) had a clinical relapse in the year prior to DMT initiation, versus 8 patients (66.7%) demonstrating MRI activity in the year prior to DMT initiation. In the year since DMT initiation, no patients in either group showed any sign of a clinical relapse, with 1 patient in the low-moderate efficacy (11.1%) and high-efficacy (8.3%) groups showing evidence of either a new or enlarging lesion on MRI.

Table 1: Patient Demographics and Clinical Data During the Study Period

Characteristics	Low-Mod Efficacy DMT (n=9)	High-Efficacy DMT (n=12)
Mean age (yrs.)	43.8 (Range: 32-57; Standard deviation: 8.2)	40.3 (Range: 26-56; Standard deviation: 9.0)
Sex (# (%)) Female Male	 7 (77.8%) 2 (22.2%)	 10 (83.3%) 2 (16.7%)
Disease phenotype (%)	RRMS: 9 (100%)	RRMS: 12 (100%)
Baseline Median EDSS	2.0 (Range: 0-2; Standard deviation: 1.05)	1.0 (Range: 0-2.5; Standard deviation: 0.73)
Mean IgG Index	n=4 (88) (Range: 60-123; Standard deviation: 27.6)	n=5 (101) (Range: 64-137; Standard deviation: 23.5)
Specific DMT (# (%))	Teriflunomide (n=6; 66.7%); Glatiramer Acetate (n=1; 11.1%); DMF (n=2; 22.2%)	Cladribine (n=4; 33.3%); Ofatumumab (n=6; 50%); Natalizumab (n=1; 8.3%); Ocrelizumab (n=1; 8.3%)
Relapse in year prior to current treatment (# (%)) Yes No	 7 (77.8%) 2 (22.2%)	 9 (75%) 3 (25%)
MRI activity in year prior to current treatment (# (%)) Yes No	 7 (77.8%) 2 (22.2%)	 8 (66.7%) 4 (33.3%)
Relapse in year since starting current treatment (# (%)) Yes No Unknown	 0 (0%) 8 (88.8%) 1 (11.1%) - completed 8 months treatment only	 0 (0%) 11 (91.7%) 1 (8.3%) - completed 3 months treatment only
MRI activity in year since starting current treatment (# (%)) Yes No Unknown	 1 (11.1%) 8 (88.8%) 1 (11.1%) - completed 8 months treatment only	 1 (8.3%) 10 (83.3%) 1 (8.3%) - completed 3 months treatment only

DMT: disease-modifying therapy; RRMS: relapsing-remitting multiple sclerosis (MS); EDSS: expanded disability status scale; DMF: dimethyl fumarate.

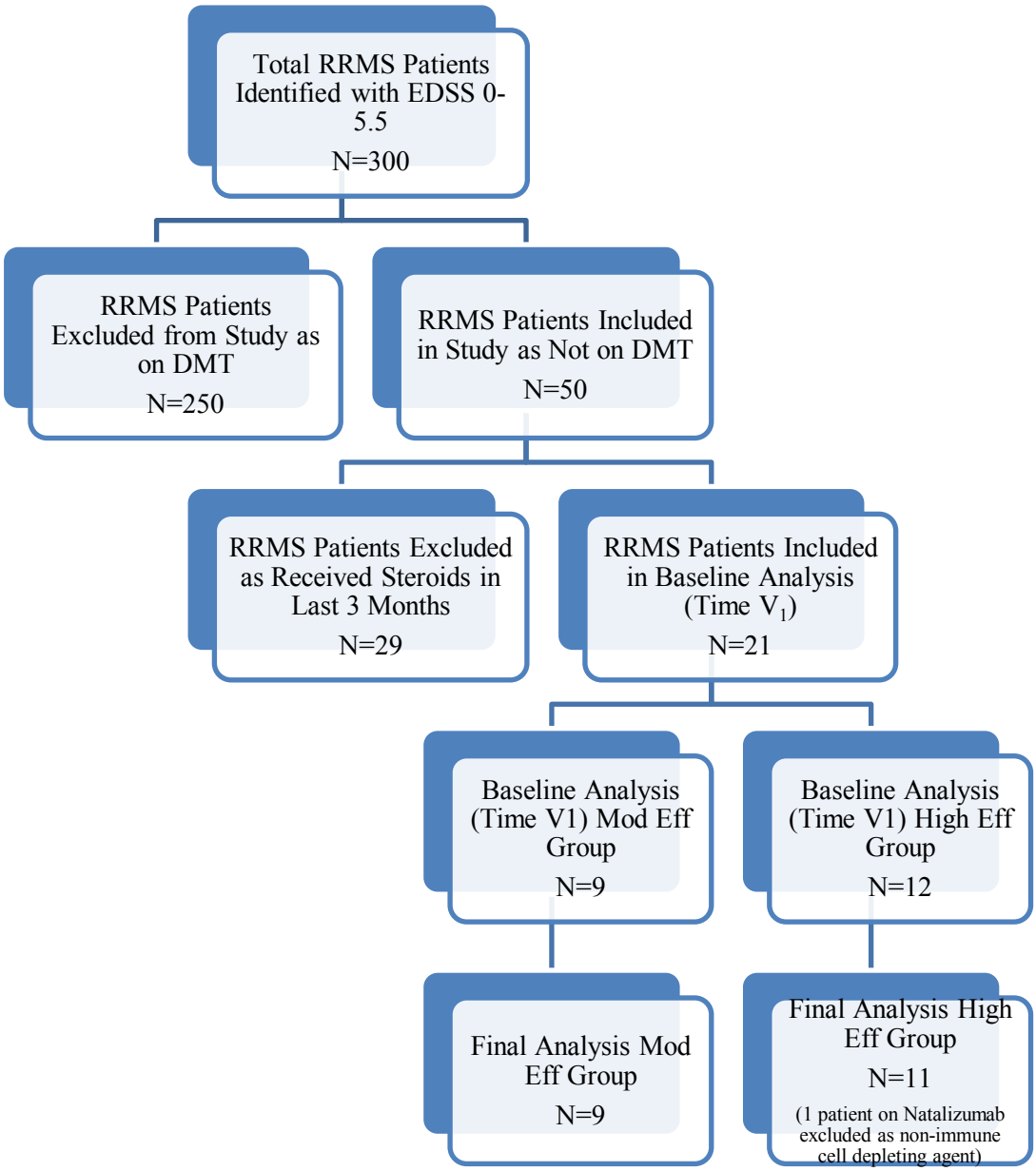

Figure 3.1. Flow chart of patient sampling and recruitment. The population of interest in this study were adults aged 18 years and older in Newfoundland and Labrador, Canada, with clinically definite RRMS, as defined by the revised 2017 McDonald diagnostic criteria (Appendix B). This study was a single center combined retrospective and prospective, longitudinal comparative cohort study that took place at the Health Sciences Centre in St. John's, NL from September 2020 to December 2022. Inclusion criteria for this study required participants to have a baseline EDSS score of 0-5.5, a diagnosis of RRMS in accordance with the revised 2017 McDonald Criteria, and the ability to perform the Timed 25-Foot Walk Test (T25FWT) (Appendix D). Specific exclusion criteria included a diagnosis of PPMS or SPMS at screening, a known diagnosis of HIV, hepatitis B/C, active or latent tuberculosis, progressive multifocal leukoencephalopathy, severe renal or hepatic disease, or significantly impaired bone marrow function or significant anemia, leukopenia, neutropenia, or thrombocytopenia. Furthermore, participants with any comorbid disease requiring chronic treatment with systemic corticosteroids/immunosuppressants during the study period were excluded, as well as those with any previous treatment with immunosuppressive medication without an appropriate washout period prior to study enrollment. The primary outcomes of interest for this study were the plasma concentrations of NfL and GFAP. The secondary outcomes consisted of the plasma concentrations of CXCL13 and the change in concentrations of the immune cell subsets. As the mechanism of action of natalizumab does not result in immune cell depletion like cladribine, ofatumumab, and ocrelizumab, this patient was removed from immune cell subset analysis, but was kept in the baseline biomarker analysis which specifically examined plasma biomarker concentrations between groups.
RRMS = Relapsing-Remitting Multiple Sclerosis; EDSS = Expanded Disability Status Scale; DMT = Disease Modifying Therapy; LP = Lumbar Puncture; High Eff = High Efficacy; Mod Eff = Moderate Efficacy

3.2 Plasma NfL Correlates Positively with CSF NfL Pre-DMT

At time point one, representing the time prior to the initiation of DMT, using the Mann-Whitney U test, the baseline CSF NfL values were found to be significantly different between the two groups ($p=0.0227$) (Figure 3.2A). The Mann-Whitney U test was implemented as a non-parametric test to compare the means of the two sample groups as the data is not normally distributed. Implementing the Mann-Whitney U test at time point one, the plasma NfL levels were not found to be significantly different between the two groups ($p=0.0693$), albeit a trend was observed (Figure 3.2B). Spearman correlation demonstrated statistical significance between baseline CSF and plasma NfL concentrations ($p<0.0001$; $r=0.800$) (Figure 3.2C).

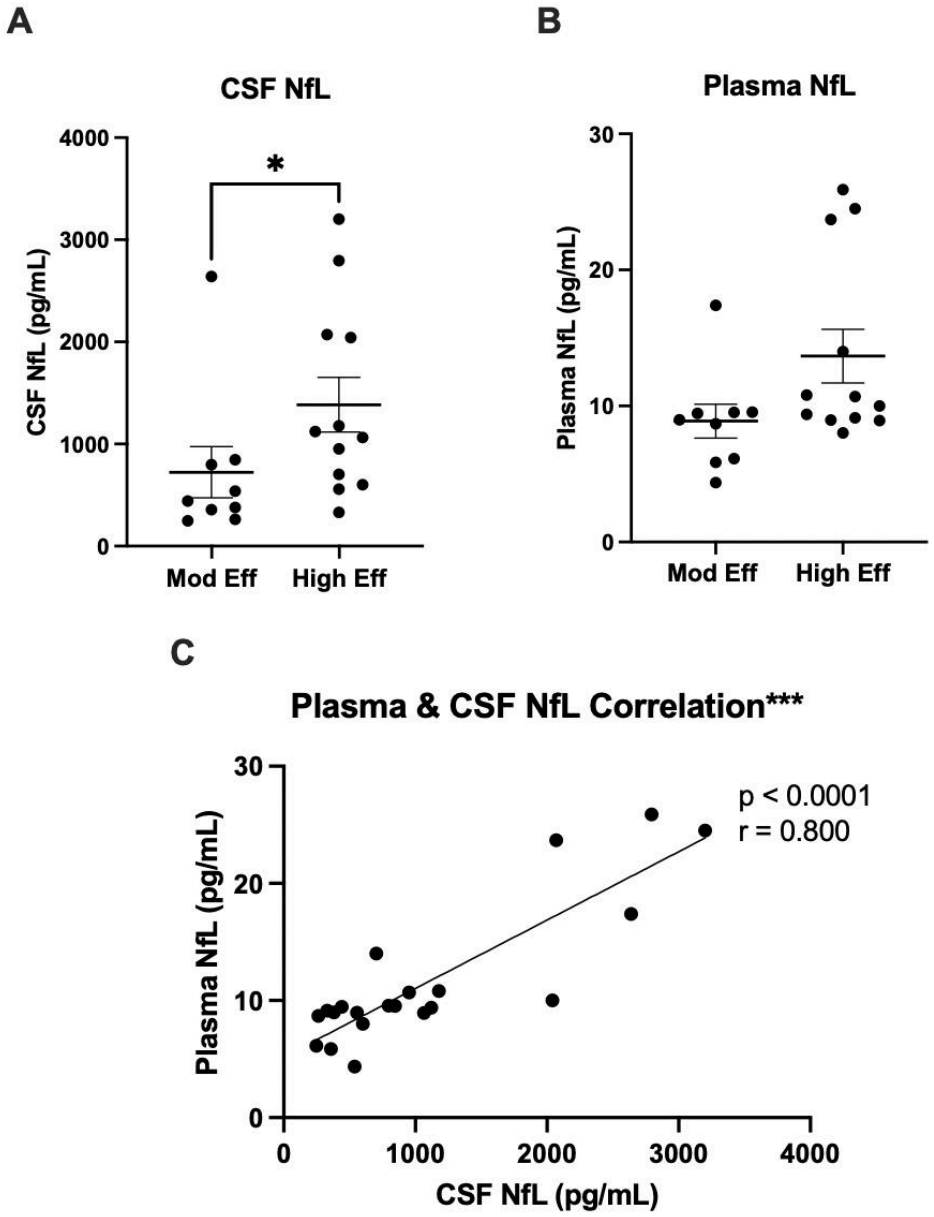

Figure 3.2. Plasma NfL demonstrates significant correlation with CSF NfL. Pre-DMT initiation, patients with RRMS had CSF and blood draws. CSF NfL was measured with commercially available ELISA (Quanterix Corporation), and plasma NfL was measured using Simoa® bead technology. Mann-Whitney U test for non-normally distributed data demonstrated a significant difference between groups pre-DMT initiation for CSF NfL ($p = 0.0227$). Mod Eff (723.6±249.9pg/mL) and High Eff (1385±267.8pg/mL) (Figure 3.2A). No significant difference between groups pre-DMT were seen for plasma NfL ($p = 0.0693$) (Figure 3.2B). Spearman correlation demonstrated a significant correlation between pre-DMT levels of CSF and plasma NfL ($p < 0.0001$; $r=0.800$) (Figure 3.2C).
SEM = Standard Error of the Mean; Mod Eff =Moderate Efficacy DMT; High Eff = High Efficacy DMT. *** $p < 0.001$.

Mann-Whitney U test of baseline plasma GFAP and CXCL13 levels were not found to be significantly different between the two groups ($p=0.1930$; $p=0.2947$) (Figure 3.3A and 3.3B). Spearman correlation of baseline plasma GFAP and CXCL13 with plasma NfL concentrations was not statistically significant ($p= 0.1545$, $r=0.3221$; $p=0.3163$, $r=-0.2361$) (Figure 3.3C and 3.3D).

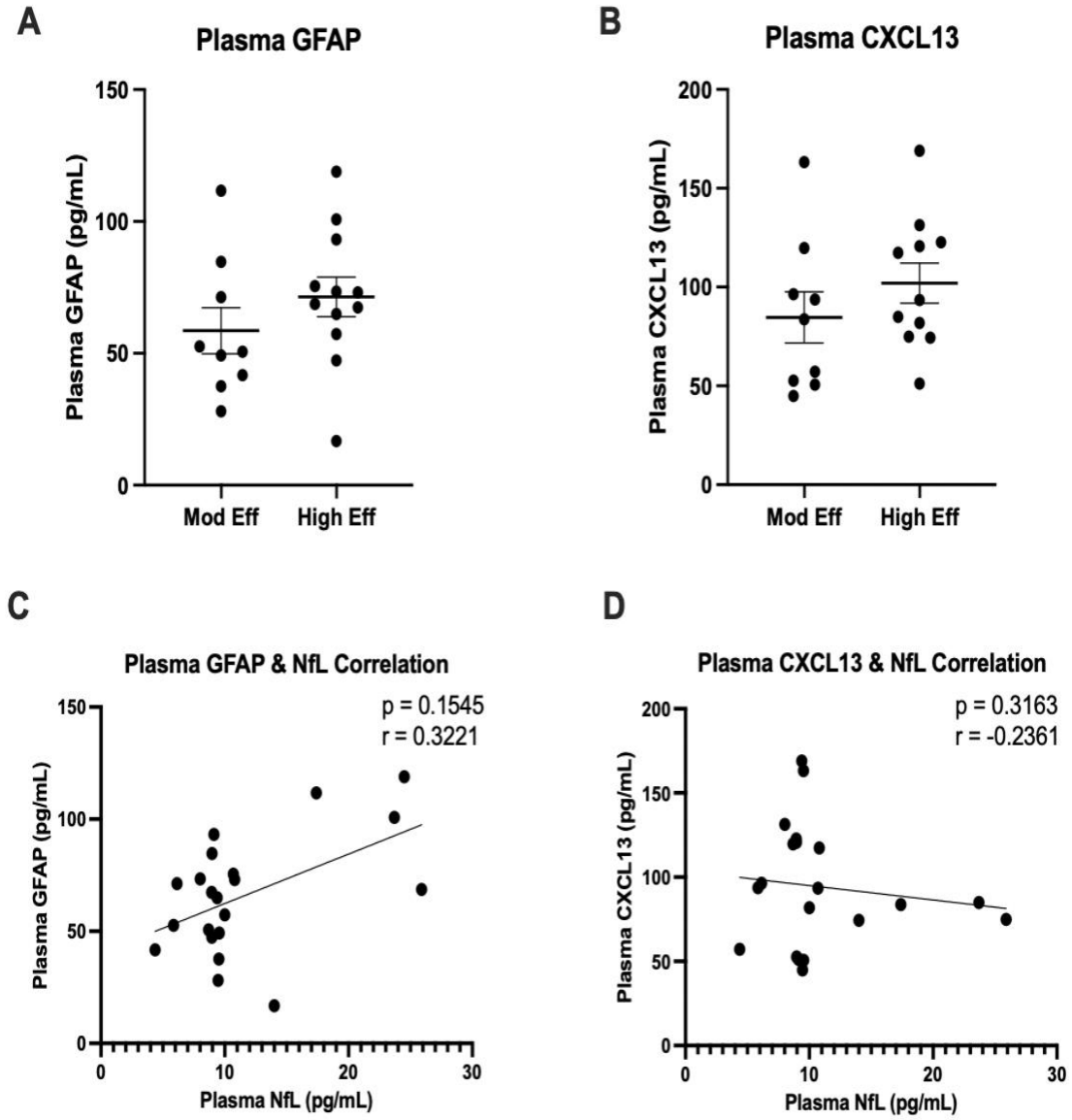

Figure 3.3. Plasma GFAP and CXCL13 are not significantly correlated with plasma NfL. Pre-DMT initiation, patients with RRMS had blood draws. Plasma GFAP was measured using Simoa® bead technology and plasma CXCL13 was measured using a Solid Phase sandwich ELISA kit (R&D systems). Mann-Whitney U test did not demonstrate a significant difference in GFAP (p= 0.1930) or CXCL13 (p= 0.2947). Mod Eff GFAP (58.59±8.748pg/mL); High Eff GFAP (71.43±7.512pg/mL); Mod Eff CXCL13 (84.67±12.98pg/mL); High Eff CXCL13 (102.0 ±10.09pg/mL) (Figure 3.3A-B). Spearman correlation did not demonstrate a significant correlation between pre-DMT levels of either plasma GFAP or CXCL13 with plasma NfL (p= 0.1545, r=0.3221; p=0.3163, r=-0.2361) (Figure 3.3C-D). SEM = Standard Error of the Mean; Mod Eff =Moderate Efficacy DMT; High Eff = High Efficacy DMT.

Further data analysis explored the relationship between baseline biomarker concentrations in patients with relapsing MS and the initial concentrations of all relevant immune cell subsets (Figures 3.4-3.6). While spearman correlation did not reveal a statistically significant association between baseline plasma NfL and normalized (i.e., normalized immune cell count to total CD45+ immune cells) plasma immune cell concentrations, there was a trend towards significance between plasma NfL and levels of CD14+ cells ($p=0.0139$; $r=0.6093$) (Figure 3.4E). Bonferroni correction requires $p=0.0013$ for statistical significance.

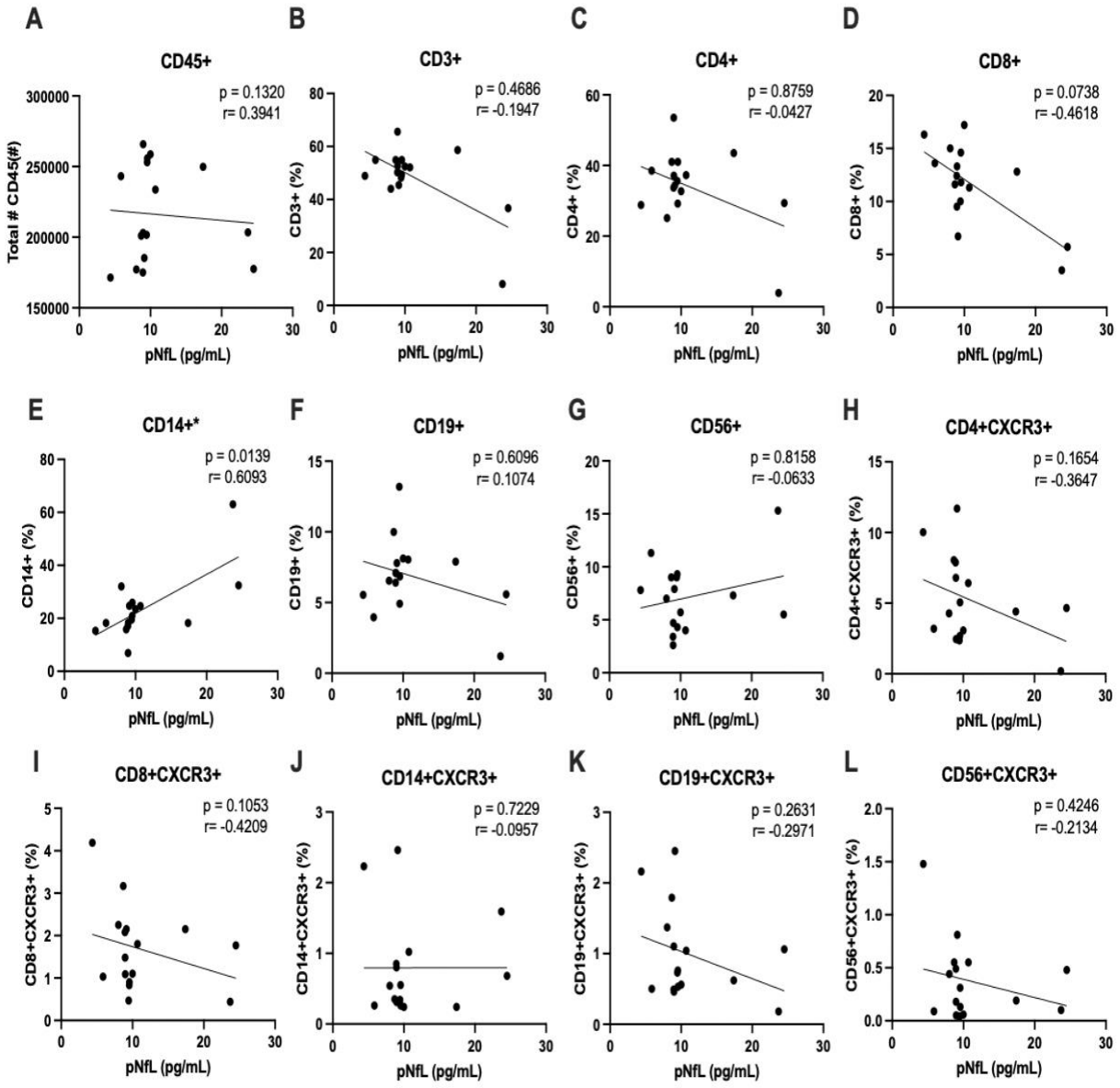

Figure 3.4. Plasma NfL does not demonstrate significant correlation with plasma immune cells. Pre-DMT initiation, patients with RRMS had blood draws. Plasma NfL was measured using Simoa® bead technology and immune cells were measured Cytoflex flow cytometer (Beckman Coulter). CD45+, CD3+, CD4+, CD8+, CD56+, CD14+, CD19+, CD4+CXCR3+, CD8+CXCR3+, CD14+CXCR3+, CD19+CXCR3+, and CD56+CXCR3+ immune cells were quantified using FlowJo software and normalized to each represent a percentage of total CD45+ cells (Figure 3.1). Spearman correlation demonstrated a trend towards significance between pre-DMT levels of plasma NfL and normalized (normalized as a percentage of total CD45+ cells) CD14+ cells ($p = 0.0139$; $r = 0.6093$) (Figure 3.4E). Normalization of immune cell to total CD45+ cells; pNfL = plasma NfL. * $p < 0.05$.

Regarding baseline plasma GFAP and CXCL13, no statistically significant associations were found with baseline measurements of normalized plasma immune cell subsets (Figures 3.5-3.6).

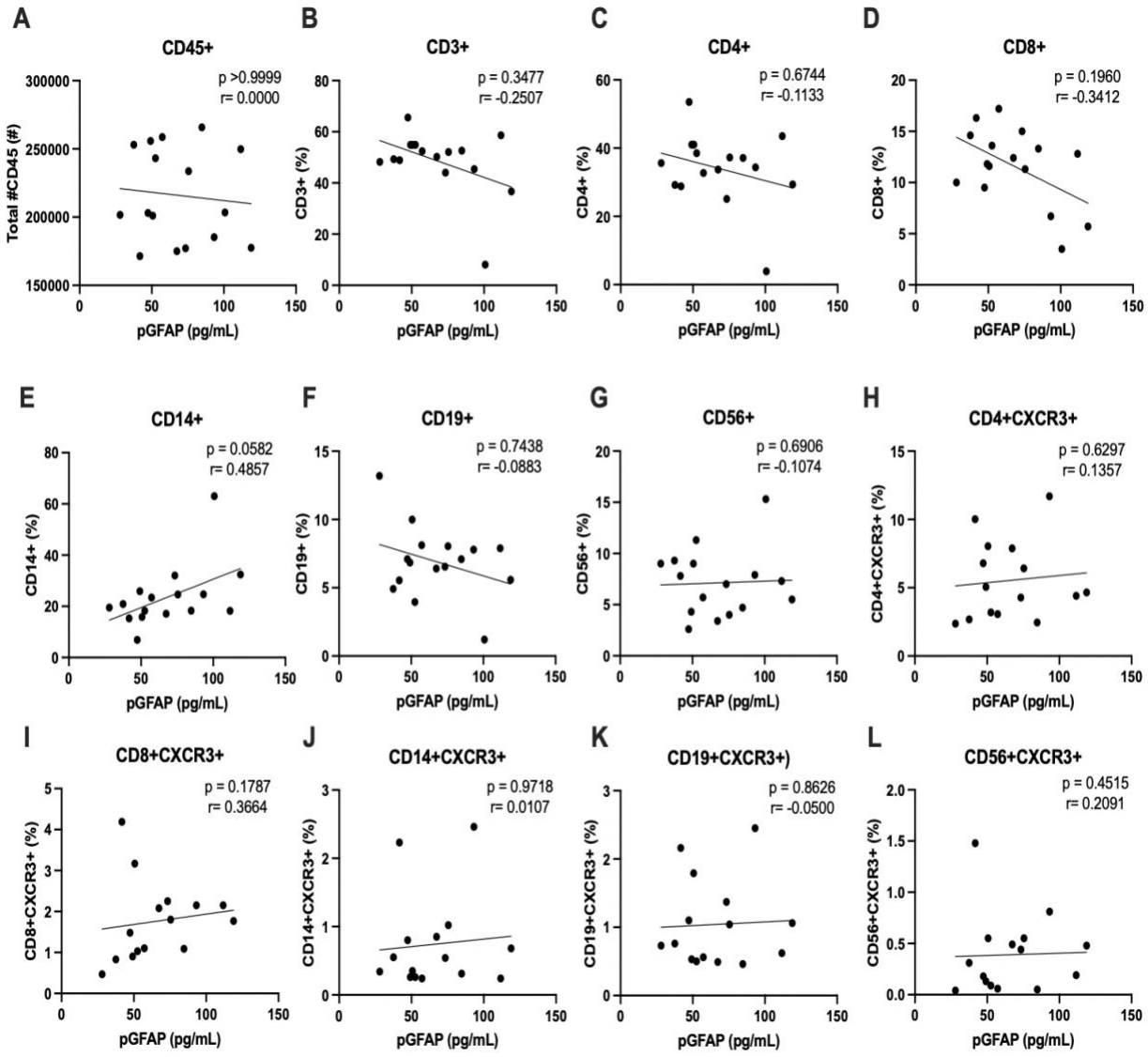

Figure 3.5. Plasma GFAP is not significantly correlated with plasma immune cells. Pre-DMT initiation, patients with RRMS had blood draws. Plasma GFAP was measured using Simoa® bead technology and immune cells were measured Cytoflex flow cytometer (Beckman Coulter). CD45+, CD3+, CD4+, CD8+, CD56+, CD14+, CD19+, CD4+CXCR3+, CD8+CXCR3+, CD14+CXCR3+, CD19+CXCR3+, and CD56+CXCR3+ immune cells were quantified using FlowJo software and normalized to each represent a percentage of total CD45+ cells (Figure 2.1). Spearman correlation did not demonstrate any significant correlations between pre-DMT levels of plasma GFAP and normalized (normalized as a percentage of total CD45+ cells) immune cells. Normalization of immune cell to total CD45+ cells; pGFAP = plasma GFAP.

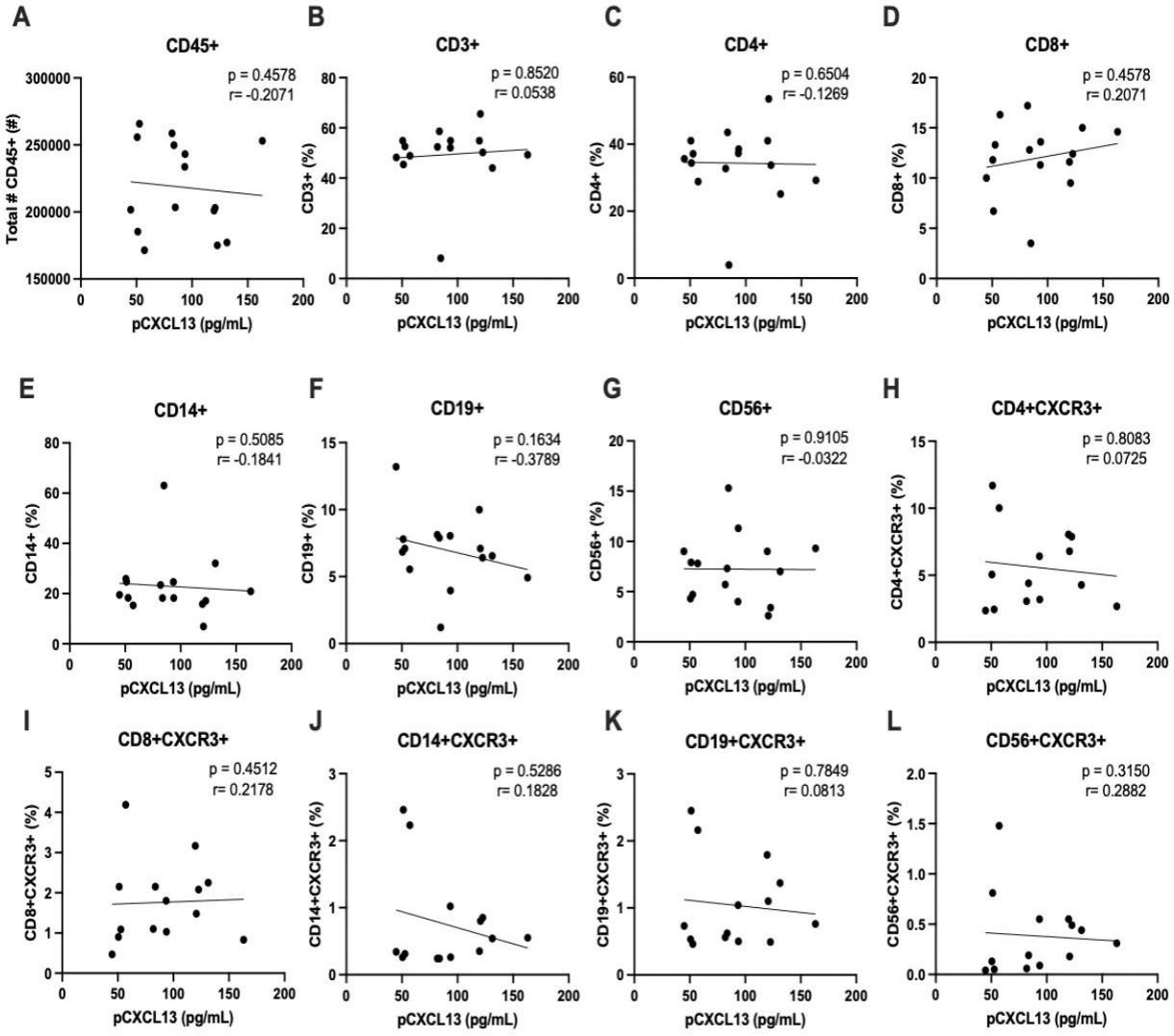

Figure 3.6. Plasma CXCL13 is not significantly correlated with plasma immune cells. Pre-DMT initiation, patients with RRMS had blood draws. A CXCL13 Solid Phase sandwich ELISA kit (R&D systems) was used to quantify CXCL13 in undiluted human plasma as per manufacturer's instructions, and immune cells were measured Cytoflex flow cytometer (Beckman Coulter). CD45+, CD3+, CD4+, CD8+, CD56+, CD14+, CD19+, CD4+CXCR3+, CD8+CXCR3+, CD14+CXCR3+, CD19+CXCR3+, and CD56+CXCR3+ immune cells were quantified using FlowJo software and normalized to each represent a percentage of total CD45+ cells (Figure 2.1). Spearman correlation did not demonstrate any significant correlations between pre-DMT levels of plasma CXCL13 and normalized (normalized as a percentage of total CD45+ cells) immune cells. Normalization of immune cell to total CD45+ cells; pCXCL13= plasma CXCL13.

3.3 Time from Relapse Association with Baseline Biomarker and Immune Cell Subset Concentrations

The time from a patient's last clinical demyelinating relapse was calculated in months via combination of clinical history and retrieval from the electronic medical record system (MediTech). Spearman correlation did not reveal any statistically significant association between time from last clinical demyelinating relapse and baseline concentrations of CSF and plasma biomarkers (Figure 3.7), albeit this did approach significance with CSF NfL ($p=0.0747$; $r=-0.4183$).

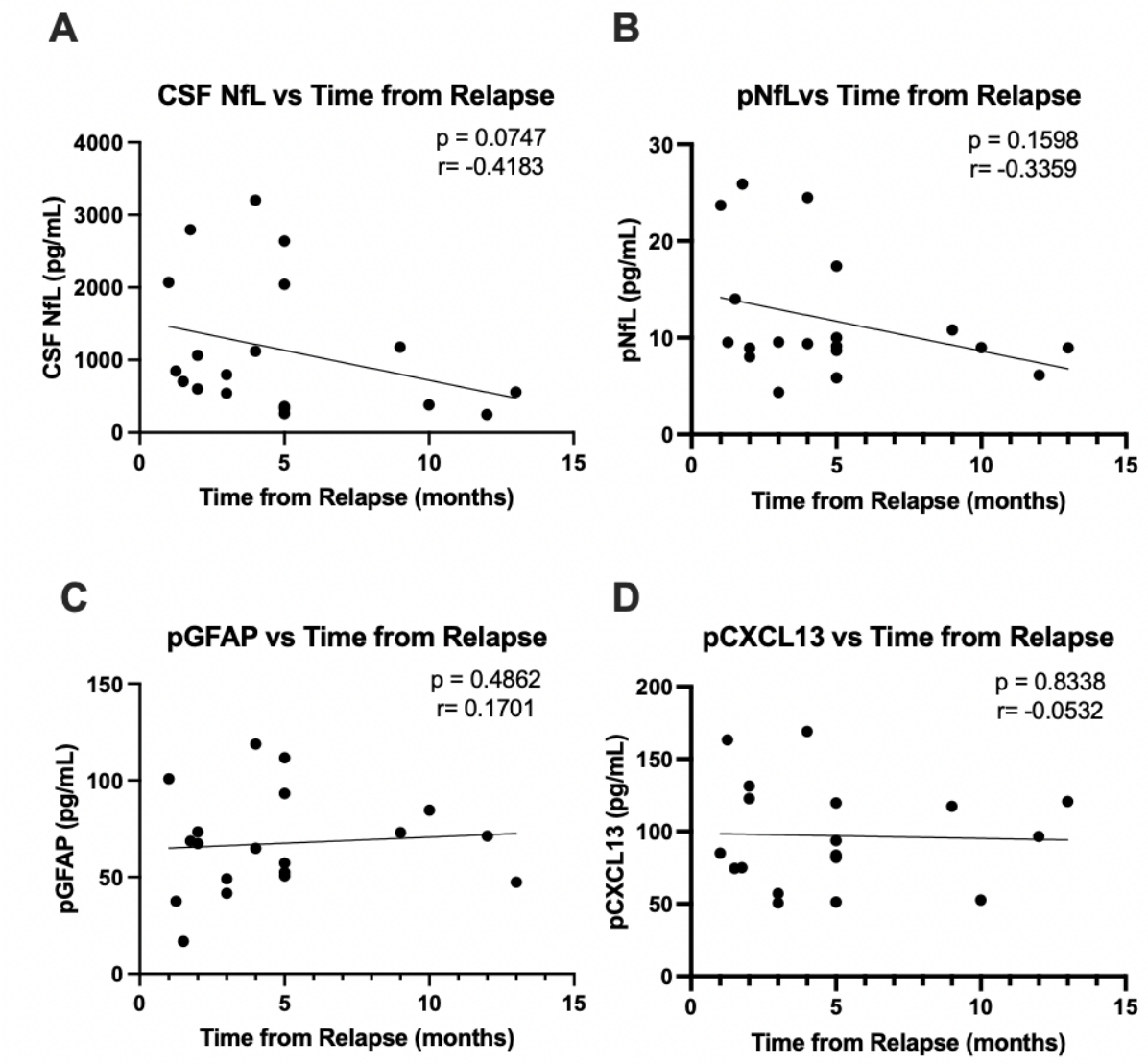

Figure 3.7. Time from last clinical relapse is not associated with plasma biomarker concentrations. Pre-DMT initiation, patients with RRMS had CSF and blood draws. Plasma NfL and GFAP were measured using Simoa® bead technology. A CXCL13 Solid Phase sandwich ELISA kit (R&D systems) was used to quantify CXCL13 in undiluted human plasma as per manufacturer's instructions and immune cells were measured Cytoflex flow cytometer (Beckman Coulter). CD45+, CD3+, CD4+, CD8+, CD56+, CD14+, CD19+, CD4+CXCR3+, CD8+CXCR3+, CD14+CXCR3+, CD19+CXCR3+, and CD56+CXCR3+ immune cells were quantified using FlowJo software and normalized (n) to each represent a percentage of total CD45+ cells (Figure 2.1). Spearman correlation did not demonstrate any significant correlations between pre-DMT levels of plasma pNFL, pGFAP or pCXCL13 and time from last clinical relapses.
pNfL = plasma NfL; pGFAP = plasma GFAP; pCXCL13= plasma CXCL13.

Further spearman correlation analysis revealed a trend towards significance between time from last clinical demyelinating relapse and baseline normalized CD3+ ($p=0.0123$; $r=0.6585$), CD4+ ($p=0.0029$; $r=0.7477$), and CD19+ ($p=0.0150$; $r=0.6428$) immune cell subsets. These correlations did not reach statistical significance when the Bonferroni correction ($p=0.0003$) was employed (Figure 3.8B, 3.8C, and 3.8F).

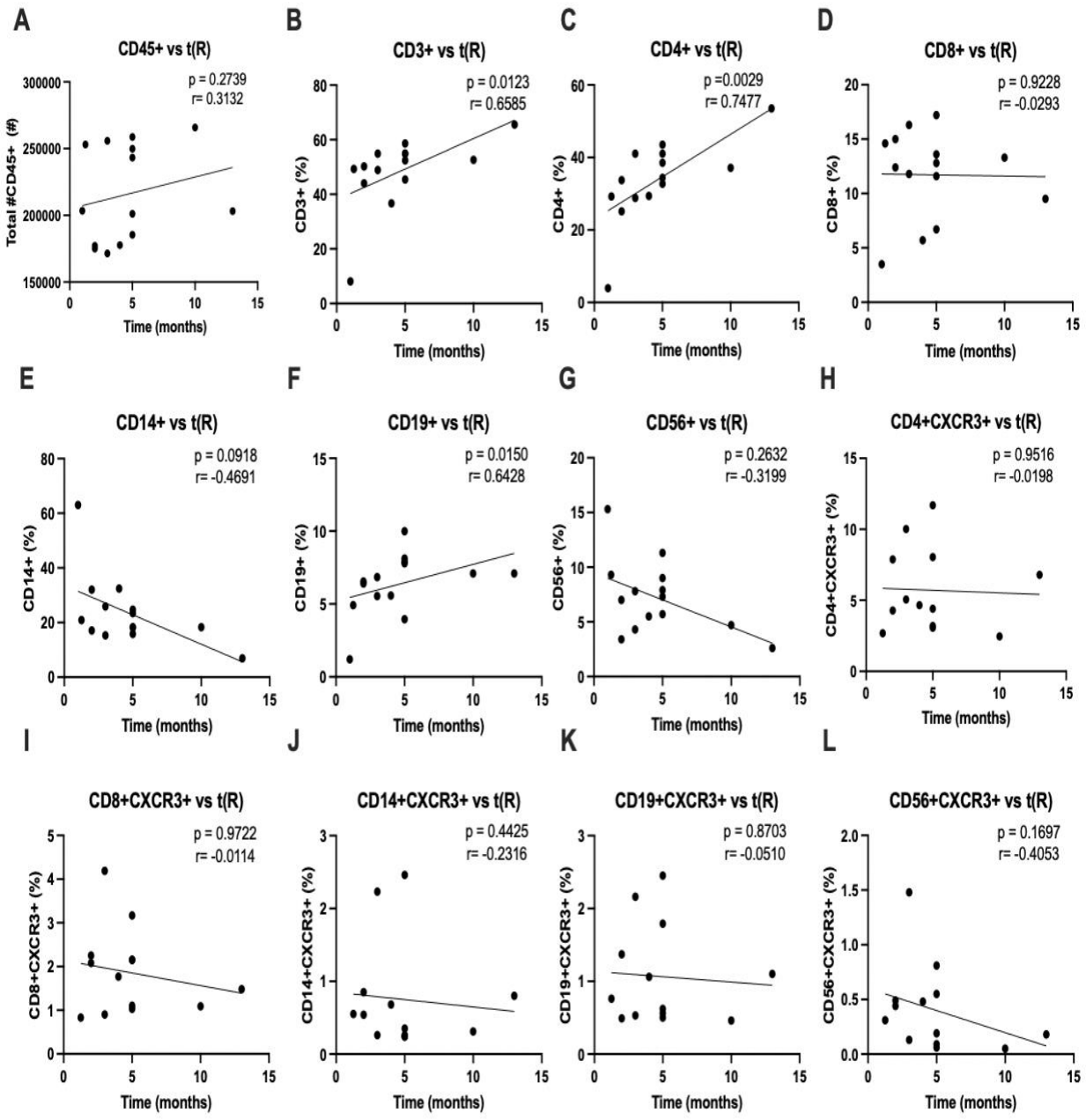

Figure 3.8. Time from last clinical relapse is not correlated with plasma immune cells. Pre-DMT initiation, patients with RRMS had blood draws. Immune cells were measured Cytoflex flow cytometer (Beckman Coulter). CD45+, CD3+, CD4+, CD8+, CD56+, CD14+, CD19+, CD4+CXCR3+, CD8+CXCR3+, CD14+CXCR3+, CD19+CXCR3+, and CD56+CXCR3+ immune cells were quantified using FlowJo software and normalized (n) to each represent a percentage of total CD45+ cells (Figure 2.1). Spearman correlation did demonstrate a significant correlation between pre-DMT levels of CD3+ (p=0.0123, r=0.6585), CD4+ (p=0.0029, r=0.7477), and CD19+ (p=0.0150, r=0.6428) immune cells and time from last clinical relapse (Figure 3.8B-C and F). Normalization of immune cell to total CD45+ cells; t(R) = time from relapse in months. * $p < 0.05$.

3.4 Patients receiving high efficacy DMT have lower levels of plasma NfL, CD19+ and CD19+CXCR3+ immune cells whereas patients receiving moderate efficacy DMT have lower levels of CD45+, CD8+ and CD19+CXCR3+ immune cells

A Wilcoxon matched pairs rank test demonstrated a statistically significant decrease in plasma NfL concentrations at follow-up for those RRMS patients in the high-efficacy DMT group ($p=0.0068$) (Figure 3.9B).

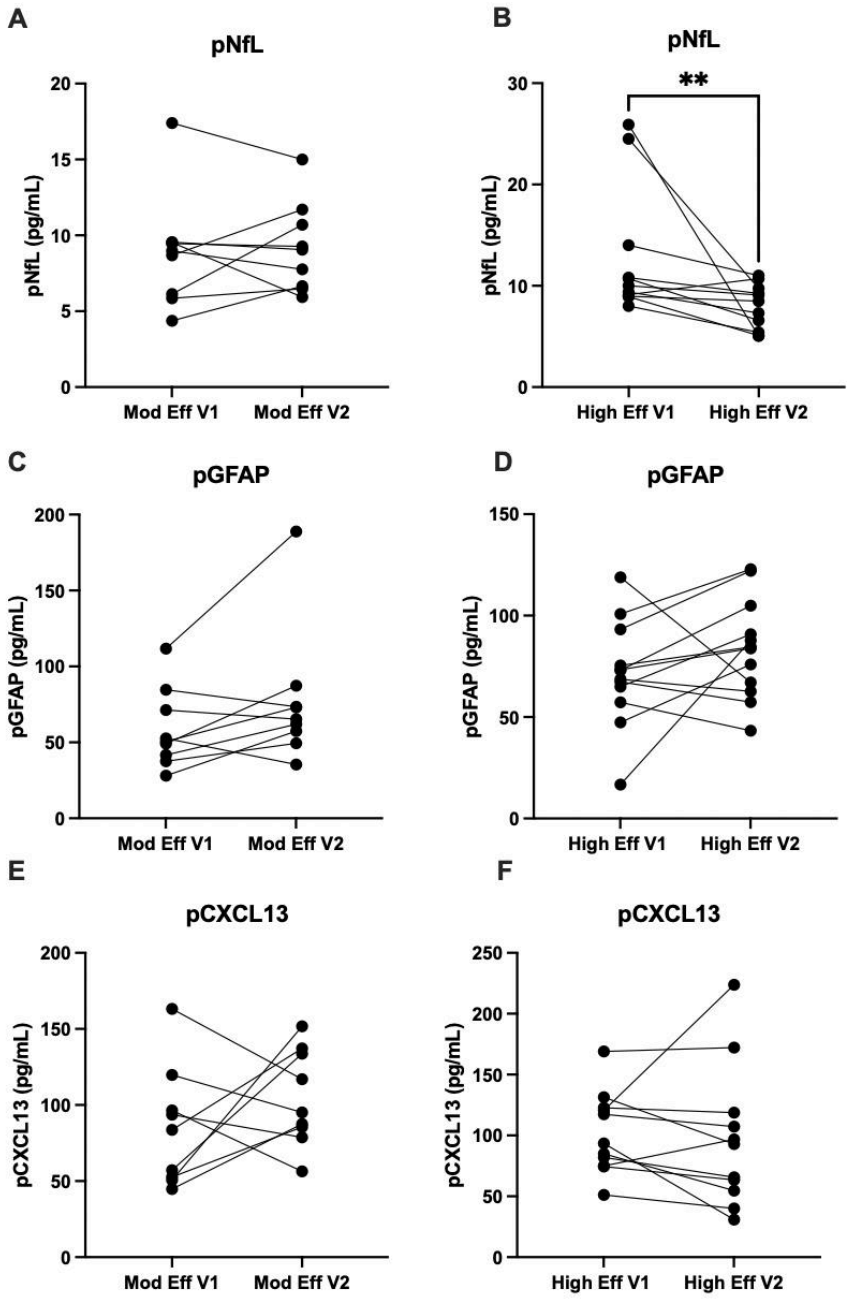

Figure 3.9. High efficacy DMT significantly reduces plasma NfL. Pre- and post-DMT initiation, patients with RRMS had blood draws. Immune cells were measured Cytoflex flow cytometer (Beckman Coulter). CD45+, CD3+, CD4+, CD8+, CD56+, CD14+, CD19+, CD4+CXCR3+, CD8+CXCR3+, CD14+CXCR3+, CD19+CXCR3+, and CD56+CXCR3+ immune cells were quantified using FlowJo software and normalized to each represent a percentage of total CD45+ cells (Figure 2.1). Wilcoxon matched pairs rank test demonstrated a significant decline in plasma NfL levels with high efficacy DMT (-4.786 pg/mL±2.042 pg/mL) (Figure 3.9B). Normalization of immune cell to total CD45+ cells; V1 = Pre-DMT; V2 = Post-DMT; Mean = Mean V2 – Mean V1; SEM = Standard Error of the Mean of V2-V1; Mod Eff =Moderate Efficacy DMT; High Eff = High Efficacy DMT. ** $p < 0.01$.

A Wilcoxon matched pairs signed rank test was performed for each immune cell subset for both the moderate-efficacy DMT and high-efficacy DMT groups, to analyze for significant changes in these individual immune cells in response to DMT. Those patients who received treatment with a moderate-efficacy DMT showed a trend towards a significant decline in their plasma CD45+ cells from baseline ($p=0.0391$) (Figure 3.10A). Bonferroni correction requires $p=0.0013$ for statistical significance. This same analysis was conducted for all further immune cell subsets for those patients who received moderate-efficacy DMT, including CD3+, CD4+, CD8+, CD14+, CD19+, CD56+, CD4+CXCR3+, CD8+CXCR3+, CD14+CXCR3+, CD19+CXCR3+, CD56+CXCR3+ immune cells (Figure 3.10B-L). In addition to CD45+ immune cells, those patients who received treatment with a moderate-efficacy DMT showed a trend towards a significant decline in their plasma CD8+ cells ($p=0.0156$) (Figure 3.10D), and CD19+CXCR3+ cells ($p=0.0078$) (Figure 3.10K).

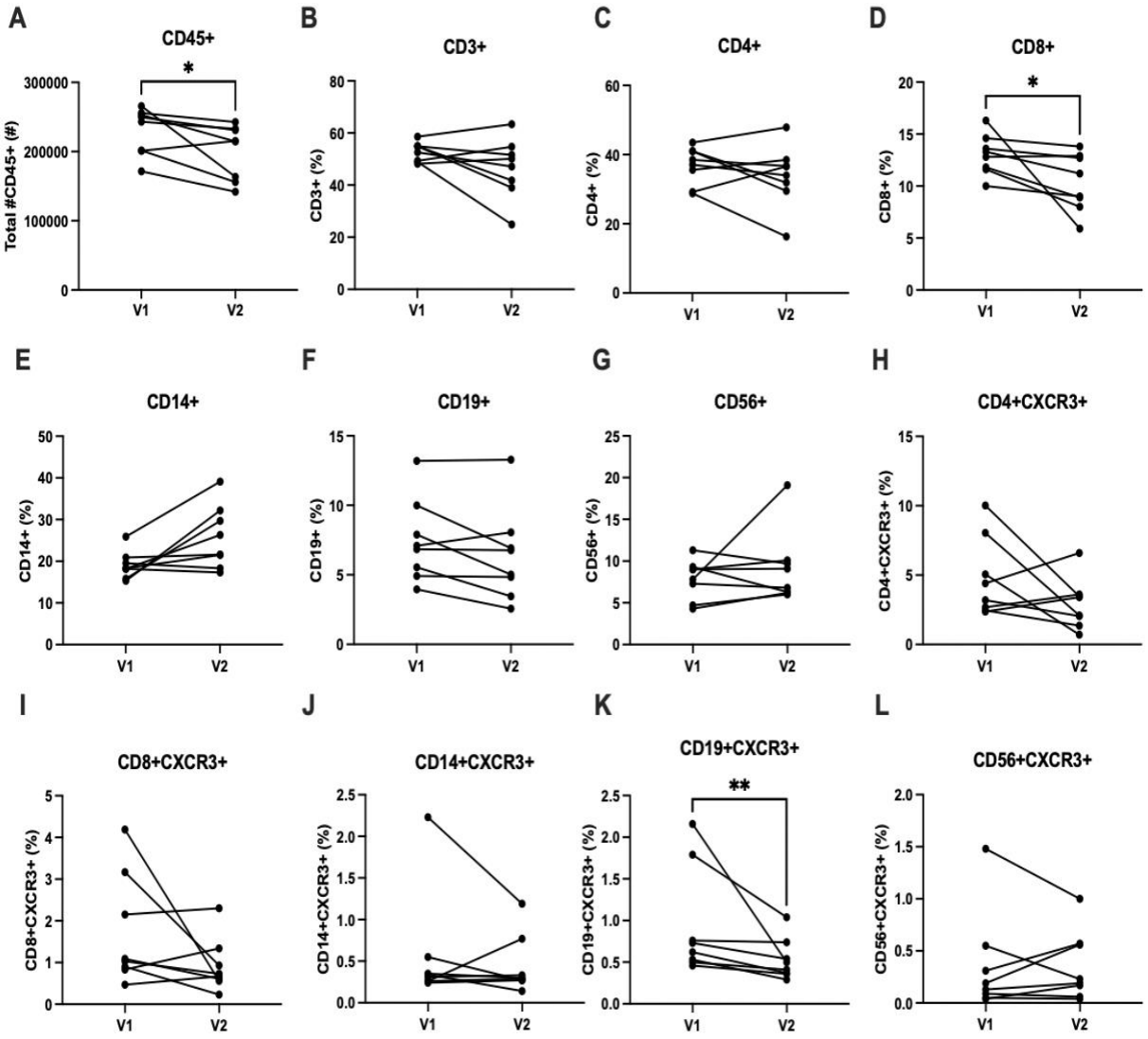

Figure 3.10. Moderate efficacy DMT significantly reduces CD19+CXCR3+ plasma immune cells. Pre- and post-DMT initiation, patients with RRMS had blood draws. Immune cells were measured Cytoflex flow cytometer (Beckman Coulter). CD45+, CD3+, CD4+, CD8+, CD56+, CD14+, CD19+, CD4+CXCR3+, CD8+CXCR3+, CD14+CXCR3+, CD19+CXCR3+, and CD56+CXCR3+ immune cells were quantified using FlowJo software and normalized to each represent a percentage of total CD45+ cells (Figure 2.1). Wilcoxon matched pairs rank test demonstrated a trend towards a significant decline in CD45+, CD8+, and CD19+CXCR3+ immune cells (Figure 3.10A, D, K). Normalization of immune cell to total CD45+ cells; V1 = Pre-DMT; V2 = Post-DMT; Mean = Mean V2 – Mean V1; SEM = Standard Error of the Mean of V2-V1; Mod Eff =Moderate Efficacy DMT pre-DMT. Bonferroni correction requires p=0.0013 for statistical significance. * $p < 0.05$; ** $p < 0.01$.

The Wilcoxon matched pairs signed rank test demonstrated a trend towards a statistically significant decrease in plasma CD19+ cells ($p=0.0156$) and CD19+CXCR3+ cells ($p=0.0156$) for those patients on high efficacy DMT (Figure 3.11F and 3.11K). Bonferroni correction requires $p=0.0013$ for statistical significance.

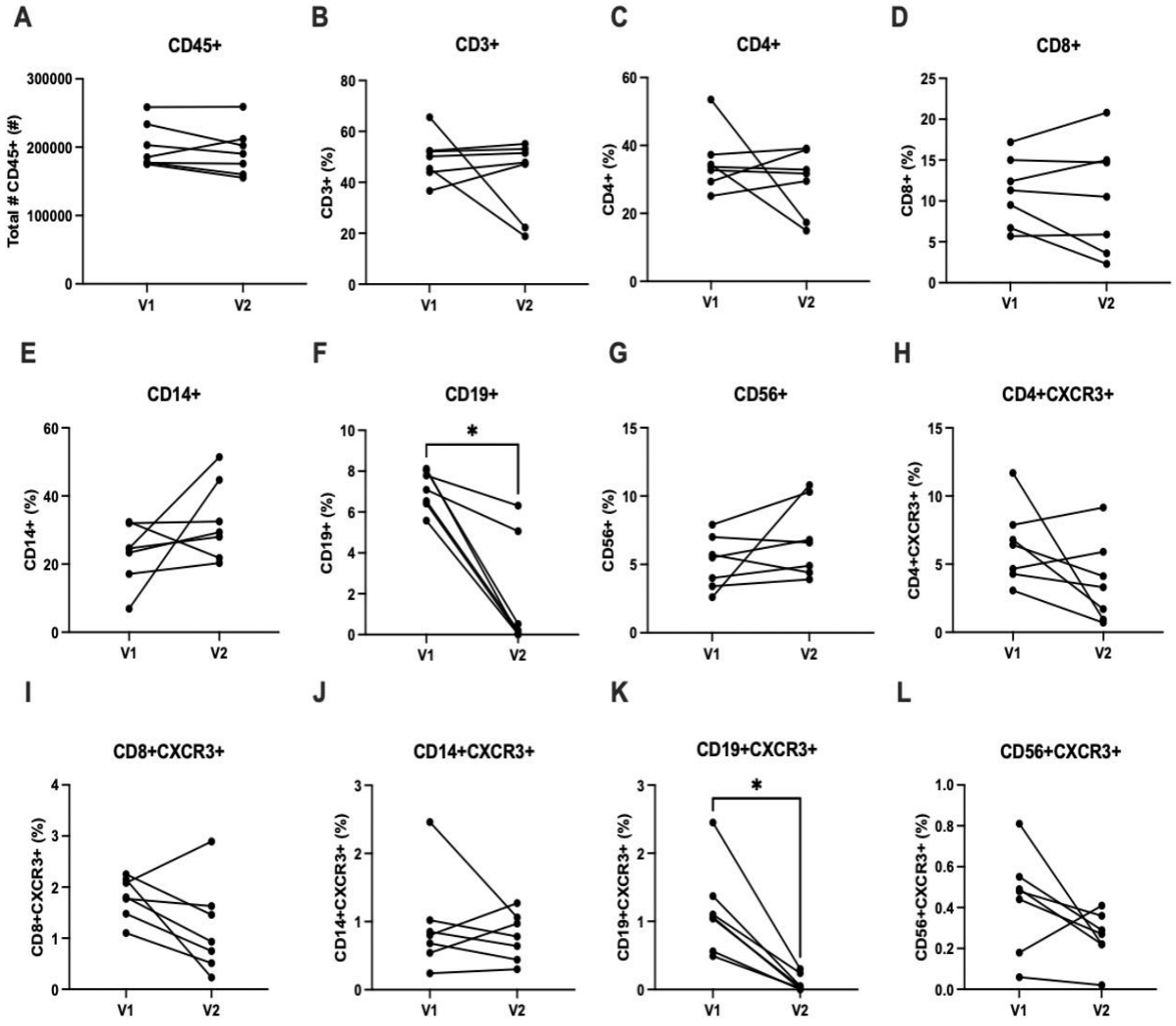

Figure 3.11. High efficacy DMT significantly reduces CD19+ and CD19+CXCR3+ plasma immune cells. Pre- and post-DMT initiation, patients with RRMS had blood draws. Immune cells were measured Cytoflex flow cytometer (Beckman Coulter). CD45+, CD3+, CD4+, CD8+, CD56+, CD14+, CD19+, CD4+CXCR3+, CD8+CXCR3+, CD14+CXCR3+, CD19+CXCR3+, and CD56+CXCR3+ immune cells were quantified using FlowJo software and normalized to each represent a percentage of total CD45+ cells (Figure 2.1). Wilcoxon matched pairs rank test demonstrated a trend towards a significant decline in CD19+ and CD19+CXCR3+ immune cells (Figure 3.11F & K). Normalization of immune cell to total CD45+ cells; V1 = Pre-DMT; V2 = Post-DMT; Mean = Mean V2 – Mean V1; SE = Standard Error of the Mean of V2-V1; High Eff = High Efficacy DMT. Bonferroni correction requires p=0.0013 for statistical significance. * $p < 0.05$.

3.5 High efficacy DMT results in a greater decline in CD19+ and CD19+CXCR3+ plasma immune cells than moderate efficacy DMT

To assess for significant differences in the changes in measured plasma immune cell subsets between the moderate and high efficacy DMT groups, the Mann-Whitney U test was employed (Figure 3.12). Plasma CD19+ and CD19+CXCR3+ immune cells, normalized to total CD45+ immune cell counts, demonstrated a trend towards a significant decrease in the high-efficacy group ($p=0.0093$; $p=0.0093$) compared to the moderate efficacy group (Figure 3.12F and 3.12K). Bonferroni correction requires $p=0.0013$ for statistical significance.

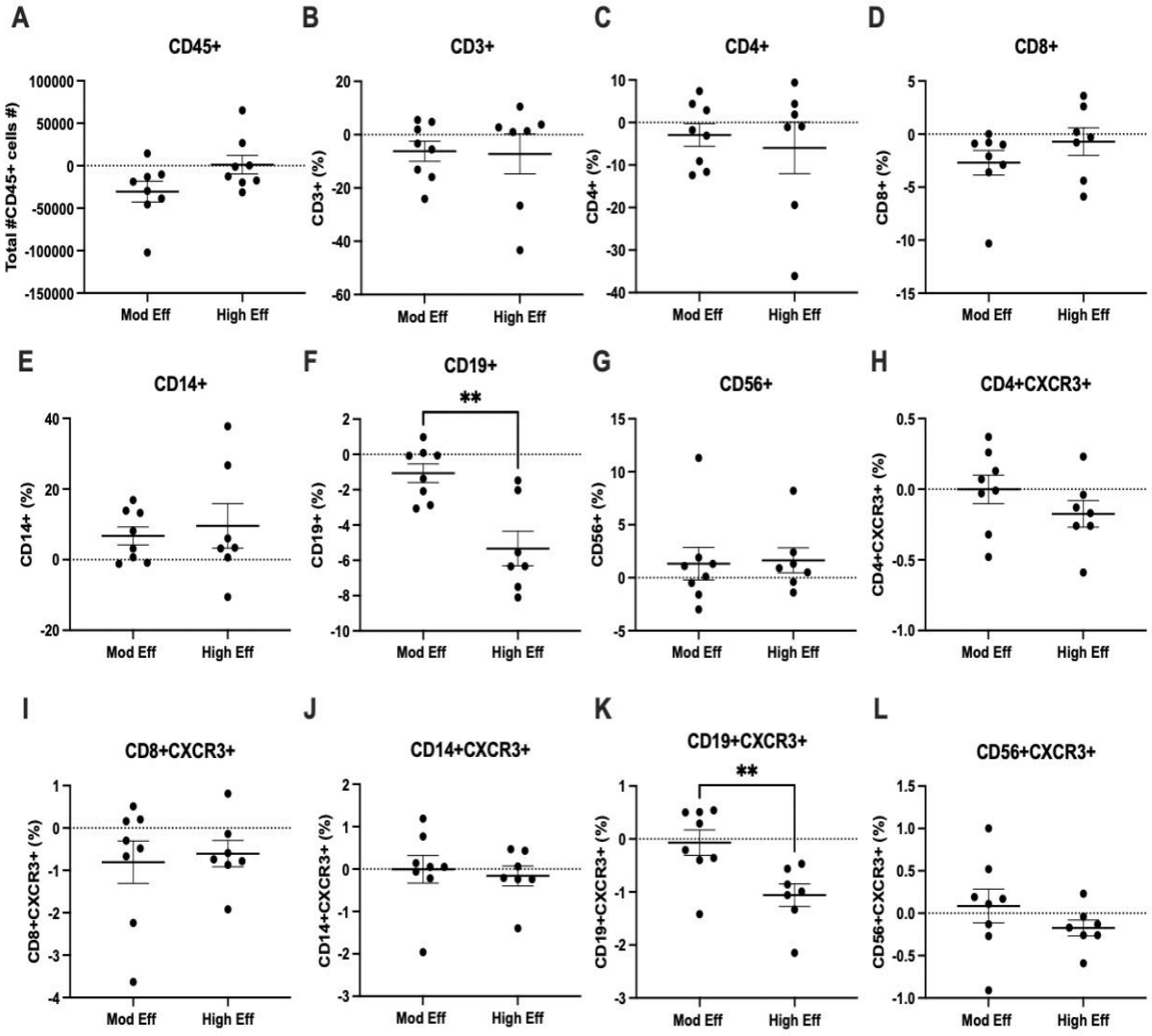

Figure 3.12. High efficacy DMT results in a greater decline in CD19+ and CD19+CXCR3+ plasma immune cells than moderate efficacy DMT. Pre- and post-DMT initiation, patients with RRMS had blood draws. Immune cells were measured Cytoflex flow cytometer (Beckman Coulter). CD45+, CD3+, CD4+, CD8+, CD56+, CD14+, CD19+, CD4+CXCR3+, CD8+CXCR3+, CD14+CXCR3+, CD19+CXCR3+, and CD56+CXCR3+ immune cells were quantified using FlowJo software and normalized to each represent a percentage of total CD45+ cells (Figure 2.1). Mann Whitney U test revealed a trend towards significant difference in the decline of levels of CD19+ immune cells between High Eff (-5.377±0.9805 pg/mL) and Mod Eff (-1.065±0.5325) groups (p=0.0093) (Figure 3.12F) and CD19+CXCR3+ immune cells between High Eff (-1.060±-0.0688 pg/mL) and Mod Eff (0.2129±0.2390 pg/mL) groups (p=0.0093) (Figure 3.12K). Normalization of immune cell to total CD45+ cells; Delta = the change in relevant normalized immune cell as percentage of total CD45+ cells; Mod Eff = Moderate Efficacy DMT; High Eff = High Efficacy DMT. Bonferroni correction requires p=0.0013 for statistical significance. ** $p < 0.01$.

The Mann Whitney U test revealed a significant decrease (i.e., larger negative delta) in plasma NfL in the high efficacy compared to moderate efficacy DMT group (p=0.0200) (Figure 3.13A). There was no significant difference in delta plasma GFAP and delta CXCL13 between groups.

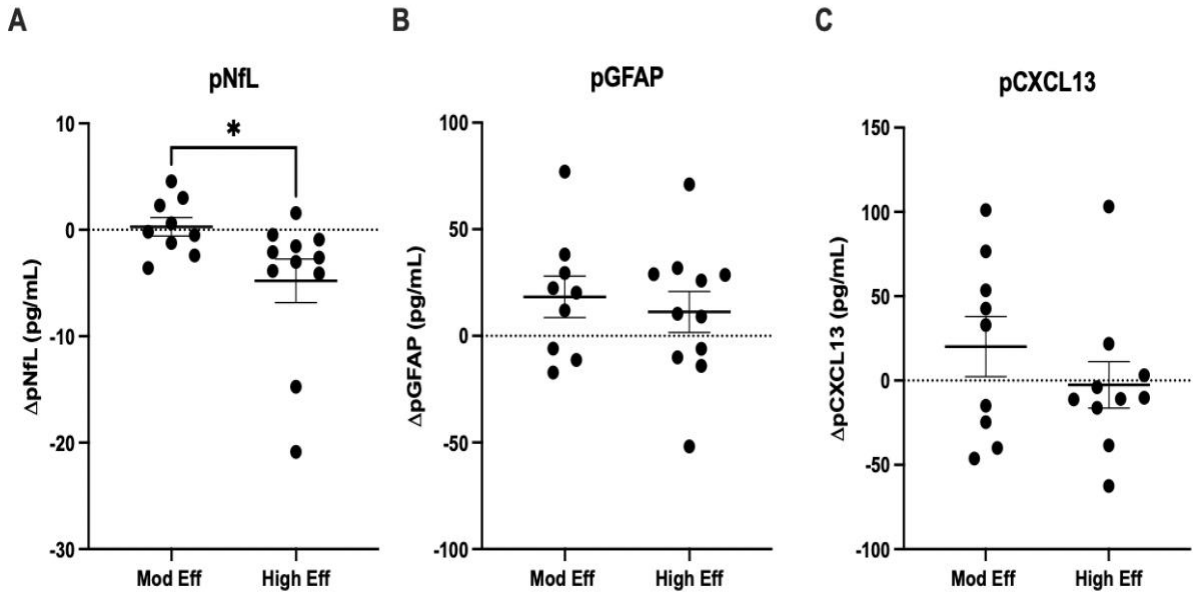

Figure 3.13. High efficacy DMT results in a significantly greater decline in plasma NfL than moderate efficacy DMT. Pre- and post-DMT initiation, patients with RRMS had blood draws. Plasma NfL and GFAP were measured using Simoa® bead technology. A CXCL13 Solid Phase sandwich ELISA kit (R&D systems) was used to quantify CXCL13 in undiluted human plasma as per manufacturer's instructions. Mann Whitney U test demonstrated a significant decline in plasma NfL levels with High Eff (-4.786±2.042 pg/mL) compared to Mod Eff (0.2878±0.8752) (Figure 3.13A). Mann Whitney U test did not demonstrate any significant difference in overall change in pGFAP or pCXCL13 between the High Eff and Mod Eff groups (Figure 3.13B-C). Normalization of immune cell to total CD45+ cells. pNfL = plasma NfL; pGFAP = plasma GFAP; pCXCL13 = plasma CXCL13; Mean = Mean V2 – Mean V1; SEM = Standard Error of the Mean of V2-V1; Mod Eff =Moderate Efficacy DMT; High Eff = High Efficacy DMT. * $p < 0.05$.

Spearman correlation was used to examine the relationship between the delta plasma NfL and delta plasma immune cell subsets for the moderate-efficacy and high-efficacy DMT subgroups (Figure 3.14 and 3.15). In the moderate-efficacy subgroup a trend towards a significant association was seen between the delta plasma NfL and the following delta normalized immune cell subsets: CD3+ cells ($p=0.0279$; $r=-0.7857$) (Figure 3.14B), CD4+ cells ($p=0.0279$; $r=-0.7857$) (Figure 3.14C), CD8+ cells ($p=0.0458$; $r=-0.7381$) (Figure 3.14D), CD4+CXCR3+ ($p=0.0107$; $r=-0.8571$) (Figure 3.14H), and CD19+CXCR3+ ($p=0.0279$; $r=0.7857$) (Figure 3.14K). Bonferroni correction requires $p=0.0003$ for statistical significance. In the high-efficacy subgroup a trend towards a significant association was seen between the delta plasma NfL, and the following delta normalized immune cell subsets: CD45+ cells ($p=0.0480$; $r=0.7857$) (Figure 3.15A), CD4+ cells ($p=0.0238$; $r=-0.8571$) (Figure 3.15C) and CD14+ cells ($p=0.0341$; $r=0.8214$) (Figure 3.15E).

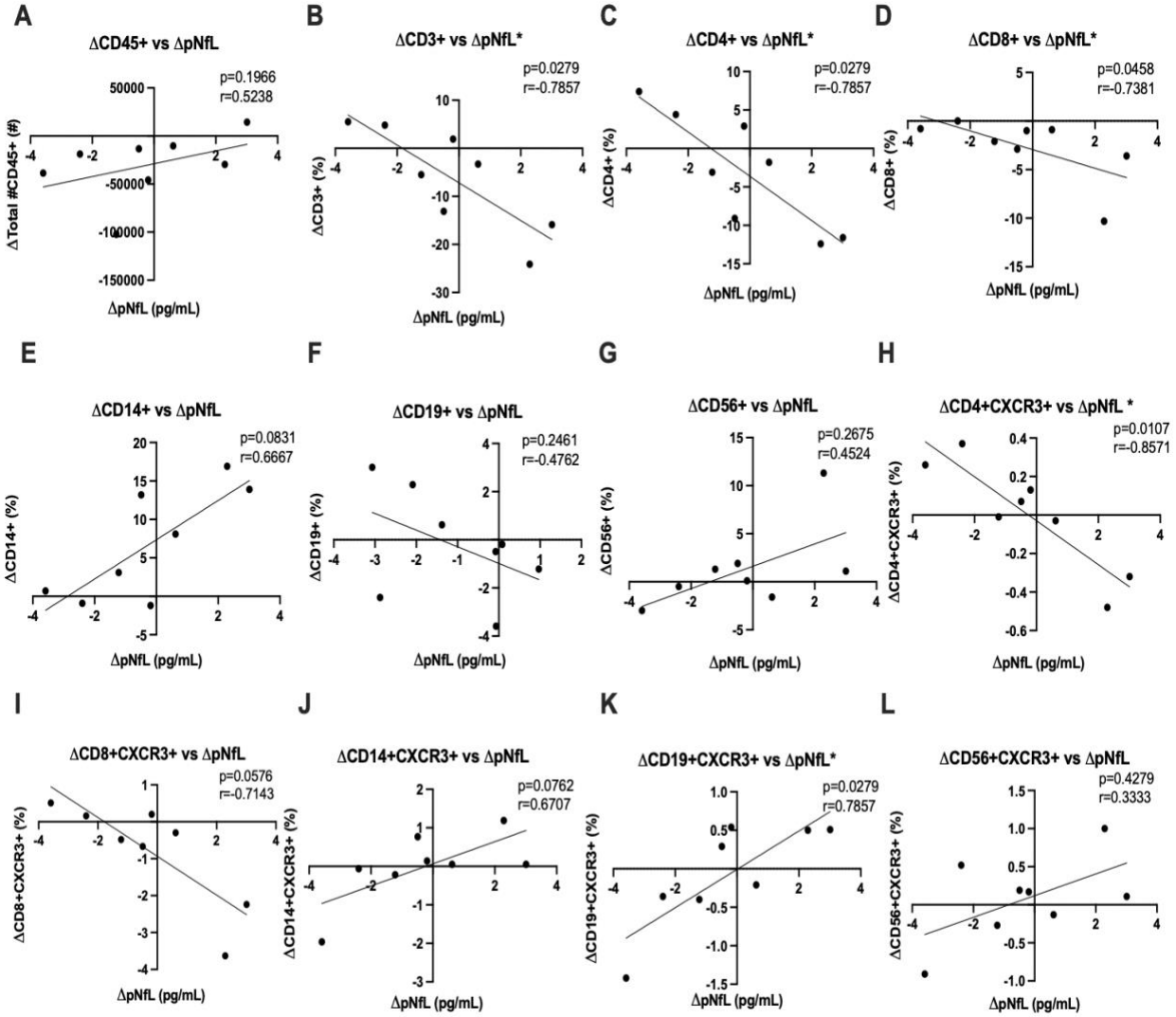

Figure 3.14. Moderate Efficacy DMT does not result in any significant change in plasma NfL or concomitant increase or decrease in immune cells. Pre- and post-DMT initiation, patients with RRMS had blood draws. Immune cells were measured Cytoflex flow cytometer (Beckman Coulter). CD45+, CD3+, CD4+, CD8+, CD56+, CD14+, CD19+, CD4+CXCR3+, CD8+CXCR3+, CD14+CXCR3+, CD19+CXCR3+, and CD56+CXCR3+ immune cells were quantified using FlowJo software and normalized (n) to each represent a percentage of total CD45+ cells (Figure 2.1). Spearman correlation demonstrated a trend towards a significant correlation between ΔpNfL and ΔCD3+ (p=0.0279; r=-0.7857), ΔCD4+ (p=0.0279; r=-0.7857), ΔCD8+(p=0.0458; r=-0.7381), ΔCD4+CXCR3+ (p=0.0107; r=-0.8571), and ΔCD19+CXCR3+ (p=0.0279; r=0.7857) (Figures 3.14B-D, H & K). Normalization of immune cell to total CD45+ cells. Mod Eff = Moderate efficacy DMT; ΔpNfL = change in plasma NfL; Δimmune cell = change in relevant immune cell. Bonferroni correction requires p=0.0003 for statistical significance.

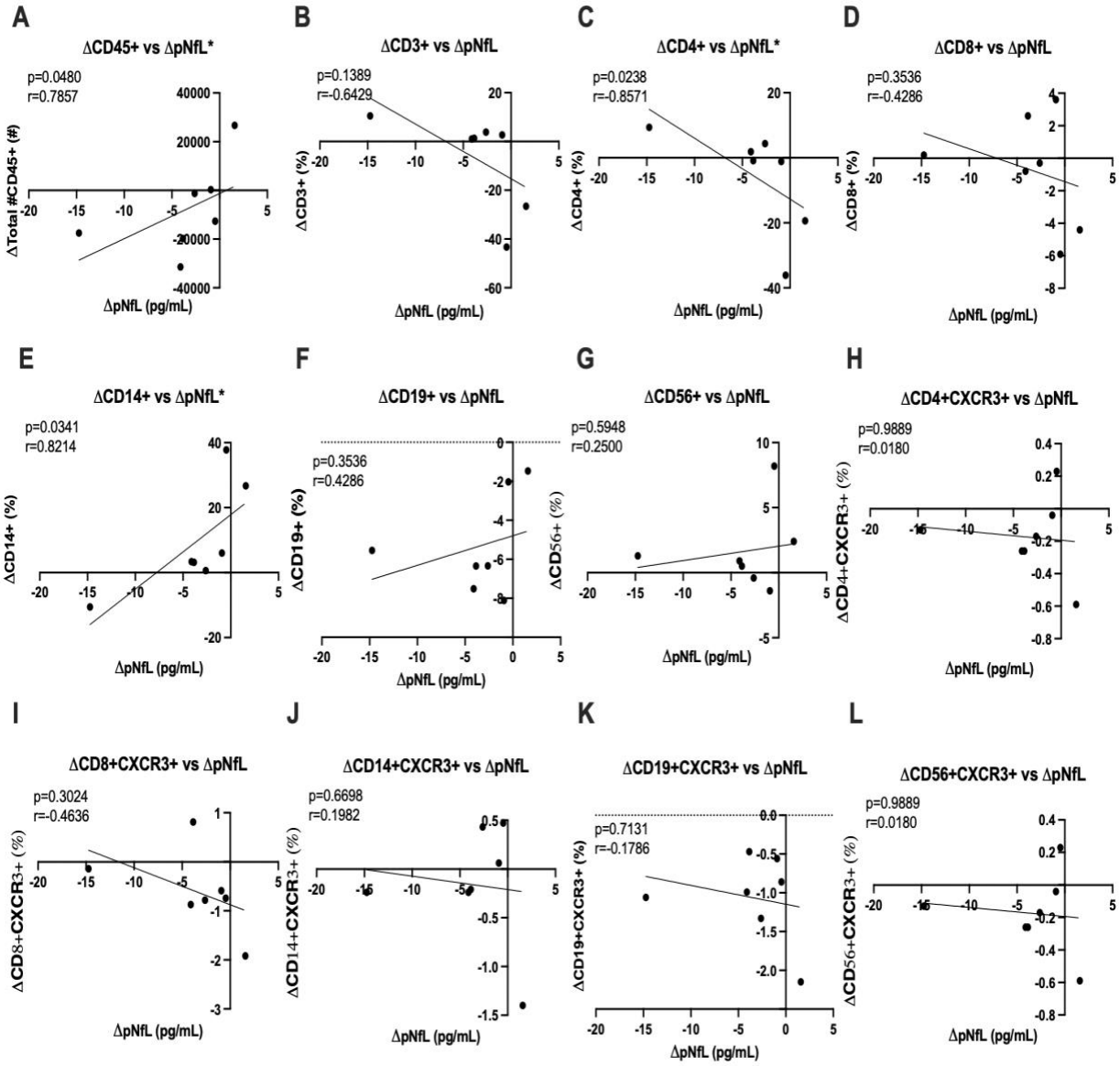

Figure 3.15. High Efficacy DMT does not result in any significant change in plasma NfL or concomitant increase or decrease in immune cells. Pre- and post-DMT initiation, patients with RRMS had blood draws. Immune cells were measured Cytoflex flow cytometer (Beckman Coulter). CD45+, CD3+, CD4+, CD8+, CD56+, CD14+, CD19+, CD4+CXCR3+, CD8+CXCR3+, CD14+CXCR3+, CD19+CXCR3+, and CD56+CXCR3+ immune cells were quantified using FlowJo software and normalized (n) to each represent a percentage of total CD45+ cells (Figure 2.1). Spearman correlation demonstrated a trend towards a significant correlation between ΔpNfL and ΔCD45+ (p=0.0480; r=0.7857), ΔCD4+ (p=0.0238; r=-0.8571) and ΔCD14+ (p=0.0341; r=0.8214) (Figure 3.15A, C and E). Normalization of immune cell to total CD45+ cells. High Eff = High efficacy DMT; ΔpNfL = change in plasma NfL; Δimmune cell = change in relevant immune cell. Bonferroni correction requires p=0.0003 for statistical significance.

Spearman correlation did not reveal any statistically significant associations between delta plasma GFAP and normalized delta plasma immune cell subsets for the moderate efficacy group (Figure 3.16).

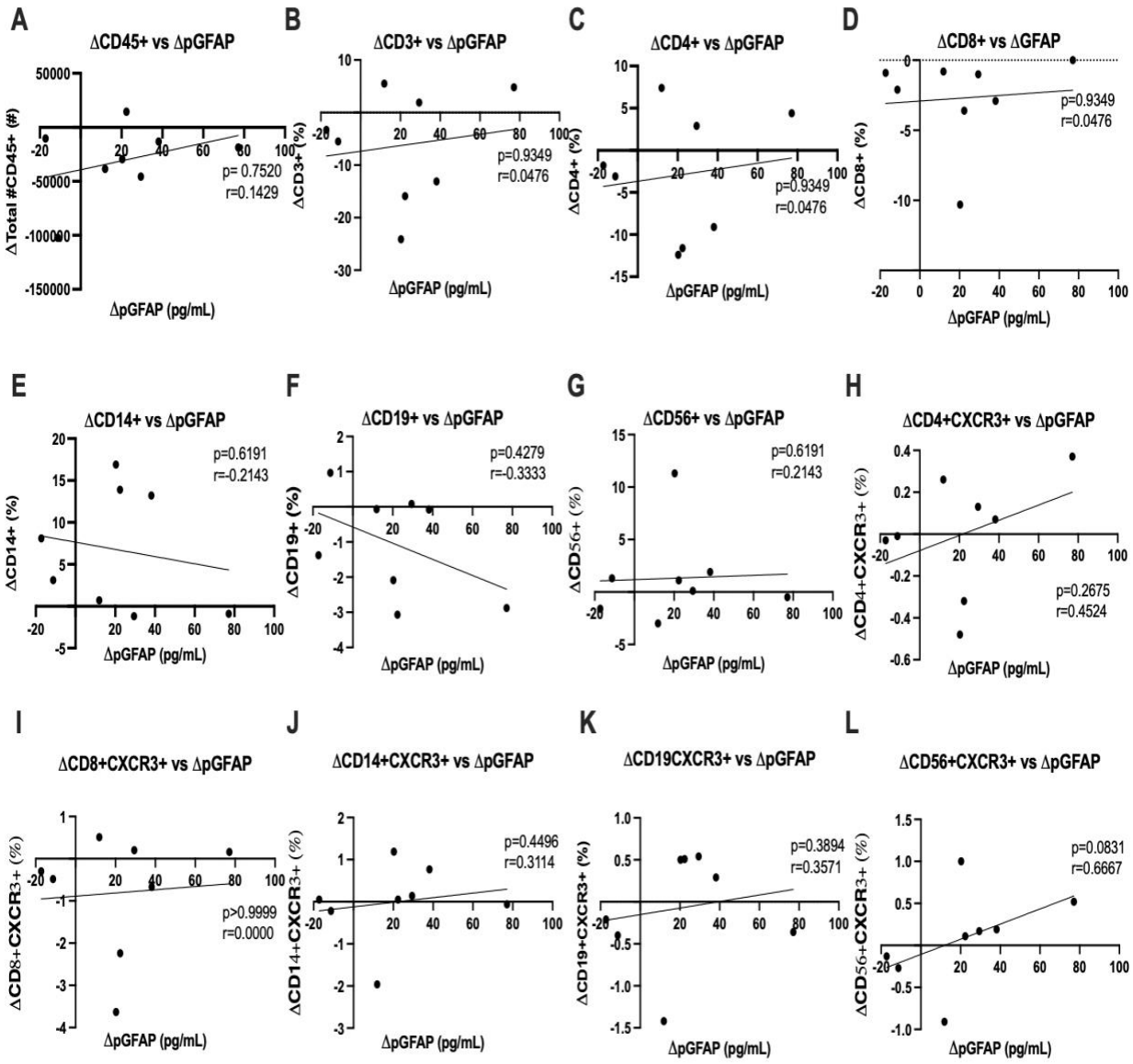

Figure 3.16. Moderate-Efficacy DMT does not result in any significant change in plasma GFAP or concomitant increase or decrease in immune cells. Pre- and post-DMT initiation, patients with RRMS had blood draws. Immune cells were measured Cytoflex flow cytometer (Beckman Coulter). CD45+, CD3+, CD4+, CD8+, CD56+, CD14+, CD19+, CD4+CXCR3+, CD8+CXCR3+, CD14+CXCR3+, CD19+CXCR3+, and CD56+CXCR3+ immune cells were quantified using FlowJo software and normalized to each represent a percentage of total CD45+ cells (Figure 2.1). Spearman correlation did not demonstrate a significant correlation between ΔpGFAP and any Δimmune cell. Normalization of immune cell to total CD45+ cells. High Eff = High efficacy DMT; ΔpGFAP = change in plasma GFAP; Δimmune cell = change in relevant immune cell. Bonferroni correction requires p=0.0003 for statistical significance.

In the high efficacy group, there was a trend towards a significant association between delta plasma GFAP and normalized delta CD8+ cells ($p=0.0341$; $r=-0.8214$) (Figure 3.17D).

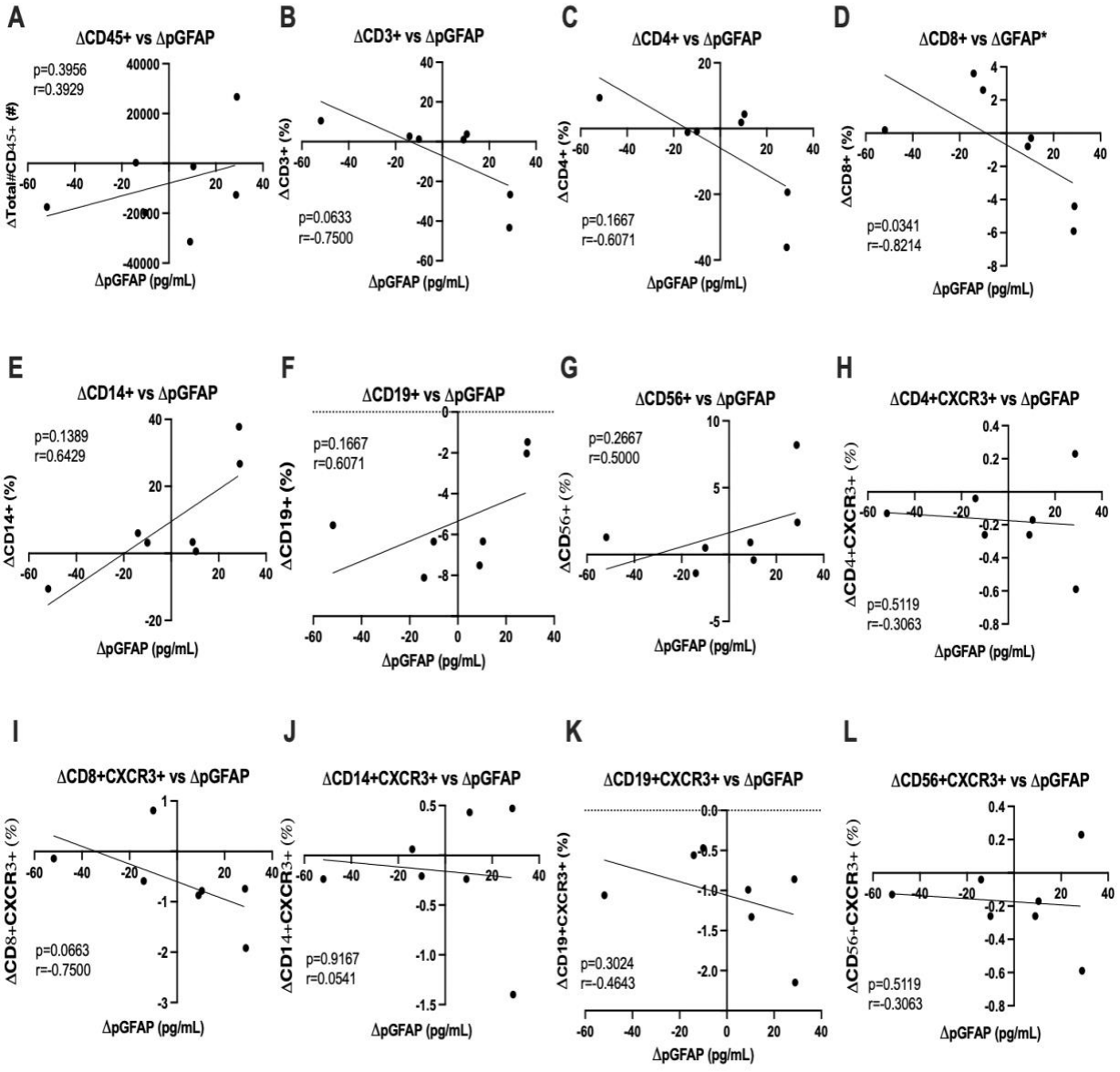

Figure 3.17. High Efficacy DMT does not result in any significant change in plasma GFAP or concomitant increase or decrease in immune cells. Pre- and post-DMT initiation, patients with RRMS had blood draws. Immune cells were measured Cytoflex flow cytometer (Beckman Coulter). CD45+, CD3+, CD4+, CD8+, CD56+, CD14+, CD19+, CD4+CXCR3+, CD8+CXCR3+, CD14+CXCR3+, CD19+CXCR3+, and CD56+CXCR3+ immune cells were quantified using FlowJo software and normalized to each represent a percentage of total CD45+ cells (Figure 2.1). Spearman correlation did demonstrate a significant correlation between ΔGFAP and ΔCD8+ (p=0.0341; r=-0.8214) (Figure 3.17D).
Normalization of immune cell to total CD45+ cells. High Eff = High efficacy DMT; ΔpGFAP = change in plasma GFAP; Δimmune cell = change in relevant immune cell. Bonferroni correction requires p=0.0003 for statistical significance.

Spearman correlation revealed a trend towards a significant association between delta plasma CXCL13 and the delta plasma CD56+CXCR3+ immune cell subsets in the moderate efficacy group ($p=0.0154$; $r=0.8333$) (Figure 3.18L).

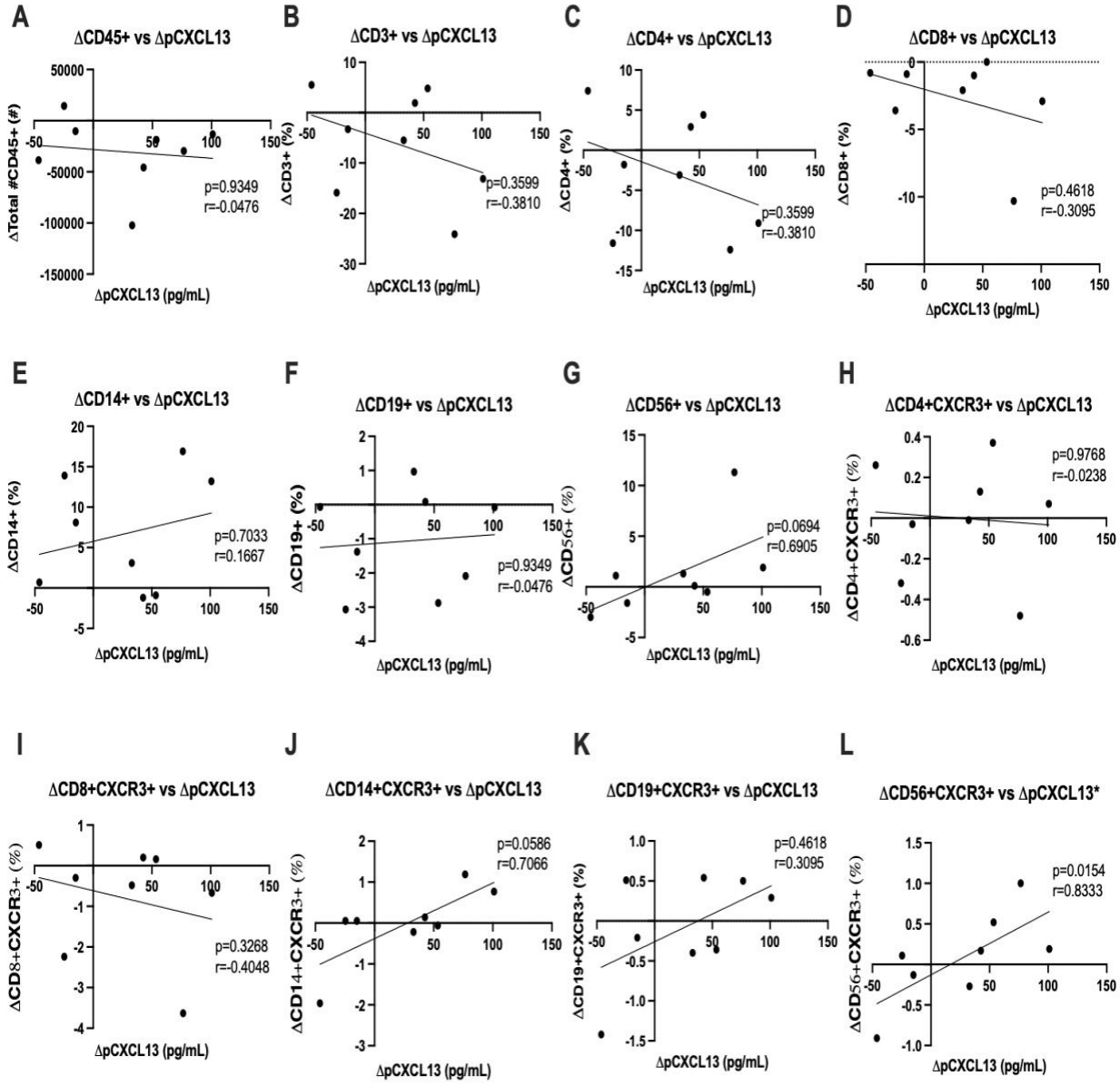

Figure 3.18. Moderate-Efficacy DMT does not result in any significant change in plasma CXCL13 or concomitant increase or decrease in immune cells.. Pre- and post-DMT initiation, patients with RRMS had blood draws. Immune cells were measured Cytoflex flow cytometer (Beckman Coulter). CD45+, CD3+, CD4+, CD8+, CD56+, CD14+, CD19+, CD4+CXCR3+, CD8+CXCR3+, CD14+CXCR3+, CD19+CXCR3+, and CD56+CXCR3+ immune cells were quantified using FlowJo software and normalized (n) to each represent a percentage of total CD45+ cells (Figure 2.1). Spearman correlation demonstrated a trend towards a significant correlation between ΔpCXCL13 and ΔCD56+CXCR3+ (p=0.0154; r=0.8333) (Figure 3.18L). Normalization of immune cell to total CD45+ cells. Mod Eff = Moderate efficacy DMT; ΔpCXCL13 = change in plasma CXCL13; Δimmune cell = change in relevant immune cell. Bonferroni correction requires p=0.0003 for statistical significance.

In the high-efficacy DMT group, there were no statistically significant associations between the plasma delta CXCL13 and the normalized delta plasma immune cells (Figure 3.19).

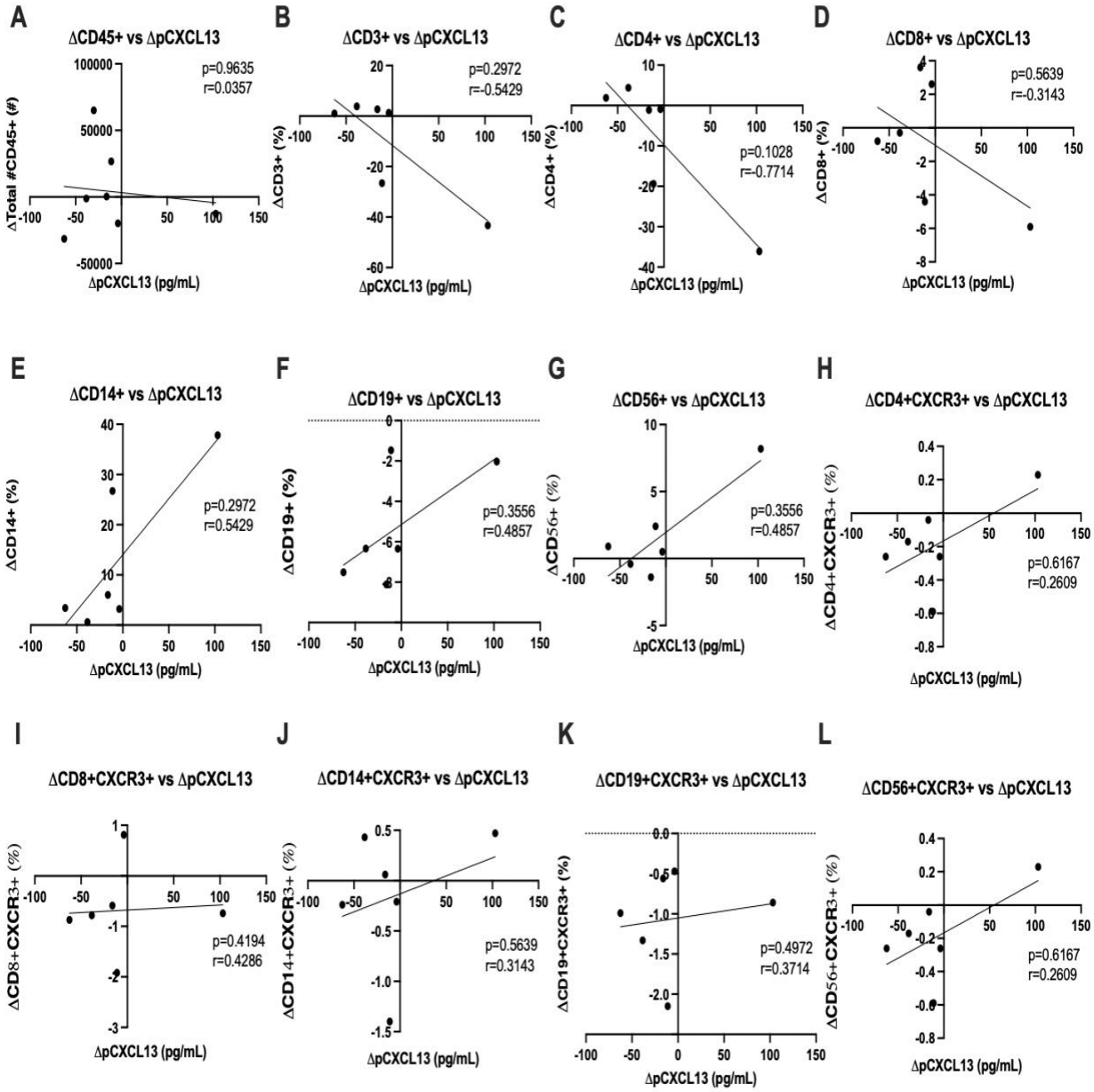

Figure 3.19. High-Efficacy DMT did not result in any significant change in plasma CXCL13 or concomitant change in immune cells. Pre- and post-DMT initiation, patients with RRMS had blood draws. Immune cells were measured Cytoflex flow cytometer (Beckman Coulter). CD45+, CD3+, CD4+, CD8+, CD56+, CD14+, CD19+, CD4+CXCR3+, CD8+CXCR3+, CD14+CXCR3+, CD19+CXCR3+, and CD56+CXCR3+ immune cells were quantified using FlowJo software and normalized to each represent a percentage of total CD45+ cells (Figure 2.1). Spearman correlation did not demonstrate a significant correlation between ΔpCXCL13 and any Δimmune cell. Normalization of immune cell to total CD45+ cells; High Eff = High efficacy DMT; ΔpCXCL13 = change in plasma CXCL13; Δimmune cell = change in relevant immune cell. Bonferroni correction requires p=0.0003 for statistical significance.

3.6 High Efficacy DMT Exerts More Effect over the Relationship Between Several Plasma Biomarkers and Immune Cell Subsets than Moderate Efficacy DMT

To discern the impact of DMT group on the relationship seen between delta plasma biomarkers and delta plasma immune cell subsets, an analysis of covariance (ANCOVA) was conducted on the relationship between each delta plasma biomarker (NfL, GFAP, and CXCL13) and delta plasma immune cell subsets between groups (moderate efficacy versus high efficacy). First, this analysis revealed a trend towards a significant difference between groups in the relationship between delta plasma NfL and delta plasma CD19+ ($p=0.0062$) (Figure 3.20F), CD4+CXCR3+ ($p=0.0172$) (Figure 3.20H), CD8+CXCR3+ ($p=0.0148$) (Figure 3.20I), CD14+CXCR3+ ($p=0.0416$) (Figure 3.20J), and CD19+CXCR3+ ($p=0.0151$) (Figure 3.20K). Bonferroni correction requires $p=0.0003$ for statistical significance.

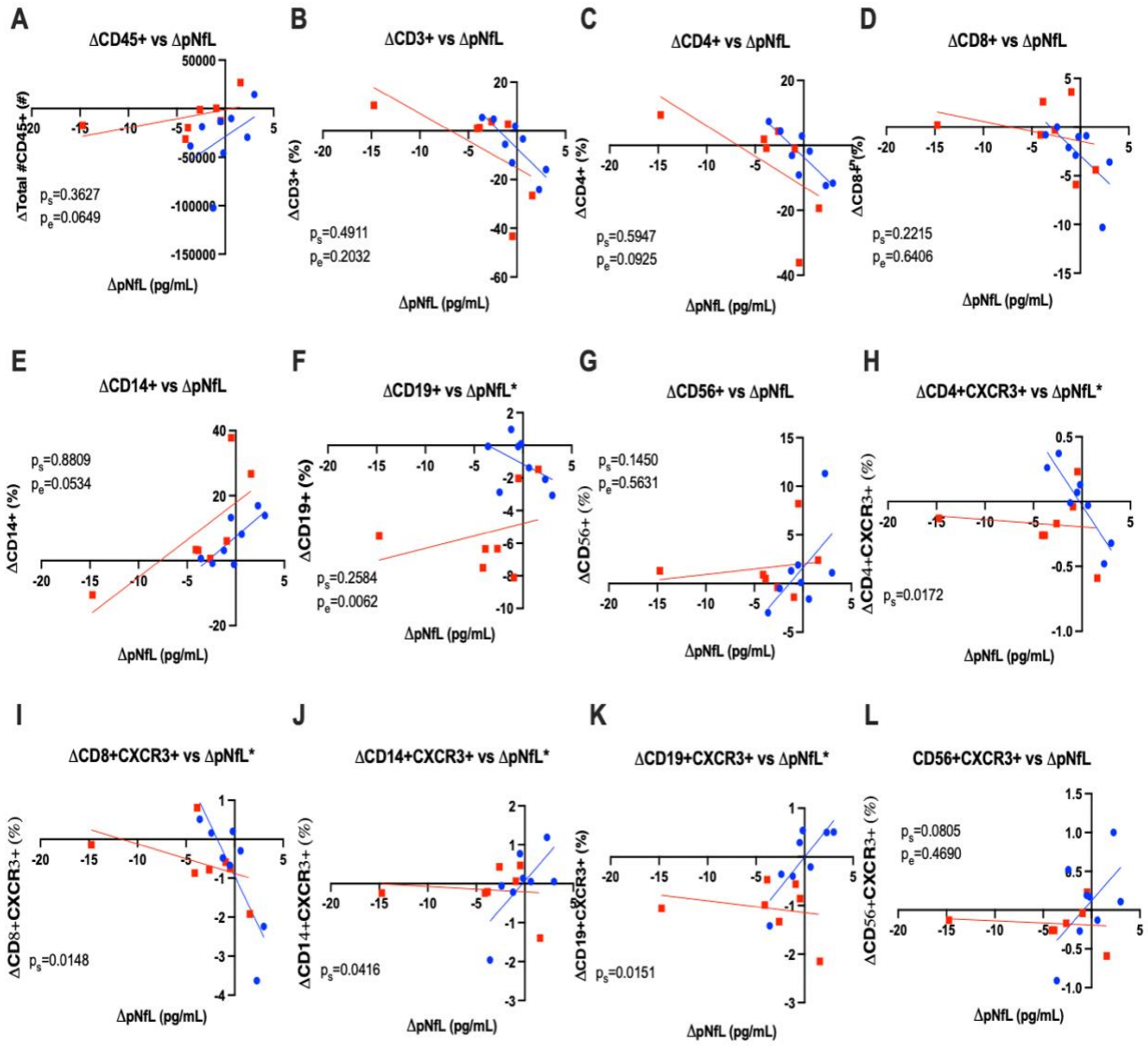

Figure 3.20. High efficacy DMT results in a larger effect on the relationship between plasma NfL and CD19+, CD4+CXCR3+, CD8+CXCR3+, CD14+CXCR3+, and CD19+CXCR3+ immune cells. Pre- and post-DMT initiation, patients with RRMS had blood draws. Immune cells were measured Cytoflex flow cytometer (Beckman Coulter). CD45+, CD3+, CD4+, CD8+, CD56+, CD14+, CD19+, CD4+CXCR3+, CD8+CXCR3+, CD14+CXCR3+, CD19+CXCR3+, and CD56+CXCR3+ immune cells were quantified using FlowJo software and normalized to each represent a percentage of total CD45+ cells (Figure 2.1). ANCOVA revealed a trend towards a significant difference in the relationship between ΔpNfL and ΔCD19+ (p_s=0.2584; p_e=0.0062), ΔCD4+CXCR3+ (p_s=0.0172), ΔCD8+CXCR3+ (p_s =0.0148); ΔCD14+CXCR3+ (p_s=0.0416), and ΔCD19+CXCR3+ (p_s=0.0151) (Figure 3.20F and H-K). Data points/lines in blue represent the moderate efficacy DMT group while data points/lines in red represent the high efficacy DMT group. ΔpNfL = change in plasma NfL; Δimmune cell = change in relevant immune cell. p_s = p-value of slope differences; p_e = p-value of elevations/intercepts. * $p < 0.05$. Bonferroni requires p=0.0003 for statistical significance.

Secondly, there was a trend towards a significant difference between groups in the relationship between delta plasma GFAP and delta plasma CD3+ (p_s=0.0373) (Figure 3.21B), CD4+ (p_s=0.0417) (Figure 3.21C), CD14+ (p_s=0.0129) (Figure 3.21E), CD19+ (p=0.0051) (Figure 3.21F), and CD19+CXCR3+ (p_e=0.0151) (Figure 3.21K) immune cell subsets. Bonferroni correction requires p=0.0003 for statistical significance.

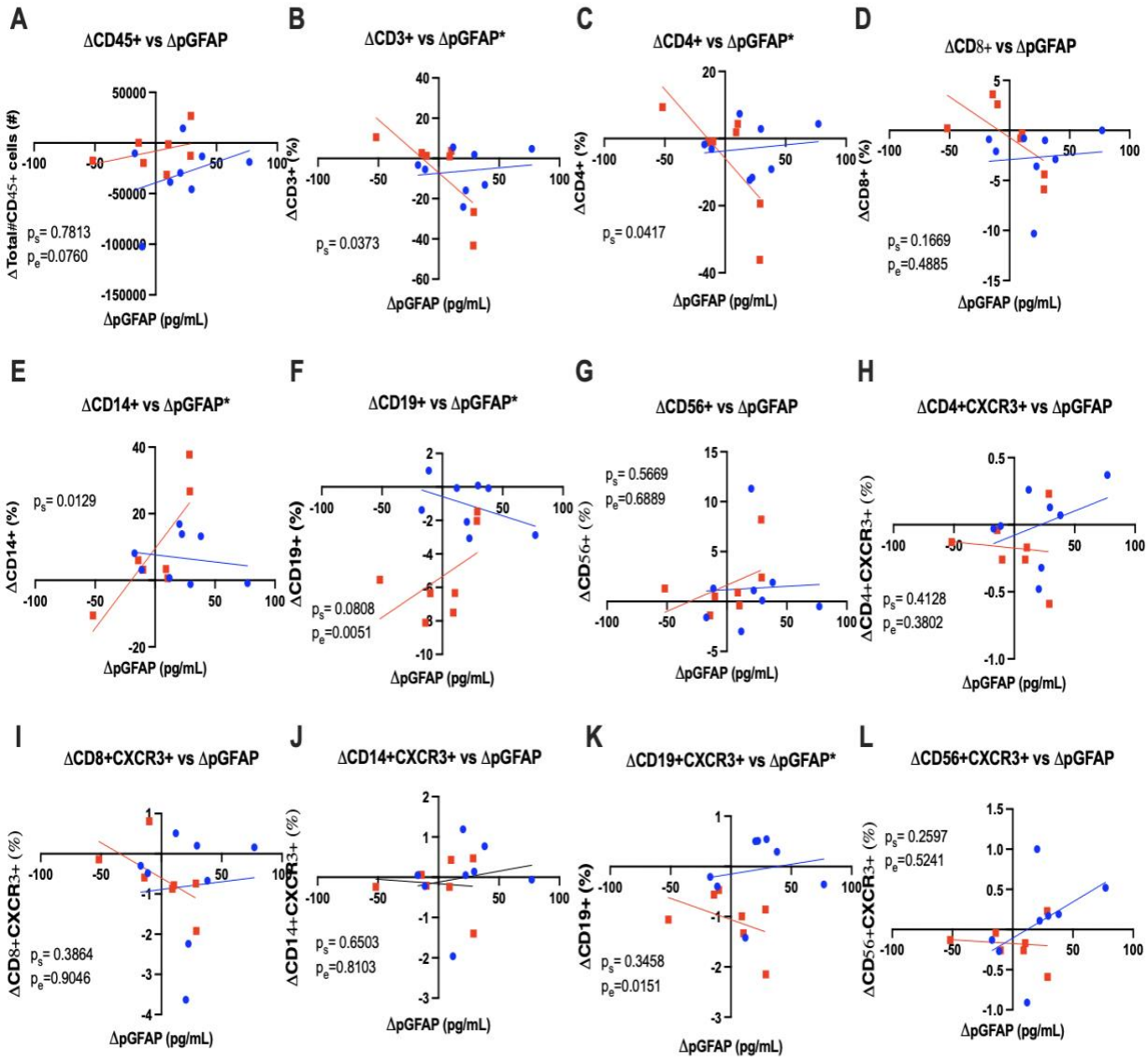

Figure 3.21. High efficacy DMT results in a larger effect on the relationship between plasma GFAP and CD14+, CD19+, and CD19+CXCR3+ immune cells. Pre- and post-DMT initiation, patients with RRMS had blood draws. Immune cells were measured Cytoflex flow cytometer (Beckman Coulter). CD45+, CD3+, CD4+, CD8+, CD56+, CD14+, CD19+, CD4+CXCR3+, CD8+CXCR3+, CD14+CXCR3+, CD19+CXCR3+, and CD56+CXCR3+ immune cells were quantified using FlowJo software and normalized to each represent a percentage of total CD45+ cells (Figure 2.1). ANCOVA revealed a trend towards a significant difference in the relationship between ΔpGFAP and ΔCD3+ (p_s=0.0373), ΔCD4+ (p_s =0.0417), ΔCD14+ (p_s=0.0129), ΔCD19+ (p_s =0.0808; p_e=0.0051), and ΔCD19+CXCR3+ (p_s=0.0151) (Figure 3.21B-C, E and F). Data points/lines in blue represent the moderate efficacy DMT group while data points/lines in red represent the high efficacy DMT group. n (immune cell) = normalization of immune cell to total CD45+ cells; ΔpNfL = change in plasma NfL; Δimmune cell = change in relevant immune cell. p_s = p-value of slope differences; p_e = p-value of elevations/intercepts. * $p < 0.05$. Bonferroni requires p=0.0003 for statistical significance.

Lastly, a trend towards a significant difference was seen between groups in the relationship between delta plasma CXCL13 and delta plasma CD4+ ($p=0.0448$) (Figure 3.22C), CD19+ ($p=0.0090$) (Figure 3.22F), and CD19+CXCR3+ ($p=0.0380$) (Figure 3.22K) immune cell subsets.

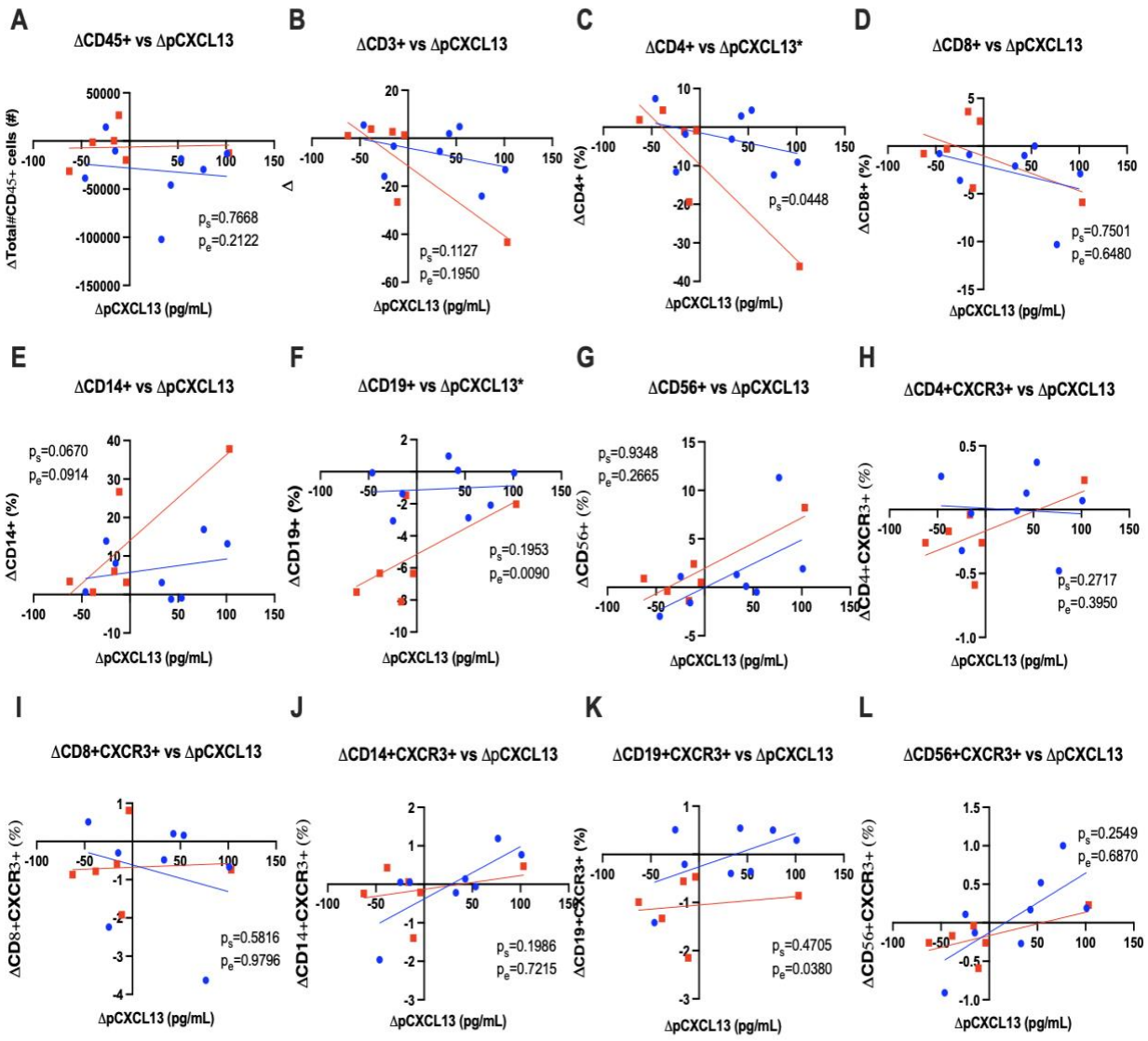

Figure 3.22. High efficacy DMT results in a larger effect on the relationship between plasma CXCL13 CD4+, CD19+, and CD19+CXCR3+ immune cells. Pre- and post-DMT initiation, patients with RRMS had blood draws. Immune cells were measured Cytoflex flow cytometer (Beckman Coulter). CD45+, CD3+, CD4+, CD8+, CD56+, CD14+, CD19+, CD4+CXCR3+, CD8+CXCR3+, CD14+CXCR3+, CD19+CXCR3+, and CD56+CXCR3+ immune cells were quantified using FlowJo software and normalized to each represent a percentage of total CD45+ cells (Figure 2.1). ANCOVA revealed a trend towards a significant difference in the relationship between ΔpCXCL13 and ΔCD4+ (p_s=0.0448, ΔCD19+ (p_s =0.1953; p_e=0.0090), and ΔCD19+CXCR3+ (p_s=0.4705; p_e=0.0380) (Figure 3.22C, F, and K). Data points/lines in blue represent the moderate efficacy DMT group while data points/lines in red represent the high efficacy DMT group. Normalization of immune cell to total CD45+ cells; High Eff = High efficacy DMT; ΔpNfL = change in plasma NfL; Δimmune cell = change in relevant immune cell. Bonferroni correction requires p=0.0003 for statistical significance.

CHAPTER 4

4. Discussion

This research study aimed to delineate the effect of DMT on plasma biomarkers and immune cell subsets and whether high efficacy DMT resulted in a greater decline in these markers over moderate efficacy DMT. The original hypothesis was that adult NL patients with RRMS who receive high efficacy DMTs will have significantly lower plasma NfL and CXCL13 concentrations lower than those adult RRMS patients receiving the "treat-to-target" therapeutic approach with moderately efficacious DMTs. Furthermore, this study hypothesized that there would be no statistically significant difference in plasma GFAP concentrations between RRMS patient cohorts. This study was successful in rejecting the null hypothesis and demonstrating that there was a significantly greater decline in plasma NfL concentrations in patients taking high efficacy DMT over those taking moderate efficacy DMT. In addition to this, several specific immune cell subsets involved in the pathogenesis of MS were also shown to be significantly reduced in patients taking high efficacy DMTs over those taking moderate efficacy DMTs.

4.1 Plasma NfL Correlates Positively with CSF NfL

The first goal of this study was to demonstrate that the baseline (pre-DMT) plasma concentrations of NfL significantly correlated with CSF NfL in patients with RRMS, allowing for plasma NfL to act as a surrogate biofluid biomarker for CSF NfL. Prior to the initiation of any DMT, those patients with confirmed RRMS demonstrated a high concordance between plasma and CSF NfL ($p<0.0001$). The second goal from this analysis was to examine whether the initial concentrations of CSF and plasma NfL, GFAP, and CXCL13 differed significantly between RRMS patients that would go on to receive moderate versus high efficacy DMT. Prior retrospective analyses have shown that CSF NfL can be used as a predictor of patients with CIS

that will eventually develop clinically definite MS up to six years prior to clinical diagnosis (Varhaug 2019). Furthermore, patients with RRMS or SPMS have demonstrated higher baseline levels of CSF NfL than healthy controls and these levels increase when patients experience a relapse (Varhaug 2019). This analysis confirmed that those RRMS patients that would go on to receive high efficacy DMT had higher CSF NfL concentrations, compared to their counterparts who would go on to receive moderate efficacy DMT. It should be noted here that age, sex, EDSS, time from last clinical demyelinating relapse, and MRI activity, were matched between the two groups. Despite the lack of differentiating clinical and radiological features, it appears that those patients who went on to receive high efficacy DMT had a higher baseline level of neuroinflammatory induced axonal injury, as evidenced by the significantly elevated levels of CSF NfL.

Previous literature identified patients with RRMS who experienced a recent relapse or disease progression, (as evidenced by increase in EDSS), have higher serum NfL levels than healthy controls and MS patients in remission, and these same patients are also more likely to develop a further relapse or EDSS progression within the following year (Disanto 2017; Disanto 2016; Varhaug 2018). These findings indicate the utility of serum NfL as a surrogate marker of recent neuronal damage, and the potential clinical use in the early identification of disease activity in the absence of clinical and radiological evidence. While the RRMS cohort in this study did not demonstrate a significantly higher level of plasma NfL at baseline in patients going on to receive high efficacy DMT, the difference approached significance ($p=0.0693$).

A prior meta-analysis of CSF and serum GFAP demonstrated a significantly higher concentration of GFAP in the CSF and serum of MS patients (all subtypes) compared to healthy controls (Sun 2021). However, while there was no significant difference seen between patients

with RRMS and healthy controls, the levels of serum GFAP were significantly higher in those patients with PPMS versus those with RRMS, indicating that CSF and serum GFAP can potentially accurately differentiate MS subtypes (Sun 2021). In this study cohort, the baseline concentrations of plasma GFAP did not significantly differ between groups, reflective of the fact that all patients carried a confirmed diagnosis of RRMS. DiSano and colleagues demonstrated that CSF and serum CXCL13 concentrations were significantly elevated in MS patients compared to NIND controls and could be used to predict future disease activity in MS patients (DiSano 2020). Our cohort did not demonstrate any significant difference in baseline plasma concentrations of CXCL13, again reflective of the fact that all patients carried a confirmed diagnosis of RRMS. The third goal of our analysis was to elucidate the relationship between baseline levels of plasma NfL, GFAP and CXCL13. Spearman correlation did not find any significant associations between baseline plasma NfL, GFAP and CXCL13, suggesting that these plasma biomarkers do not denote the same pathophysiological processes underpinning MS pathogenesis.

The last portion of the baseline analysis involved examining the correlations between baseline concentrations of plasma biomarkers (NfL, GFAP, and CXCL13), and plasma immune cell subsets. Spearman correlation revealed a trend towards a statistically significant association between baseline plasma NfL and levels of CD14+ cells ($p=0.0139$; $r=0.6093$) (Figure 3.3E). In other words, higher concentrations of plasma NfL result in higher plasma CD14+ immune cell counts. As concentrations of CD14+ immune cells were seen to rise in accordance with plasma NfL, this builds on previous evidence that has outlined the role of CD14+ monocytes in MS pathophysiology (Gjelstrup 2017). Gjelstrup and colleagues discovered that there is expansion of the CD16+ monocyte population in MS patients when compared to health controls, and

presented data to suggest that this expansion is primarily attributable to nonclassical monocyte populations (Gjelstrup 2017).

4.2 Time from Relapse Association with Baseline Biomarker and Immune Cell Subset Concentrations

Spearman correlation did not reveal any significant association between time from last clinical demyelinating relapse and baseline concentrations of CSF or plasma NfL, or plasma GFAP and CXCL13, albeit this did approach significance for CSF NfL (Figure 3.6). With this said, all patients in this study were at least 1 month away from their last relapse. Thus, if patients received a LP and blood draw closer to their last relapse, it is possible that we would have seen a significant correlation with these biomarkers. One patient within this cohort represented an outlier (i.e., time from relapse of 37 months), and given the potential significant confounding effects on the data, this patient was removed from this analysis, as well as from subsequent analysis of time from relapse versus baseline normalized plasma immune cell subset concentration. As previous literature has identified and proposed immune cell subset changes in PBMCs as surrogate biomarkers of disease activity, progression, and response to treatment, spearman correlation was conducted for time from last clinical relapse and baseline levels of immune cell subsets (Brune-Ingebretsen 2023). This same prior analysis identified that the most significant deviation in immunophenotype was based upon DMT choice and not disease course (Brune-Ingebretsen 2023). There was a trend towards a significant association between time from last clinical demyelinating relapse and baseline normalized CD3+ ($p=0.0123$; $r=0.6585$), CD4+ ($p=0.0029$; $r=0.7477$), and CD19+ ($p=0.0150$; $r=0.6428$) immune cell subsets in this cohort (Figure 3.7B, 3.7C, and 3.7F).

CD3 is expressed at all stages of T cell development and marks many circulating T cells in the blood, on which it forms a complex with the T cell receptor (TCR) (Munschauer 1993). CD4+ T cells have classically been viewed as the primary cellular drivers of MS (Carnero 2020; Compston 2008). In general, when an antigen is presented to the adaptive immune system, APCs provide the relevant antigen to CD4+ T cells in the periphery, with subsequent activation of the CD4+ T cells, resulting in generation of autoreactive proinflammatory Th1 and Th17 subsets (Riley, 2016). While MS is classically thought of as a T cell mediated disease, B cells have been shown to play a role in acute demyelination and contribute to disease progression, and trials demonstrating the effect of anti-CD20 B cell therapies (rituximab and ocrelizumab) in MS have strengthened this notion (Dal Bianco 2008; Wootla 2011; Sospedra 2016; Hauser 2008; Kappos 2011). CD20 is a surface antigen with expression on pre-B and mature B cells and previous studies investigating the efficacy of rituximab in MS patients have revealed that CD20 may target antigen presentation by B cells and activation of T cells, influencing the production of proinflammatory and regulatory cytokines (Wootla 2011). The CD19 cell marker encompasses a greater portion of the lifespan of the B cell, from the pro B cell formation to plasmablast (Baker 2017).

In this study it has been shown that pre-DMT levels of CD3+ and CD4+ T cells and CD19+ B cells (lymphoid lineage) increase in plasma the further away a RRMS patient is from a clinical demyelinating relapse. This could signal that despite apparent clinical remission, there is ongoing peripheral activation of both the T and B cell lymphoid lineage, representing active pathophysiological processes underpinning MS. As such, active surveillance of plasma immune cell subsets could represent a novel biofluid biomarker to assess for ongoing disease state in patients whose disease appears well controlled clinically and radiographically.

4.3 Patients receiving high efficacy DMT have lower levels of plasma NfL, CD19+ and CD19+CXCR3+ immune cells whereas patients receiving moderate efficacy DMT have lower levels of CD45+, CD8+ and CD19+CXCR3+ immune cells

The Wilcoxon matched pairs rank test demonstrated a trend towards a significant reduction in the plasma NfL concentrations in RRMS patients who were treated with high efficacy DMT (cladribine, ocrelizumab, and ofatumumab) ($p=0.0068$) (Figure 8B). Bonferroni correction requires $p < 0.0003$. Given that plasma NfL has been identified as a potential biomarker of disease activity, and that this study has shown that plasma NfL is differentially decreased between moderate and high efficacy DMT, this finding has potential implications for guiding clinical practice towards higher efficacy treatment early in RRMS disease course.

Previous studies have identified a significant reduction of total leukocyte and lymphocyte counts, CD4+ and CD8+ T cells, and T regulatory cells (Tregs) after 1 year of treatment with DMF (moderate efficacy DMT), and an increased frequency of myeloid cells (CD14+) with minimal effect on both NK and B cells (Diebold 2022; Walo-Delgado 2021). Furthermore, this same analysis found that significant reductions in the CXCR3 effector-memory T cells, and that this immune cell subset could potentially serve as a biomarker for treatment response (Diebold 2022). The findings of this current study are in line with these findings, as patients who received treatment with a moderate-efficacy DMT showed a trend towards a significant decline in their plasma CD45+ cells ($p=0.0391$) (Figure 9A), CD8+ cells ($p=0.0156$) (Figure 9D), and CD19+CXCR3+ cells ($p=0.0078$) (Figure 9K) from baseline. Furthermore, the patients in the high efficacy DMT group demonstrated a trend towards a significant decline in plasma CD19+ cells ($p=0.0156$) and CD19+CXCR3+ cells ($p=0.0156$) (Figure 10F and 10K). This study elucidates the differential effects of DMT subtype on the peripheral immune cell milieu, with

moderate efficacy DMT suppressing T cell lineages (CD45+ total and CD8+), and high efficacy DMT suppressing B cell lineages to a greater degree (CD19+ and CD19+CXCR3+). This finding is not surprising, as the majority of RRMS patients on high efficacy DMT in this cohort were taking B cell depleting therapies and this has been verified in previous literature (Brune-Ingebretsen 2023).

CXCR3+ expression in peripheral T cells has previously been shown to be higher compared to NIND controls, with a higher proportion of CXCR3+ T cells in the CSF compared to the peripheral compartment, a finding which suggests that CXCR3 is an important mediator of T cell trafficking into the CNS (Teleshova 2002; Blandford 2023). Other studies have reported enrichment of CXCR3+ B cells in the CSF of RRMS patients when compared to matched blood samples, suggesting that there is a common CXCR3 driven lymphocyte recruitment pathway in MS (van Langelaar 2019). The results of this study demonstrate that pre-DMT, CD19+CXCR3+ immune cell subsets were elevated, and that with any type of DMT, CD19+CXCR3+ cells are reduced in the periphery. Unfortunately, no CD19+CXCR3+ CSF samples pre- and post-DMT were measured to examine prior hypothesis, and this would be of interest moving forward. Nevertheless, the results of this study do demonstrate that no matter the choice of DMT, peripheral activation of CD19+CXCR3+ immune function is reduced.

4.4 High efficacy DMT results in a greater decline in CD19+ and CD19+CXCR3+ plasma immune cells than moderate efficacy DMT

In the high efficacy DMT group, normalized plasma CD19+ and CD19+CXCR3+ immune cells were approached a significant decrease in comparison to levels in patients treated with moderate efficacy DMT ($p=0.0093$; $p=0.0093$) (Figure 3.11F and 3.11K). This finding

supports the notion that high efficacy DMT can more drastically dampen the peripheral neuroinflammatory activity seen in MS, potentially leading to better long-term disease control. There were no significant differences seen in delta plasma GFAP and delta CXCL13 between groups. As GFAP is emerging as a potential biomarker of MS disease progression, all patients in this study were diagnosed as having RRMS, and as the follow-up period of this study was 1 year, differences in plasma GFAP between groups was not expected.

Further delineation of the relationship between the change in plasma biomarker concentrations and immune cell subsets within each DMT group was conducted via a spearman correlation of delta plasma biomarker versus and delta plasma immune cell subsets. In the moderate efficacy group, with a decrease in plasma NfL levels (i.e., negative delta), a concomitant decrease in CD19+CXCR3+ immune cells, and increase in CD3+, CD4+, CD8+, and CD4+CXCR3+ immune cells (i.e., positive delta) was seen. In other words, based upon the nature of this relationship, plasma NfL would be expected to increase with increasing concentrations of plasma CD19+CXCR3+, and declining concentrations of CD3+, CD4+ and CD8+ T cells. This study elucidates the preferential positive relationship between plasma NfL and B cell lineage immune cell markers, as well as the negative relationship seen between plasma NfL and T cell lineage immune cell markers. Furthermore, this study demonstrates that for those RRMS patients taking high efficacy DMT, with a decrease in plasma NfL levels, a concomitant decrease in CD45+ and CD14+ immune cells and increase in CD4+ immune cells occur. In addition to delineating the relationship between plasma NfL and immune cell subsets, this research highlights the key preferential changes that occur in immune cell subsets depending on choice of DMT.

In addition to the associations seen between delta plasma NfL and immune cell subsets, a

trend towards a significant negative relationship was seen between delta plasma GFAP and delta CD8+ cells in those patients taking high efficacy DMT. In other words, as plasma GFAP increases, the levels of CD8+ immune cells will decrease in the periphery. Plasma GFAP is proposed as an emerging biofluid biomarker of disease progression, whereby inflammation in this phase becomes compartmentalized within the CNS, with minimal peripheral immune inflammation. As such, the finding from this study that plasma GFAP is negatively correlated with peripheral CD8+ immune cell concentration could help strengthen this hypothesis. Furthermore, a trend towards a significant positive relationship was seen between delta plasma CXCL13 and delta CD56+CXCR3+ immune cells, meaning that with increasing concentrations of CXCL13 in the periphery, a concomitant rise in CD56+CXCR3+ immune cells would be seen. While the implications of this finding require further research in a larger prospective cohort, one can hypothesize that as CXCL13 is produced in the periphery, but not intrathecally, that CXCL13 in the periphery co-activates CD56+CXCR3+ immune cells, driving an innate immune inflammatory activity (DiSano 2020).

4.5 High Efficacy DMT Exerts More Effect over the Relationship Between Several Plasma Biomarkers and Immune Cell Subsets than Moderate Efficacy DMT

The final analysis of this study focused on partitioning out the true impact of DMT choice on the relationship between delta plasma biomarkers and immune cell subsets. ANCOVA analysis revealed that the choice of high efficacy DMT exerted a larger effect on the relationship between plasma NfL and CD19+, CD4+CXCR3+, CD8+CXCR3+, CD14+CXCR3+, and CD19+CXCR3+ immune cell subsets. In other words, when compared to moderate efficacy DMT, high efficacy DMT lowered the CD19+, CD4+CXCR3+, CD8+CXCR3+, CD14+CXCR3+, and CD19+CXCR3+ immune cell subset concentrations in plasma in tandem

with decreasing plasma NfL.

ANCOVA between group analysis of DMT effect over the relationship between delta plasma GFAP and immune cell subsets revealed a trend towards high efficacy DMT having a greater modulatory effect over the relationship between plasma GFAP and CD3+, CD4+, CD14+, CD19+, and CD19+CXCR3+ immune cell subsets when compared to moderate efficacy DMT. Bonferroni correction required $p < 0.0003$. While not significant, when compared to moderate efficacy DMT, high efficacy DMT modulated and lowered the CD3+, CD4+, CD14+, CD19+, and CD19+CXCR3+ immune cell subsets in tandem with decreasing plasma GFAP.

ANCOVA between group analysis of DMT effect over the relationship between delta plasma CXCL13 and immune cell subsets revealed a trend towards high efficacy DMT modulating the relationship between plasma CXCL13 and CD4+, CD19+, and CD19+CXCR3+ immune cell subsets to a greater degree than moderate efficacy DMT. Although not statistically significant, when compared to moderate efficacy DMT, high efficacy DMT altered and lowered the CD4+, CD19+, and CD19+CXCR3+ immune cell subsets in tandem with decreasing plasma CXCL13. In essence, this study, while a small, combined retrospective and prospective, provides evidence that immune cell subsets and plasma NfL are differentially modulated by high versus moderate DMTs, and that incorporating specific immune cell subsets with plasma biomarkers may provide insights into DMT effectiveness in MS.

4.6 Conclusion and Future Directions

Overall, this analysis revealed many trends towards significance between plasma NfL and immune cell subpopulations. In addition to this, high efficacy DMT, while not significantly different, did demonstrate a trend towards differential modulation of this relationship over moderate efficacy DMTs. As this was an exploratory analysis with a small patient sample, future

studies employing a larger group of patients, with focused hypotheses centered around the trends seen in this analysis, would be beneficial to further elucidate these relationships. Given these findings, this suggests that early implementation of high efficacy DMT may have a better chance at reducing the proinflammatory cascade seen in the pathogenesis of MS, and that combining circulating immune cell subset frequencies with plasma concentrations may be a better predictor of DMT response, and potential prognosis of disease course overall.

A limitation of this study lies in the specificity of NfL as a potential MS biomarker. NfL is not specific to MS, even though it has been validated as a potentially clinically useful marker in multiple studies. As neurofilaments are found in the cytoplasm of neurons, all diseases that lead to neuronal and axonal damage can result in an increased concentration of these proteins in the CSF. In addition to this, NfL CSF concentrations steadily increase by approximately 2.2% per year in healthy controls (Disanto 2017). Despite these limitations, plasma NfL, when combined with other molecular biomarkers for MS, give valuable information regarding MS diagnosis, prognosis, and treatment response. Furthermore, post-treatment samples were collected over a variable range of time (~6mos-2 years), which may contribute to variability within the cohorts. Other limitations of this study include the lack of healthy or NIND controls, the small sample size (although adequately powered for the primary analysis), the exploratory nature of the study leading to the need for Bonferroni correction, the grouping of patients into two broad DMT categories as opposed to individual DMT, as well as the relatively short follow-up period.

Future directions of this research would include longitudinal analysis of this patient cohort clinical data, including EDSS scores (to determine change in EDSS in response to DMT and potential association with plasma NfL and immune cell subsets). Ideally, this patient cohort

will be followed clinically for several years, allowing neurologists and researchers to monitor EDSS, ARR and quantitative radiological data (MRI T1-weighted enhancing lesions or T2-weighted lesion load). Through serial measurements of paraclinical data such as immune cell subsets, plasma NfL, GFAP, CXCL13, MRI data, as well as clinical course through EDSS and ARR, it will be possible to draw more concrete conclusions regarding the association of plasma biomarkers and immune cell subsets with overall disease course. Furthermore, IgG index was available on only a subset of the patients within this cohort, and as such, was not included in the analysis due to low numbers. Ideally, measurement of the IgG index of these patients would be conducted and correlated with the aforementioned biomarkers and immune cell subsets.

In summary, the results of this study demonstrate that there was a significant association between plasma NfL and several different immune cell subpopulations, and that this relationship is differentially modulated by the use of high and moderate efficacy DMT. The results of this analysis support the preliminary findings from TREAT-MS and DELIVER-MS, demonstrating that earlier implementation of high efficacy DMT allows for a greater reduction in the pathogenic proinflammatory cascade in MS, potentially resulting in better patient outcomes. Furthermore, combining circulating immune cell subset frequencies with plasma concentrations of NfL may prove to be a better predictor of DMT response, and potential prognosis of disease course overall.

References

Abdelhak A, Huss A, Kassubek J, Tumani H, Otto M. Serum GFAP as a biomarker for disease severity in multiple sclerosis. Sci Rep. 2018 Oct 4;8(1):14798. doi: 10.1038/s41598-018-33158-8. Erratum in: Sci Rep. 2019 Jun 5;9(1):8433. PMID: 30287870; PMCID: PMC6172254.

Absinta M, Sati P, Masuzzo F, Nair G, Sethi V, Kolb H, Ohayon J, Wu T, Cortese ICM, Reich DS. Association of Chronic Active Multiple Sclerosis Lesions With Disability In Vivo. JAMA Neurol. 2019 Dec 1;76(12):1474-1483. doi: 10.1001/jamaneurol.2019.2399. Erratum in: JAMA Neurol. 2019 Dec 1;76(12):1520. PMID: 31403674; PMCID: PMC6692692.

Absinta M, Sati P, Schindler M, Leibovitch EC, Ohayon J, Wu T, Meani A, Filippi M, Jacobson S, Cortese IC, Reich DS. Persistent 7-tesla phase rim predicts poor outcome in new multiple sclerosis patient lesions. J Clin Invest. 2016 Jul 1;126(7):2597-609. doi: 10.1172/JCI86198. Epub 2016 Jun 6. PMID: 27270171; PMCID: PMC4922708.

Absinta M, Sati P, Fechner A, Schindler MK, Nair G, Reich DS. Identification of Chronic Active Multiple Sclerosis Lesions on 3T MRI. AJNR Am J Neuroradiol. 2018 Jul;39(7):1233-1238. doi: 10.3174/ajnr.A5660. Epub 2018 May 3. PMID: 29724768; PMCID: PMC6039266.

Achiron A, Mandel M, Dreyer-Alster S, Harari G, Magalashvili D, Sonis P, Dolev M, Menascu S, Flechter S, Falb R, Gurevich M. Humoral immune response to COVID-19 mRNA vaccine in patients with multiple sclerosis treated with high-efficacy disease-modifying therapies. Ther Adv Neurol Disord. 2021 Apr 22;14:17562864211012835. doi: 10.1177/17562864211012835. PMID: 34035836; PMCID: PMC8072850.

AlSharoqi IA, Aljumah M, Bohlega S, Boz C, Daif A, El-Koussa S, Inshasi J, Kurtuncu M, Müller T, Retief C, Sahraian MA, Shaygannejad V, Slassi I, Taha K, Zakaria M, Sørensen PS. Immune Reconstitution Therapy or Continuous Immunosuppression for the Management of Active Relapsing-Remitting Multiple Sclerosis Patients? A Narrative Review. Neurol Ther. 2020 Jun;9(1):55-66. doi: 10.1007/s40120-020-00187-3. Epub 2020 Apr 15. PMID: 32297127; PMCID: PMC7229056.

Amankwah N, Marrie RA, Bancej C, Garner R, Manuel DG, Wall R, Finès P, Bernier J, Tu K, Reimer K. Multiple sclerosis in Canada 2011 to 2031: results of a microsimulation modelling study of epidemiological and economic impacts. Health Promot Chronic Dis Prev Can. 2017 Feb;37(2):37-48. doi: 10.24095/hpcdp.37.2.02. PMID: 28273039; PMCID: PMC5607528.

Arsenault S, Benoit RY, Clift F, Moore CS. Does the use of the Bruton Tyrosine Kinase inhibitors and the c-kit inhibitor masitinib result in clinically significant outcomes among patients with various forms of multiple sclerosis? Mult Scler Relat Disord. 2022 Nov;67:104164. doi: 10.1016/j.msard.2022.104164. Epub 2022 Sep 6. PMID: 36126539.

Ayrignac X, Le Bars E, Duflos C, Hirtz C, Maleska Maceski A, Carra-Dallière C, Charif M, Pinna F, Prin P, Menjot de Champfleur N, Deverdun J, Kober T, Marechal B, Fartaria MJ, Corredor Jerez R, Labauge P, Lehmann S. Serum GFAP in multiple sclerosis: correlation with disease type and MRI markers of disease severity. Sci Rep. 2020 Jul 2;10(1):10923. doi: 10.1038/s41598-020-67934-2. PMID: 32616916; PMCID: PMC7331703.

Baker D, Marta M, Pryce G, Giovannoni G, Schmierer K. Memory B Cells are Major Targets for Effective Immunotherapy in Relapsing Multiple Sclerosis. EBioMedicine. 2017 Feb;16:41-50. doi: 10.1016/j.ebiom.2017.01.042. Epub 2017 Jan 31. PMID: 28161400; PMCID: PMC5474520.

Balashov KE, Rottman JB, Weiner HL, Hancock WW. CCR5(+) and CXCR3(+) T cells are increased in multiple sclerosis and their ligands MIP-1alpha and IP-10 are expressed in demyelinating brain lesions. Proc Natl Acad Sci U S A. 1999 Jun 8;96(12):6873-8. doi: 10.1073/pnas.96.12.6873. PMID: 10359806; PMCID: PMC22009.

Banwell B, Giovannoni G, Hawkes C, Lublin F. Editors' welcome and a working definition for a multiple sclerosis cure. Mult Scler Relat Disord. 2013 Apr;2(2):65-7. doi: 10.1016/j.msard.2012.12.001. Epub 2013 Jan 21. PMID: 25877624.

Barkhof F. The clinico-radiological paradox in multiple sclerosis revisited. Curr Opin Neurol. 2002 Jun;15(3):239-45. doi: 10.1097/00019052-200206000-00003. PMID: 12045719.

Bar-Or A, Fawaz L, Fan B, Darlington PJ, Rieger A, Ghorayeb C, Calabresi PA, Waubant E, Hauser SL, Zhang J, Smith CH. Abnormal B-cell cytokine responses a trigger of T-cell-mediated disease in MS? Ann Neurol. 2010 Apr;67(4):452-61. doi: 10.1002/ana.21939. PMID: 20437580.

Bar-Or A, Pachner A, Menguy-Vacheron F, Kaplan J, Wiendl H. Teriflunomide and its mechanism of action in multiple sclerosis. Drugs. 2014 Apr;74(6):659-74. doi: 10.1007/s40265-014-0212-x. PMID: 24740824; PMCID: PMC4003395.

Bar-Or A, Calkwood JC, Chognot C, Evershed J, Fox EJ, Herman A, Manfrini M, McNamara J, Robertson DS, Stokmaier D, Wendt JK, Winthrop KL, Traboulsee A. Effect of ocrelizumab on vaccine responses in patients with multiple sclerosis: The VELOCE study. Neurology. 2020 Oct 6;95(14):e1999-e2008. doi: 10.1212/WNL.0000000000010380. Epub 2020 Jul 29. PMID: 32727835; PMCID: PMC7843152.

Barry B, Erwin AA, Stevens J, Tornatore C. Fingolimod Rebound: A Review of the Clinical Experience and Management Considerations. Neurol Ther. 2019 Dec;8(2):241-250. doi: 10.1007/s40120-019-00160-9. Epub 2019 Nov 1. PMID: 31677060; PMCID: PMC6858914.

Benedict RHB, Amato MP, DeLuca J, Geurts JJG. Cognitive impairment in multiple sclerosis: clinical management, MRI, and therapeutic avenues. Lancet Neurol. 2020 Oct;19(10):860-871. doi: 10.1016/S1474-4422(20)30277-5. Epub 2020 Sep 16. PMID: 32949546; PMCID: PMC10011205.

Bermel RA, Rae-Grant AD, Fox RJ. Diagnosing multiple sclerosis at a later age: more than just progressive myelopathy. Mult Scler. 2010 Nov;16(11):1335-40. doi: 10.1177/1352458510377334. Epub 2010 Jul 29. PMID: 20670982.

Blandford SN, Fudge NJ, Moore CS. CXCL10 Is Associated with Increased Cerebrospinal Fluid Immune Cell Infiltration and Disease Duration in Multiple Sclerosis. Biomolecules. 2023 Aug 1;13(8):1204. doi: 10.3390/biom13081204. PMID: 37627269; PMCID: PMC10452246.

Bodini B, Chard D, Altmann DR, Tozer D, Miller DH, Thompson AJ, Wheeler-Kingshott C, Ciccarelli O. White and gray matter damage in primary progressive MS: The chicken or the egg? Neurology. 2016 Jan 12;86(2):170-6. doi: 10.1212/WNL.0000000000002237. Epub 2015 Dec 16. PMID: 26674332; PMCID: PMC4731689.

Boyko AN, Boyko OV. Cladribine tablets' potential role as a key example of selective immune reconstitution therapy in multiple sclerosis. Degener Neurol Neuromuscul Dis. 2018 May 3;8:35-44. doi: 10.2147/DNND.S161450. PMID: 30050387; PMCID: PMC6053904.

Brown JWL, Coles A, Horakova D, Havrdova E, Izquierdo G, Prat A, Girard M, Duquette P, Trojano M, Lugaresi A, Bergamaschi R, Grammond P, Alroughani R, Hupperts R, McCombe P, Van Pesch V, Sola P, Ferraro D, Grand'Maison F, Terzi M, Lechner-Scott J, Flechter S, Slee M, Shaygannejad V, Pucci E, Granella F, Jokubaitis V, Willis M, Rice C, Scolding N, Wilkins A, Pearson OR, Ziemssen T, Hutchinson M, Harding K, Jones J, McGuigan C, Butzkueven H, Kalincik T, Robertson N; MSBase Study Group. Association of Initial Disease-Modifying Therapy With Later Conversion to Secondary Progressive Multiple Sclerosis. JAMA. 2019 Jan 15;321(2):175-187. doi: 10.1001/jama.2018.20588. Erratum in: JAMA. 2020 Apr 7;323(13):1318. PMID: 30644981; PMCID: PMC6439772.

Brownlee WJ, Hardy TA, Fazekas F, Miller DH. Diagnosis of multiple sclerosis: progress and challenges. Lancet. 2017 Apr 1;389(10076):1336-1346. doi: 10.1016/S0140-6736(16)30959-X. Epub 2016 Nov 24. PMID: 27889190.

Brune-Ingebretsen S, Høgestøl EA, de Rosbo NK, Berg-Hansen P, Brunborg C, Blennow K, Zetterberg H, Paul F, Uccelli A, Villoslada P, Harbo HF, Berge T. Immune cell subpopulations and serum neurofilament light chain are associated with increased risk of disease worsening in multiple sclerosis. J Neuroimmunol. 2023 Sep 15;382:578175. doi: 10.1016/j.jneuroim.2023.578175. Epub 2023 Aug 7. PMID: 37573634.

Bussas M, El Husseini M, Harabacz L, Pineker V, Grahl S, Pongratz V, Berthele A, Riederer I, Zimmer C, Hemmer B, Kirschke JS, Mühlau M. Multiple sclerosis lesions and atrophy in the spinal cord: Distribution across vertebral levels and correlation with disability. Neuroimage Clin. 2022;34:103006. doi: 10.1016/j.nicl.2022.103006. Epub 2022 Apr 13. PMID: 35468568; PMCID: PMC9059154.

Calabrese M, Poretto V, Favaretto A, Alessio S, Bernardi V, Romualdi C, Rinaldi F, Perini P, Gallo P. Cortical lesion load associates with progression of disability in multiple sclerosis. Brain. 2012 Oct;135(Pt 10):2952-61. doi: 10.1093/brain/aws246. PMID: 23065788.

Calabresi PA, Tranquill LR, Dambrosia JM, Stone LA, Maloni H, Bash CN, Frank JA, McFarland HF. Increases in soluble VCAM-1 correlate with a decrease in MRI lesions in multiple sclerosis treated with interferon beta-1b. Ann Neurol. 1997 May;41(5):669-74. doi: 10.1002/ana.410410517. PMID: 9153530.

Carnero Contentti E, Correale J. Bruton's tyrosine kinase inhibitors: a promising emerging treatment option for multiple sclerosis. Expert Opin Emerg Drugs. 2020 Dec;25(4):377-381. doi: 10.1080/14728214.2020.1822817. Epub 2020 Sep 21. PMID: 32910702.

Chitnis T, Arnold DL, Banwell B, Brück W, Ghezzi A, Giovannoni G, Greenberg B, Krupp L, Rostásy K, Tardieu M, Waubant E, Wolinsky JS, Bar-Or A, Stites T, Chen Y, Putzki N, Merschhemke M, Gärtner J; PARADIGMS Study Group. Trial of Fingolimod versus Interferon Beta-1a in Pediatric Multiple Sclerosis. N Engl J Med. 2018 Sep 13;379(11):1017-1027. doi: 10.1056/NEJMoa1800149. PMID: 30207920.

Chitnis T, Gonzalez C, Healy BC, Saxena S, Rosso M, Barro C, Michalak Z, Paul A, Kivisakk P, Diaz-Cruz C, Sattarnezhad N, Pierre IV, Glanz BI, Tomic D, Kropshofer H, Häring D, Leppert D, Kappos L, Bakshi R, Weiner HL, Kuhle J. Neurofilament light chain serum levels correlate with 10-year MRI outcomes in multiple sclerosis. Ann Clin Transl Neurol. 2018 Oct 16;5(12):1478-1491. doi: 10.1002/acn3.638. PMID: 30564615; PMCID: PMC6292183.

Ciotti JR, Valtcheva MV, Cross AH. Effects of MS disease-modifying therapies on responses to vaccinations: A review. Mult Scler Relat Disord. 2020 Oct;45:102439. doi: 10.1016/j.msard.2020.102439. Epub 2020 Aug 1. PMID: 32769063; PMCID: PMC7395588.

Cohen JA, Barkhof F, Comi G, Hartung HP, Khatri BO, Montalban X, Pelletier J, Capra R, Gallo P, Izquierdo G, Tiel-Wilck K, de Vera A, Jin J, Stites T, Wu S, Aradhye S, Kappos L; TRANSFORMS Study Group. Oral fingolimod or intramuscular interferon for relapsing multiple sclerosis. N Engl J Med. 2010 Feb 4;362(5):402-15. doi: 10.1056/NEJMoa0907839. Epub 2010 Jan 20. PMID: 20089954.

Cohen JA, Coles AJ, Arnold DL, Confavreux C, Fox EJ, Hartung HP, Havrdova E, Selmaj KW, Weiner HL, Fisher E, Brinar VV, Giovannoni G, Stojanovic M, Ertik BI, Lake SL, Margolin DH, Panzara MA, Compston DA; CARE-MS I investigators. Alemtuzumab versus interferon beta 1a as first-line treatment for patients with relapsing-remitting multiple sclerosis: a randomised controlled phase 3 trial. Lancet. 2012 Nov 24;380(9856):1819-28. doi: 10.1016/S0140-6736(12)61769-3. Epub 2012 Nov 1. PMID: 23122652.

Cohen JA, Comi G, Selmaj KW, Bar-Or A, Arnold DL, Steinman L, Hartung HP, Montalban X, Kubala Havrdová E, Cree BAC, Sheffield JK, Minton N, Raghupathi K, Huang V, Kappos L; RADIANCE Trial Investigators. Safety and efficacy of ozanimod versus interferon beta-1a in relapsing multiple sclerosis (RADIANCE): a multicentre, randomised, 24-month, phase 3 trial. Lancet Neurol. 2019 Nov;18(11):1021-1033. doi: 10.1016/S1474-4422(19)30238-8. Epub 2019 Sep 3. PMID: 31492652.

Coles AJ, Twyman CL, Arnold DL, Cohen JA, Confavreux C, Fox EJ, Hartung HP, Havrdova E, Selmaj KW, Weiner HL, Miller T, Fisher E, Sandbrink R, Lake SL, Margolin DH, Oyuela P, Panzara MA, Compston DA; CARE-MS II investigators. Alemtuzumab for patients with relapsing multiple sclerosis after disease-modifying therapy: a randomised controlled phase 3 trial. Lancet. 2012 Nov 24;380(9856):1829-39. doi: 10.1016/S0140-6736(12)61768-1. Epub 2012 Nov 1. PMID: 23122650.

Comabella M, Pericot I, Goertsches R, Nos C, Castillo M, Blas Navarro J, Río J, Montalban X. Plasma osteopontin levels in multiple sclerosis. J Neuroimmunol. 2005 Jan;158(1-2):231-9. doi: 10.1016/j.jneuroim.2004.09.004. PMID: 15589058.

Comabella M, Fernández M, Martin R, Rivera-Vallvé S, Borrás E, Chiva C, Julià E, Rovira A, Cantó E, Alvarez-Cermeño JC, Villar LM, Tintoré M, Montalban X. Cerebrospinal fluid chitinase 3-like 1 levels are associated with conversion to multiple sclerosis. Brain. 2010 Apr;133(Pt 4):1082-93. doi: 10.1093/brain/awq035. Epub 2010 Mar 17. PMID: 20237129.

Comabella M, Montalban X. Body fluid biomarkers in multiple sclerosis. Lancet Neurol. 2014 Jan;13(1):113-26. doi: 10.1016/S1474-4422(13)70233-3. PMID: 24331797.

Comi G, Martinelli V, Rodegher M, Moiola L, Bajenaru O, Carra A, Elovaara I, Fazekas F, Hartung HP, Hillert J, King J, Komoly S, Lubetzki C, Montalban X, Myhr KM, Ravnborg M, Rieckmann P, Wynn D, Young C, Filippi M; PreCISe study group. Effect of glatiramer acetate on conversion to clinically definite multiple sclerosis in patients with clinically isolated syndrome (PreCISe study): a randomised, double-blind, placebo-controlled trial. Lancet. 2009 Oct 31;374(9700):1503-11. doi: 10.1016/S0140-6736(09)61259-9. Epub 2009 Oct 6. Erratum in: Lancet. 2010 Apr 24;375(9724):1436. PMID: 19815268.

Comi G, Kappos L, Selmaj KW, Bar-Or A, Arnold DL, Steinman L, Hartung HP, Montalban X, Kubala Havrdová E, Cree BAC, Sheffield JK, Minton N, Raghupathi K, Ding N, Cohen JA; SUNBEAM Study Investigators. Safety and efficacy of ozanimod versus interferon beta-1a in relapsing multiple sclerosis (SUNBEAM): a multicentre, randomised, minimum 12-month, phase 3 trial. Lancet Neurol. 2019 Nov;18(11):1009-1020. doi: 10.1016/S1474-4422(19)30239-X. Epub 2019 Sep 3. PMID: 31492651.

Comi G, Bar-Or A, Lassmann H, Uccelli A, Hartung HP, Montalban X, Sørensen PS, Hohlfeld R, Hauser SL; Expert Panel of the 27th Annual Meeting of the European Charcot Foundation. Role of B Cells in Multiple Sclerosis and Related Disorders. Ann Neurol. 2021 Jan;89(1):13-23. doi: 10.1002/ana.25927. Epub 2020 Nov 4. PMID: 33091175; PMCID: PMC8007167.

Confavreux C, Vukusic S, Moreau T, Adeleine P. Relapses and progression of disability in multiple sclerosis. N Engl J Med. 2000 Nov 16;343(20):1430-8. doi: 10.1056/NEJM200011163432001. PMID: 11078767.

Correale J, Gaitán MI, Ysrraelit MC, Fiol MP. Progressive multiple sclerosis: from pathogenic mechanisms to treatment. Brain. 2017 Mar 1;140(3):527-546. doi: 10.1093/brain/aww258. PMID: 27794524.

Cree BAC, Mares J, Hartung HP. Current therapeutic landscape in multiple sclerosis: an evolving treatment paradigm. Curr Opin Neurol. 2019 Jun;32(3):365-377. doi: 10.1097/WCO.0000000000000700. Erratum in: Curr Opin Neurol. 2019 Oct;32(5):782. PMID: 30985372.

Cree BAC, Arnold DL, Chataway J, Chitnis T, Fox RJ, Pozo Ramajo A, Murphy N, Lassmann H. Secondary Progressive Multiple Sclerosis: New Insights. Neurology. 2021 Aug 24;97(8):378-388. doi: 10.1212/WNL.0000000000012323. Epub 2021 Jun 4. PMID: 34088878; PMCID: PMC8397587.

Cross AH, Stark JL, Lauber J, Ramsbottom MJ, Lyons JA. Rituximab reduces B cells and T cells in cerebrospinal fluid of multiple sclerosis patients. J Neuroimmunol. 2006 Nov;180(1-2):63-70.

doi: 10.1016/j.jneuroim.2006.06.029. Epub 2006 Aug 14. PMID: 16904756; PMCID: PMC1769354.

Cross A, Riley C. Treatment of Multiple Sclerosis. Continuum (Minneap Minn). 2022 Aug 1;28(4):1025-1051. doi: 10.1212/CON.0000000000001170. PMID: 35938656.

Dal Bianco A, Bradl M, Frischer J, Kutzelnigg A, Jellinger K, Lassmann H. Multiple sclerosis and Alzheimer's disease. Ann Neurol. 2008 Feb;63(2):174-83. doi: 10.1002/ana.21240. PMID: 17924575.

Deisenhammer F, Zetterberg H, Fitzner B, Zettl UK. The Cerebrospinal Fluid in Multiple Sclerosis. Front Immunol. 2019 Apr 12;10:726. doi: 10.3389/fimmu.2019.00726. PMID: 31031747; PMCID: PMC6473053.

Demortiere S, Rico A, Maarouf A, Boutiere C, Pelletier J, Audoin B. Maintenance of natalizumab during the first trimester of pregnancy in active multiple sclerosis. Mult Scler. 2021 Apr;27(5):712-718. doi: 10.1177/1352458520912637. Epub 2020 Mar 23. PMID: 32202216.

Diebold M, Galli E, Kopf A, Sanderson NSR, Callegari I, Benkert P, Gonzalo Núñez N, Ingelfinger F, Herms S, Cichon S, Kappos L, Kuhle J, Becher B, Claassen M, Derfuss T. High-dimensional immune profiling identifies a biomarker to monitor dimethyl fumarate response in multiple sclerosis. Proc Natl Acad Sci U S A. 2022 Aug 2;119(31):e2205042119. doi: 10.1073/pnas.2205042119. Epub 2022 Jul 26. PMID: 35881799; PMCID: PMC9351505.

DiSano KD, Gilli F, Pachner AR. Intrathecally produced CXCL13: A predictive biomarker in multiple sclerosis. Mult Scler J Exp Transl Clin. 2020 Dec 16;6(4):2055217320981396. doi: 10.1177/2055217320981396. PMID: 33403120; PMCID: PMC7747124.

Disanto G, Adiutori R, Dobson R, Martinelli V, Dalla Costa G, Runia T, Evdoshenko E, Thouvenot E, Trojano M, Norgren N, Teunissen C, Kappos L, Giovannoni G, Kuhle J; International Clinically Isolated Syndrome Study Group. Serum neurofilament light chain levels are increased in patients with a clinically isolated syndrome. J Neurol Neurosurg Psychiatry. 2016 Feb;87(2):126-9. doi: 10.1136/jnnp-2014-309690. Epub 2015 Feb 25. PMID: 25716934.

Disanto G, Barro C, Benkert P, Naegelin Y, Schädelin S, Giardiello A, Zecca C, Blennow K, Zetterberg H, Leppert D, Kappos L, Gobbi C, Kuhle J; Swiss Multiple Sclerosis Cohort Study Group. Serum Neurofilament light: A biomarker of neuronal damage in multiple sclerosis. Ann Neurol. 2017 Jun;81(6):857-870. doi: 10.1002/ana.24954. PMID: 28512753; PMCID: PMC5519945.

Duddy M, Niino M, Adatia F, Hebert S, Freedman M, Atkins H, Kim HJ, Bar-Or A. Distinct effector cytokine profiles of memory and naive human B cell subsets and implication in multiple sclerosis. J Immunol. 2007 May 15;178(10):6092-9. doi: 10.4049/jimmunol.178.10.6092. PMID: 17475834.

Edan G, Miller D, Clanet M, Confavreux C, Lyon-Caen O, Lubetzki C, Brochet B, Berry I, Rolland Y, Froment JC, Cabanis E, Iba-Zizen MT, Gandon JM, Lai HM, Moseley I, Sabouraud

O. Therapeutic effect of mitoxantrone combined with methylprednisolone in multiple sclerosis: a randomised multicentre study of active disease using MRI and clinical criteria. J Neurol Neurosurg Psychiatry. 1997 Feb;62(2):112-8. doi: 10.1136/jnnp.62.2.112. PMID: 9048709; PMCID: PMC486720.

Eshaghi A, Prados F, Brownlee WJ, Altmann DR, Tur C, Cardoso MJ, De Angelis F, van de Pavert SH, Cawley N, De Stefano N, Stromillo ML, Battaglini M, Ruggieri S, Gasperini C, Filippi M, Rocca MA, Rovira A, Sastre-Garriga J, Vrenken H, Leurs CE, Killestein J, Pirpamer L, Enzinger C, Ourselin S, Wheeler-Kingshott CAMG, Chard D, Thompson AJ, Alexander DC, Barkhof F, Ciccarelli O; MAGNIMS study group. Deep gray matter volume loss drives disability worsening in multiple sclerosis. Ann Neurol. 2018 Feb;83(2):210-222. doi: 10.1002/ana.25145. Epub 2018 Feb 6. PMID: 29331092; PMCID: PMC5838522.

Filippi M, Preziosa P, Langdon D, Lassmann H, Paul F, Rovira À, Schoonheim MM, Solari A, Stankoff B, Rocca MA. Identifying Progression in Multiple Sclerosis: New Perspectives. Ann Neurol. 2020 Sep;88(3):438-452. doi: 10.1002/ana.25808. Epub 2020 Jul 6. PMID: 32506714.

Fillatreau S, Sweenie CH, McGeachy MJ, Gray D, Anderton SM. B cells regulate autoimmunity by provision of IL-10. Nat Immunol. 2002 Oct;3(10):944-50. doi: 10.1038/ni833. Epub 2002 Sep 3. PMID: 12244307.

Fischer JS, Rudick RA, Cutter GR, Reingold SC. The Multiple Sclerosis Functional Composite Measure (MSFC): an integrated approach to MS clinical outcome assessment. National MS Society Clinical Outcomes Assessment Task Force. Mult Scler. 1999 Aug;5(4):244-50. doi: 10.1177/135245859900500409. PMID: 10467383.

Floro S, Carandini T, Pietroboni AM, De Riz MA, Scarpini E, Galimberti D. Role of Chitinase 3-like 1 as a Biomarker in Multiple Sclerosis: A Systematic Review and Meta-analysis. Neurol Neuroimmunol Neuroinflamm. 2022 May 9;9(4):e1164. doi: 10.1212/NXI.0000000000001164. PMID: 35534236; PMCID: PMC9128043.

Fox RJ, Cree BA, De Sèze J, Gold R, Hartung HP, Jeffery D, Kappos L, Kaufman M, Montalbán X, Weinstock-Guttman B, Anderson B, Natarajan A, Ticho B, Duda P; RESTORE. MS disease activity in RESTORE: a randomized 24-week natalizumab treatment interruption study. Neurology. 2014 Apr 29;82(17):1491-8. doi: 10.1212/WNL.0000000000000355. Epub 2014 Mar 28. Erratum in: Neurology. 2015 Feb 24;84(8):862. multiple investigator names added. PMID: 24682966; PMCID: PMC4011468.

Friend S, Richman S, Bloomgren G, Cristiano LM, Wenten M. Evaluation of pregnancy outcomes from the Tysabri® (natalizumab) pregnancy exposure registry: a global, observational, follow-up study. BMC Neurol. 2016 Aug 24;16(1):150. doi: 10.1186/s12883-016-0674-4. PMID: 27552976; PMCID: PMC4995778.

Gjelstrup MC, Stilund M, Petersen T, Møller HJ, Petersen EL, Christensen T. Subsets of activated monocytes and markers of inflammation in incipient and progressed multiple sclerosis. Immunol Cell Biol. 2018 Feb;96(2):160-174. doi: 10.1111/imcb.1025. Epub 2017 Dec 11. PMID: 29363161; PMCID: PMC5836924.

Gill AJ, Schorr EM, Gadani SP, Calabresi PA. Emerging imaging and liquid biomarkers in multiple sclerosis. Eur J Immunol. 2023 Aug;53(8):e2250228. doi: 10.1002/eji.202250228. Epub 2023 May 28. PMID: 37194443; PMCID: PMC10524168.

Giovannoni G, Comi G, Cook S, Rammohan K, Rieckmann P, Soelberg Sørensen P, Vermersch P, Chang P, Hamlett A, Musch B, Greenberg SJ; CLARITY Study Group. A placebo-controlled trial of oral cladribine for relapsing multiple sclerosis. N Engl J Med. 2010 Feb 4;362(5):416-26. doi: 10.1056/NEJMoa0902533. Epub 2010 Jan 20. PMID: 20089960.

Giovannoni G, Soelberg Sorensen P, Cook S, Rammohan K, Rieckmann P, Comi G, Dangond F, Adeniji AK, Vermersch P. Safety and efficacy of cladribine tablets in patients with relapsing-remitting multiple sclerosis: Results from the randomized extension trial of the CLARITY study. Mult Scler. 2018 Oct;24(12):1594-1604. doi: 10.1177/1352458517727603. Epub 2017 Sep 5. PMID: 28870107.

Giovannoni G, Mathews J. Cladribine Tablets for Relapsing-Remitting Multiple Sclerosis: A Clinician's Review. Neurol Ther. 2022 Jun;11(2):571-595. doi: 10.1007/s40120-022-00339-7. Epub 2022 Mar 23. PMID: 35318617; PMCID: PMC8940595.

Greenfield AL, Hauser SL. B-cell Therapy for Multiple Sclerosis: Entering an era. Ann Neurol. 2018 Jan;83(1):13-26. doi: 10.1002/ana.25119. PMID: 29244240; PMCID: PMC5876115.

Guarnera C, Bramanti P, Mazzon E. Alemtuzumab: a review of efficacy and risks in the treatment of relapsing remitting multiple sclerosis. Ther Clin Risk Manag. 2017 Jul 14;13:871-879. doi: 10.2147/TCRM.S134398. PMID: 28761351; PMCID: PMC5522829.

Guerrero BL, Sicotte NL. Microglia in Multiple Sclerosis: Friend or Foe? Front Immunol. 2020 Mar 20;11:374. doi: 10.3389/fimmu.2020.00374. PMID: 32265902; PMCID: PMC7098953.

Haghikia A, Langer-Gould A, Rellensmann G, Schneider H, Tenenbaum T, Elias-Hamp B, Menck S, Zimmermann J, Herbstritt S, Marziniak M, Kümpfel T, Meinl I, Plavina T, Gold R, Hellwig K. Natalizumab use during the third trimester of pregnancy. JAMA Neurol. 2014 Jul 1;71(7):891-5. doi: 10.1001/jamaneurol.2014.209. PMID: 24821217.

Harding K, Williams O, Willis M, Hrastelj J, Rimmer A, Joseph F, Tomassini V, Wardle M, Pickersgill T, Robertson N, Tallantyre E. Clinical Outcomes of Escalation vs Early Intensive Disease-Modifying Therapy in Patients With Multiple Sclerosis. JAMA Neurol. 2019 May 1;76(5):536-541. doi: 10.1001/jamaneurol.2018.4905. PMID: 30776055; PMCID: PMC6515582.

Hartung HP, Gonsette R, König N, Kwiecinski H, Guseo A, Morrissey SP, Krapf H, Zwingers T; Mitoxantrone in Multiple Sclerosis Study Group (MIMS). Mitoxantrone in progressive multiple sclerosis: a placebo-controlled, double-blind, randomised, multicentre trial. Lancet. 2002 Dec 21-28;360(9350):2018-25. doi: 10.1016/S0140-6736(02)12023-X. PMID: 12504397.Hauser SL, Waubant E, Arnold DL, et al. B-cell depletion with rituximab in relapsing-remitting multiple sclerosis. *N Engl J Med*. 2008;358(7):676-688. doi:10.1056/NEJMoa0706383.

Hauser SL, Bar-Or A, Comi G, Giovannoni G, Hartung HP, Hemmer B, Lublin F, Montalban X, Rammohan KW, Selmaj K, Traboulsee A, Wolinsky JS, Arnold DL, Klingelschmitt G,

Masterman D, Fontoura P, Belachew S, Chin P, Mairon N, Garren H, Kappos L; OPERA I and OPERA II Clinical Investigators. Ocrelizumab versus Interferon Beta-1a in Relapsing Multiple Sclerosis. N Engl J Med. 2017 Jan 19;376(3):221-234. doi: 10.1056/NEJMoa1601277. Epub 2016 Dec 21. PMID: 28002679.

Hauser SL, Bar-Or A, Cohen JA, Comi G, Correale J, Coyle PK, Cross AH, de Seze J, Leppert D, Montalban X, Selmaj K, Wiendl H, Kerloeguen C, Willi R, Li B, Kakarieka A, Tomic D, Goodyear A, Pingili R, Häring DA, Ramanathan K, Merschhemke M, Kappos L; ASCLEPIOS I and ASCLEPIOS II Trial Groups. Ofatumumab versus Teriflunomide in Multiple Sclerosis. N Engl J Med. 2020 Aug 6;383(6):546-557. doi: 10.1056/NEJMoa1917246. PMID: 32757523.

He A, Merkel B, Brown JWL, Zhovits Ryerson L, Kister I, Malpas CB, Sharmin S, Horakova D, Kubala Havrdova E, Spelman T, Izquierdo G, Eichau S, Trojano M, Lugaresi A, Hupperts R, Sola P, Ferraro D, Lycke J, Grand'Maison F, Prat A, Girard M, Duquette P, Larochelle C, Svenningsson A, Petersen T, Grammond P, Granella F, Van Pesch V, Bergamaschi R, McGuigan C, Coles A, Hillert J, Piehl F, Butzkueven H, Kalincik T; MSBase study group. Timing of high-efficacy therapy for multiple sclerosis: a retrospective observational cohort study. Lancet Neurol. 2020 Apr;19(4):307-316. doi: 10.1016/S1474-4422(20)30067-3. Epub 2020 Mar 18. PMID: 32199096.

Hillert J, Magyari M, Soelberg Sørensen P, Butzkueven H, Van Der Welt A, Vukusic S, Trojano M, Iaffaldano P, Pellegrini F, Hyde R, Stawiarz L, Manouchehrinia A, Spelman T. Treatment Switching and Discontinuation Over 20 Years in the Big Multiple Sclerosis Data Network. Front Neurol. 2021 Mar 17;12:647811. doi: 10.3389/fneur.2021.647811. PMID: 33815259; PMCID: PMC8010264.

Huss A, Otto M, Senel M, Ludolph AC, Abdelhak A, Tumani H. A Score Based on NfL and Glial Markers May Differentiate Between Relapsing-Remitting and Progressive MS Course. Front Neurol. 2020 Jul 16;11:608. doi: 10.3389/fneur.2020.00608. PMID: 32765393; PMCID: PMC7378743.

Johnson KP, Brooks BR, Cohen JA, Ford CC, Goldstein J, Lisak RP, Myers LW, Panitch HS, Rose JW, Schiffer RB. Copolymer 1 reduces relapse rate and improves disability in relapsing-remitting multiple sclerosis: results of a phase III multicenter, double-blind placebo-controlled trial. The Copolymer 1 Multiple Sclerosis Study Group. Neurology. 1995 Jul;45(7):1268-76. doi: 10.1212/wnl.45.7.1268. PMID: 7617181.

Kalincik T, Cutter G, Spelman T, Jokubaitis V, Havrdova E, Horakova D, Trojano M, Izquierdo G, Girard M, Duquette P, Prat A, Lugaresi A, Grand'Maison F, Grammond P, Hupperts R, Oreja-Guevara C, Boz C, Pucci E, Bergamaschi R, Lechner-Scott J, Alroughani R, Van Pesch V, Iuliano G, Fernandez-Bolaños R, Ramo C, Terzi M, Slee M, Spitaleri D, Verheul F, Cristiano E, Sánchez-Menoyo JL, Fiol M, Gray O, Cabrera-Gomez JA, Barnett M, Butzkueven H. Defining reliable disability outcomes in multiple sclerosis. Brain. 2015 Nov;138(Pt 11):3287-98. doi: 10.1093/brain/awv258. Epub 2015 Sep 10. PMID: 26359291.

Kalincik T, Horakova D, Spelman T, Jokubaitis V, Trojano M, Lugaresi A, Izquierdo G, Rozsa C, Grammond P, Alroughani R, Duquette P, Girard M, Pucci E, Lechner-Scott J, Slee M,

Fernandez-Bolanos R, Grand'Maison F, Hupperts R, Verheul F, Hodgkinson S, Oreja-Guevara C, Spitaleri D, Barnett M, Terzi M, Bergamaschi R, McCombe P, Sanchez-Menoyo J, Simo M, Csepany T, Rum G, Boz C, Havrdova E, Butzkueven H; MSBase Study Group. Switch to natalizumab versus fingolimod in active relapsing-remitting multiple sclerosis. Ann Neurol. 2015 Mar;77(3):425-35. doi: 10.1002/ana.24339. Epub 2015 Jan 17. PMID: 25546031.

Kalincik T, Diouf I, Sharmin S, Malpas C, Spelman T, Horakova D, Havrdova EK, Trojano M, Izquierdo G, Lugaresi A, Prat A, Girard M, Duquette P, Grammond P, Jokubaitis V, van der Walt A, Grand'Maison F, Sola P, Ferraro D, Shaygannejad V, Alroughani R, Hupperts R, Terzi M, Boz C, Lechner-Scott J, Pucci E, Van Pesch V, Granella F, Bergamaschi R, Spitaleri D, Slee M, Vucic S, Ampapa R, McCombe P, Ramo-Tello C, Prevost J, Olascoaga J, Cristiano E, Barnett M, Saladino ML, Sanchez-Menoyo JL, Hodgkinson S, Rozsa C, Hughes S, Moore F, Shaw C, Butler E, Skibina O, Gray O, Kermode A, Csepany T, Singhal B, Shuey N, Piroska I, Taylor B, Simo M, Sirbu CA, Sas A, Butzkueven H; MSBase Study Group. Effect of Disease-Modifying Therapy on Disability in Relapsing-Remitting Multiple Sclerosis Over 15 Years. Neurology. 2021 Feb 2;96(5):e783-e797. doi: 10.1212/WNL.0000000000011242. Epub 2020 Dec 28. PMID: 33372028; PMCID: PMC7884998.

Kamma E, Lasisi W, Libner C, Ng HS, Plemel JR. Central nervous system macrophages in progressive multiple sclerosis: relationship to neurodegeneration and therapeutics. J Neuroinflammation. 2022 Feb 10;19(1):45. doi: 10.1186/s12974-022-02408-y. PMID: 35144628; PMCID: PMC8830034.

Kappos L, Radue EW, O'Connor P, Polman C, Hohlfeld R, Calabresi P, Selmaj K, Agoropoulou C, Leyk M, Zhang-Auberson L, Burtin P; FREEDOMS Study Group. A placebo-controlled trial of oral fingolimod in relapsing multiple sclerosis. N Engl J Med. 2010 Feb 4;362(5):387-401. doi: 10.1056/NEJMoa0909494. Epub 2010 Jan 20. PMID: 20089952.

Kappos L, Li D, Calabresi PA, O'Connor P, Bar-Or A, Barkhof F, Yin M, Leppert D, Glanzman R, Tinbergen J, Hauser SL. Ocrelizumab in relapsing-remitting multiple sclerosis: a phase 2, randomised, placebo-controlled, multicentre trial. Lancet. 2011 Nov 19;378(9805):1779-87. doi: 10.1016/S0140-6736(11)61649-8. Epub 2011 Oct 31. PMID: 22047971.

Kappos L, Mehling M, Arroyo R, Izquierdo G, Selmaj K, Curovic-Perisic V, Keil A, Bijarnia M, Singh A, von Rosenstiel P. Randomized trial of vaccination in fingolimod-treated patients with multiple sclerosis. Neurology. 2015 Mar 3;84(9):872-9. doi: 10.1212/WNL.0000000000001302. Epub 2015 Jan 30. PMID: 25636714.

Kappos L, De Stefano N, Freedman MS, Cree BA, Radue EW, Sprenger T, Sormani MP, Smith T, Häring DA, Piani Meier D, Tomic D. Inclusion of brain volume loss in a revised measure of 'no evidence of disease activity' (NEDA-4) in relapsing-remitting multiple sclerosis. Mult Scler. 2016 Sep;22(10):1297-305. doi: 10.1177/1352458515616701. Epub 2015 Nov 19. PMID: 26585439; PMCID: PMC5015759.

Kappos L, Fox RJ, Burcklen M, Freedman MS, Havrdová EK, Hennessy B, Hohlfeld R, Lublin F, Montalban X, Pozzilli C, Scherz T, D'Ambrosio D, Linscheid P, Vaclavkova A, Pirozek-Lawniczek M, Kracker H, Sprenger T. Ponesimod Compared With Teriflunomide in Patients

With Relapsing Multiple Sclerosis in the Active-Comparator Phase 3 OPTIMUM Study: A Randomized Clinical Trial. JAMA Neurol. 2021 May 1;78(5):558-567. doi: 10.1001/jamaneurol.2021.0405. PMID: 33779698; PMCID: PMC8008435.

Karpus WJ. Cytokines and chemokines in the pathogenesis of experimental autoimmune encephalomyelitis. *J Immunol*. 2020;204(2):316–326. doi:10.4049/jimmunol.1900914.

Kearney H, Altmann DR, Samson RS, Yiannakas MC, Wheeler-Kingshott CA, Ciccarelli O, Miller DH. Cervical cord lesion load is associated with disability independently from atrophy in MS. Neurology. 2015 Jan 27;84(4):367-73. doi: 10.1212/WNL.0000000000001186. Epub 2014 Dec 24. PMID: 25540312.

Khademi M, Kockum I, Andersson ML, Iacobaeus E, Brundin L, Sellebjerg F, Hillert J, Piehl F, Olsson T. Cerebrospinal fluid CXCL13 in multiple sclerosis: a suggestive prognostic marker for the disease course. Mult Scler. 2011 Mar;17(3):335-43. doi: 10.1177/1352458510389102. Epub 2010 Dec 6. PMID: 21135023.

Khan O, Rieckmann P, Boyko A, Selmaj K, Zivadinov R; GALA Study Group. Three times weekly glatiramer acetate in relapsing-remitting multiple sclerosis. Ann Neurol. 2013 Jun;73(6):705-13. doi: 10.1002/ana.23938. Epub 2013 Jun 28. PMID: 23686821.

Klineova S, Lublin FD. Clinical Course of Multiple Sclerosis. Cold Spring Harb Perspect Med. 2018 Sep 4;8(9):a028928. doi: 10.1101/cshperspect.a028928. PMID: 29358317; PMCID: PMC6120692.

Klotz L, Havla J, Schwab N, Hohlfeld R, Barnett M, Reddel S, Wiendl H. Risks and risk management in modern multiple sclerosis immunotherapeutic treatment. Ther Adv Neurol Disord. 2019 Apr 1;12:1756286419836571. doi: 10.1177/1756286419836571. PMID: 30967901; PMCID: PMC6444778.

Kuhle J, Pohl C, Mehling M, Edan G, Freedman MS, Hartung HP, Polman CH, Miller DH, Montalban X, Barkhof F, Bauer L, Dahms S, Lindberg R, Kappos L, Sandbrink R. Lack of association between antimyelin antibodies and progression to multiple sclerosis. N Engl J Med. 2007 Jan 25;356(4):371-8. doi: 10.1056/NEJMoa063602. PMID: 17251533.

Kuhle J, Barro C, Disanto G, Mathias A, Soneson C, Bonnier G, Yaldizli Ö, Regeniter A, Derfuss T, Canales M, Schluep M, Du Pasquier R, Krueger G, Granziera C. Serum neurofilament light chain in early relapsing remitting MS is increased and correlates with CSF levels and with MRI measures of disease severity. Mult Scler. 2016 Oct;22(12):1550-1559. doi: 10.1177/1352458515623365. Epub 2016 Jan 11. PMID: 26754800.

Lamers KJ, de Reus HP, Jongen PJ. Myelin basic protein in CSF as indicator of disease activity in multiple sclerosis. Mult Scler. 1998 Jun;4(3):124-6. doi: 10.1177/135245859800400306. PMID: 9762659.

Lassmann H, van Horssen J, Mahad D. Progressive multiple sclerosis: pathology and pathogenesis. Nat Rev Neurol. 2012 Nov 5;8(11):647-56. doi: 10.1038/nrneurol.2012.168. Epub 2012 Sep 25. PMID: 23007702.

Lublin FD, Reingold SC. Defining the clinical course of multiple sclerosis: results of an international survey. National Multiple Sclerosis Society (USA) Advisory Committee on Clinical Trials of New Agents in Multiple Sclerosis. Neurology. 1996 Apr;46(4):907-11. doi: 10.1212/wnl.46.4.907. PMID: 8780061.

Lublin FD, Reingold SC, Cohen JA, Cutter GR, Sørensen PS, Thompson AJ, Wolinsky JS, Balcer LJ, Banwell B, Barkhof F, Bebo B Jr, Calabresi PA, Clanet M, Comi G, Fox RJ, Freedman MS, Goodman AD, Inglese M, Kappos L, Kieseier BC, Lincoln JA, Lubetzki C, Miller AE, Montalban X, O'Connor PW, Petkau J, Pozzilli C, Rudick RA, Sormani MP, Stüve O, Waubant E, Polman CH. Defining the clinical course of multiple sclerosis: the 2013 revisions. Neurology. 2014 Jul 15;83(3):278-86. doi: 10.1212/WNL.0000000000000560. Epub 2014 May 28. PMID: 24871874; PMCID: PMC4117366.

Madeddu R, Farace C, Tolu P, Solinas G, Asara Y, Sotgiu MA, Delogu LG, Prados JC, Sotgiu S, Montella A. Cytoskeletal proteins in the cerebrospinal fluid as biomarker of multiple sclerosis. Neurol Sci. 2013 Feb;34(2):181-6. doi: 10.1007/s10072-012-0974-4. Epub 2012 Feb 24. PMID: 22362332.

Maghazachi AA. G protein-coupled receptors in natural killer cells. J Leukoc Biol. 2003 Jul;74(1):16-24. doi: 10.1189/jlb.0103019. PMID: 12832438.

Magliozzi R, Howell O, Vora A, Serafini B, Nicholas R, Puopolo M, Reynolds R, Aloisi F. Meningeal B-cell follicles in secondary progressive multiple sclerosis associate with early onset of disease and severe cortical pathology. Brain. 2007 Apr;130(Pt 4):1089-104. doi: 10.1093/brain/awm038. PMID: 17438020.

Mahajan KR, Ontaneda D. The Role of Advanced Magnetic Resonance Imaging Techniques in Multiple Sclerosis Clinical Trials. Neurotherapeutics. 2017 Oct;14(4):905-923. doi: 10.1007/s13311-017-0561-8. PMID: 28770481; PMCID: PMC5722766.

Marriott JJ, Miyasaki JM, Gronseth G, O'Connor PW; Therapeutics and Technology Assessment Subcommittee of the American Academy of Neurology. Evidence Report: The efficacy and safety of mitoxantrone (Novantrone) in the treatment of multiple sclerosis: Report of the Therapeutics and Technology Assessment Subcommittee of the American Academy of Neurology. Neurology. 2010 May 4;74(18):1463-70. doi: 10.1212/WNL.0b013e3181dc1ae0. PMID: 20439849; PMCID: PMC2871006.

Martinsen V, Kursula P. Multiple sclerosis and myelin basic protein: insights into protein disorder and disease. Amino Acids. 2022 Jan;54(1):99-109. doi: 10.1007/s00726-021-03111-7. Epub 2021 Dec 10. PMID: 34889995; PMCID: PMC8810476.

Matsui M, Araya S, Wang HY, Matsushima K, Saida T. Differences in systemic and central nervous system cellular immunity relevant to relapsing-remitting multiple sclerosis. J Neurol. 2005 Aug;252(8):908-15. doi: 10.1007/s00415-005-0778-z. Epub 2005 Mar 21. PMID: 15772738.

Mattsson N, Andreasson U, Zetterberg H, Blennow K; Alzheimer's Disease Neuroimaging Initiative. Association of Plasma Neurofilament Light With Neurodegeneration in Patients With Alzheimer Disease. JAMA Neurol. 2017 May 1;74(5):557-566. doi: 10.1001/jamaneurol.2016.6117. PMID: 28346578; PMCID: PMC5822204.

McCarthy CL, Tuohy O, Compston DA, Kumararatne DS, Coles AJ, Jones JL. Immune competence after alemtuzumab treatment of multiple sclerosis. Neurology. 2013 Sep 3;81(10):872-6. doi: 10.1212/WNL.0b013e3182a35215. Epub 2013 Aug 7. PMID: 23925762; PMCID: PMC3885219.

McDonald WI, Compston A, Edan G, Goodkin D, Hartung HP, Lublin FD, McFarland HF, Paty DW, Polman CH, Reingold SC, Sandberg-Wollheim M, Sibley W, Thompson A, van den Noort S, Weinshenker BY, Wolinsky JS. Recommended diagnostic criteria for multiple sclerosis: guidelines from the International Panel on the diagnosis of multiple sclerosis. Ann Neurol. 2001 Jul;50(1):121-7. doi: 10.1002/ana.1032. PMID: 11456302.

Metze C, Winkelmann A, Loebermann M, Hecker M, Schweiger B, Reisinger EC, Zettl UK. Immunogenicity and predictors of response to a single dose trivalent seasonal influenza vaccine in multiple sclerosis patients receiving disease-modifying therapies. CNS Neurosci Ther. 2019 Feb;25(2):245-254. doi: 10.1111/cns.13034. Epub 2018 Jul 25. PMID: 30044050; PMCID: PMC6488907.

Millefiorini E, Gasperini C, Pozzilli C, D'Andrea F, Bastianello S, Trojano M, Morino S, Morra VB, Bozzao A, Calo' A, Bernini ML, Gambi D, Prencipe M. Randomized placebo-controlled trial of mitoxantrone in relapsing-remitting multiple sclerosis: 24-month clinical and MRI outcome. J Neurol. 1997 Mar;244(3):153-9. doi: 10.1007/s004150050066. PMID: 9050955.

Mills EA, Ogrodnik MA, Plave A, Mao-Draayer Y. Emerging Understanding of the Mechanism of Action for Dimethyl Fumarate in the Treatment of Multiple Sclerosis. Front Neurol. 2018 Jan 23;9:5. doi: 10.3389/fneur.2018.00005. PMID: 29410647; PMCID: PMC5787128.

Mistry N, Abdel-Fahim R, Samaraweera A, Mougin O, Tallantyre E, Tench C, Jaspan T, Morris P, Morgan PS, Evangelou N. Imaging central veins in brain lesions with 3-T T2*-weighted magnetic resonance imaging differentiates multiple sclerosis from microangiopathic brain lesions. Mult Scler. 2016 Sep;22(10):1289-96. doi: 10.1177/1352458515616700. Epub 2015 Dec 10. PMID: 26658816.

Montalban X, Hauser SL, Kappos L, Arnold DL, Bar-Or A, Comi G, de Seze J, Giovannoni G, Hartung HP, Hemmer B, Lublin F, Rammohan KW, Selmaj K, Traboulsee A, Sauter A, Masterman D, Fontoura P, Belachew S, Garren H, Mairon N, Chin P, Wolinsky JS; ORATORIO Clinical Investigators. Ocrelizumab versus Placebo in Primary Progressive Multiple Sclerosis. N Engl J Med. 2017 Jan 19;376(3):209-220. doi: 10.1056/NEJMoa1606468. Epub 2016 Dec 21. PMID: 28002688.

Morrow SA, Clift F, Devonshire V, Lapointe E, Schneider R, Stefanelli M, Vosoughi R. Use of natalizumab in persons with multiple sclerosis: 2022 update. Mult Scler Relat Disord. 2022 Sep;65:103995. doi: 10.1016/j.msard.2022.103995. Epub 2022 Jun 26. PMID: 35810718.

Multiple Sclerosis International Federation. Number of people with MS: Atlas of MS. https://www.atlasofms.org/map/global/epidemiology/number-of-people-with-ms. Updated 2020. Accessed November 11, 2020.

Munschauer FE, Stewart C, Jacobs L, Kaba S, Ghorishi Z, Greenberg SJ, Cookfair D. Circulating CD3+ CD4+ CD8+ T lymphocytes in multiple sclerosis. J Clin Immunol. 1993 Mar;13(2):113-8. doi: 10.1007/BF00919267. PMID: 8100570.

Naismith RT, Wundes A, Ziemssen T, Jasinska E, Freedman MS, Lembo AJ, Selmaj K, Bidollari I, Chen H, Hanna J, Leigh-Pemberton R, Lopez-Bresnahan M, Lyons J, Miller C, Rezendes D, Wolinsky JS; EVOLVE-MS-2 Study Group. Diroximel Fumarate Demonstrates an Improved Gastrointestinal Tolerability Profile Compared with Dimethyl Fumarate in Patients with Relapsing-Remitting Multiple Sclerosis: Results from the Randomized, Double-Blind, Phase III EVOLVE-MS-2 Study. CNS Drugs. 2020 Feb;34(2):185-196. doi: 10.1007/s40263-020-00700-0. PMID: 31953790; PMCID: PMC7018784.

Nomiyama H, Osada N, Yoshie O. A family tree of vertebrate chemokine receptors for a unified nomenclature. Dev Comp Immunol. 2011 Jul;35(7):705-15. doi: 10.1016/j.dci.2011.01.019. Epub 2011 Feb 2. PMID: 21295066.

O'Connor P, Wolinsky JS, Confavreux C, Comi G, Kappos L, Olsson TP, Benzerdjeb H, Truffinet P, Wang L, Miller A, Freedman MS; TEMSO Trial Group. Randomized trial of oral teriflunomide for relapsing multiple sclerosis. N Engl J Med. 2011 Oct 6;365(14):1293-303. doi: 10.1056/NEJMoa1014656. PMID: 21991951.

Oh J, O'Connor PW. Teriflunomide in the treatment of multiple sclerosis: current evidence and future prospects. Ther Adv Neurol Disord. 2014 Sep;7(5):239-52. doi: 10.1177/1756285614546855. PMID: 25342978; PMCID: PMC4206621.

Oh J. Diagnosis of Multiple Sclerosis. Continuum (Minneap Minn). 2022 Aug 1;28(4):1006-1024. doi: 10.1212/CON.0000000000001156. PMID: 35938655.

Ontaneda D, Fox RJ, Chataway J. Clinical trials in progressive multiple sclerosis: lessons learned and future perspectives. Lancet Neurol. 2015 Feb;14(2):208-23. doi: 10.1016/S1474-4422(14)70264-9. PMID: 25772899; PMCID: PMC4361791.

Orsi G, Hayden Z, Cseh T, Berki T, Illes Z. Osteopontin levels are associated with late-time lower regional brain volumes in multiple sclerosis. Sci Rep. 2021 Dec 8;11(1):23604. doi: 10.1038/s41598-021-03173-3. PMID: 34880402; PMCID: PMC8654976.

Panitch H, Goodin DS, Francis G, Chang P, Coyle PK, O'Connor P, Monaghan E, Li D, Weinshenker B; EVIDENCE Study Group. EVidence of Interferon Dose-response: Europian North American Compartative Efficacy; University of British Columbia MS/MRI Research Group. Randomized, comparative study of interferon beta-1a treatment regimens in MS: The EVIDENCE Trial. Neurology. 2002 Nov 26;59(10):1496-506. doi: 10.1212/01.wnl.0000034080.43681.da. PMID: 12451188.

Petzold A, Eikelenboom MJ, Gveric D, Keir G, Chapman M, Lazeron RH, Cuzner ML, Polman CH, Uitdehaag BM, Thompson EJ, Giovannoni G. Markers for different glial cell responses in multiple sclerosis: clinical and pathological correlations. Brain. 2002 Jul;125(Pt 7):1462-73. doi: 10.1093/brain/awf165. PMID: 12076997.

Piehl F, Kockum I, Khademi M, Blennow K, Lycke J, Zetterberg H, Olsson T. Plasma neurofilament light chain levels in patients with MS switching from injectable therapies to fingolimod. Mult Scler. 2018 Jul;24(8):1046-1054. doi: 10.1177/1352458517715132. Epub 2017 Jun 19. PMID: 28627962.

Polman CH, Reingold SC, Edan G, Filippi M, Hartung HP, Kappos L, Lublin FD, Metz LM, McFarland HF, O'Connor PW, Sandberg-Wollheim M, Thompson AJ, Weinshenker BG, Wolinsky JS. Diagnostic criteria for multiple sclerosis: 2005 revisions to the "McDonald Criteria". Ann Neurol. 2005 Dec;58(6):840-6. doi: 10.1002/ana.20703. PMID: 16283615.

Polman CH, O'Connor PW, Havrdova E, Hutchinson M, Kappos L, Miller DH, Phillips JT, Lublin FD, Giovannoni G, Wajgt A, Toal M, Lynn F, Panzara MA, Sandrock AW; AFFIRM Investigators. A randomized, placebo-controlled trial of natalizumab for relapsing multiple sclerosis. N Engl J Med. 2006 Mar 2;354(9):899-910. doi: 10.1056/NEJMoa044397. PMID: 16510744.

Polman CH, Reingold SC, Banwell B, Clanet M, Cohen JA, Filippi M, Fujihara K, Havrdova E, Hutchinson M, Kappos L, Lublin FD, Montalban X, O'Connor P, Sandberg-Wollheim M, Thompson AJ, Waubant E, Weinshenker B, Wolinsky JS. Diagnostic criteria for multiple sclerosis: 2010 revisions to the McDonald criteria. Ann Neurol. 2011 Feb;69(2):292-302. doi: 10.1002/ana.22366. PMID: 21387374; PMCID: PMC3084507.

Preische O, Schultz SA, Apel A, Kuhle J, Kaeser SA, Barro C, Gräber S, Kuder-Buletta E, LaFougere C, Laske C, Vöglein J, Levin J, Masters CL, Martins R, Schofield PR, Rossor MN, Graff-Radford NR, Salloway S, Ghetti B, Ringman JM, Noble JM, Chhatwal J, Goate AM, Benzinger TLS, Morris JC, Bateman RJ, Wang G, Fagan AM, McDade EM, Gordon BA, Jucker M; Dominantly Inherited Alzheimer Network. Serum neurofilament dynamics predicts neurodegeneration and clinical progression in presymptomatic Alzheimer's disease. Nat Med. 2019 Feb;25(2):277-283. doi: 10.1038/s41591-018-0304-3. Epub 2019 Jan 21. PMID: 30664784; PMCID: PMC6367005.

Raman D, Sobolik-Delmaire T, Richmond A. Chemokines in health and disease. Exp Cell Res. 2011 Mar 10;317(5):575-89. doi: 10.1016/j.yexcr.2011.01.005. Epub 2011 Jan 9. PMID: 21223965; PMCID: PMC3063402.

Ribbons KA, McElduff P, Boz C, Trojano M, Izquierdo G, Duquette P, Girard M, Grand'Maison F, Hupperts R, Grammond P, Oreja-Guevara C, Petersen T, Bergamaschi R, Giuliani G, Barnett M, van Pesch V, Amato MP, Iuliano G, Fiol M, Slee M, Verheul F, Cristiano E, Fernandez-Bolanos R, Saladino ML, Rio ME, Cabrera-Gomez J, Butzkueven H, van Munster E, Den Braber-Moerland L, La Spitaleri D, Lugaresi A, Shaygannejad V, Gray O, Deri N, Alroughani R, Lechner-Scott J. Male Sex Is Independently Associated with Faster Disability Accumulation in

Relapse-Onset MS but Not in Primary Progressive MS. PLoS One. 2015 Jun 5;10(6):e0122686. doi: 10.1371/journal.pone.0122686. PMID: 26046348; PMCID: PMC4457630.

Rice CM, Cottrell D, Wilkins A, Scolding NJ. Primary progressive multiple sclerosis: progress and challenges. J Neurol Neurosurg Psychiatry. 2013 Oct;84(10):1100-6. doi: 10.1136/jnnp-2012-304140. Epub 2013 Feb 16. PMID: 23418213.

Riley, C. S. Multiple Sclerosis and Allied Demyelinating Diseases. In: ED Louis, SA Mayer, LP Rowland & GM Abrams. *Merritt's Neurology.* 13th ed. Philadelphia, PA: Lippincott Williams & Wilkins; 2016:593-630.

Rosengren LE, Lycke J, Andersen O. Glial fibrillary acidic protein in CSF of multiple sclerosis patients: relation to neurological deficit. J Neurol Sci. 1995 Nov;133(1-2):61-5. doi: 10.1016/0022-510x(95)00152-r. PMID: 8583233.

Rotstein D, Montalban X. Reaching an evidence-based prognosis for personalized treatment of multiple sclerosis. Nat Rev Neurol. 2019 May;15(5):287-300. doi: 10.1038/s41582-019-0170-8. PMID: 30940920.

Rotstein D, Solomon JM, Sormani MP, Montalban X, Ye XY, Dababneh D, Muccilli A, Saab G, Shah P. Association of NEDA-4 With No Long-term Disability Progression in Multiple Sclerosis and Comparison With NEDA-3: A Systematic Review and Meta-analysis. Neurol Neuroimmunol Neuroinflamm. 2022 Oct 12;9(6):e200032. doi: 10.1212/NXI.0000000000200032. PMID: 36224046; PMCID: PMC9558627.

Rudick RA, Ransohoff RM, Peppler R, VanderBrug Medendorp S, Lehmann P, Alam J. Interferon beta induces interleukin-10 expression: relevance to multiple sclerosis. Ann Neurol. 1996 Oct;40(4):618-27. doi: 10.1002/ana.410400412. PMID: 8871582.

Rudick RA, Stuart WH, Calabresi PA, Confavreux C, Galetta SL, Radue EW, Lublin FD, Weinstock-Guttman B, Wynn DR, Lynn F, Panzara MA, Sandrock AW; SENTINEL Investigators. Natalizumab plus interferon beta-1a for relapsing multiple sclerosis. N Engl J Med. 2006 Mar 2;354(9):911-23. doi: 10.1056/NEJMoa044396. PMID: 16510745.

Ryerson LZ, Foley J, Chang I, Kister I, Cutter G, Metzger RR, Goldberg JD, Li X, Riddle E, Smirnakis K, Kasliwal R, Ren Z, Hotermans C, Ho PR, Campbell N. Risk of natalizumab-associated PML in patients with MS is reduced with extended interval dosing. Neurology. 2019 Oct 8;93(15):e1452-e1462. doi: 10.1212/WNL.0000000000008243. Epub 2019 Sep 12. PMID: 31515290; PMCID: PMC7010325.

Sandberg-Wollheim M, Neudorfer O, Grinspan A, Weinstock-Guttman B, Haas J, Izquierdo G, Riley C, Ross AP, Baruch P, Drillman T, Coyle PK. Pregnancy Outcomes from the Branded Glatiramer Acetate Pregnancy Database. Int J MS Care. 2018 Jan-Feb;20(1):9-14. doi: 10.7224/1537-2073.2016-079. PMID: 29507538; PMCID: PMC5825987.

Sati P, Thomasson DM, Li N, Pham DL, Biassou NM, Reich DS, Butman JA. Rapid, high-resolution, whole-brain, susceptibility-based MRI of multiple sclerosis. Mult Scler. 2014

Oct;20(11):1464-70. doi: 10.1177/1352458514525868. Epub 2014 Mar 17. PMID: 24639479; PMCID: PMC4167170.

Sati P, Oh J, Constable RT, Evangelou N, Guttmann CR, Henry RG, Klawiter EC, Mainero C, Massacesi L, McFarland H, Nelson F, Ontaneda D, Rauscher A, Rooney WD, Samaraweera AP, Shinohara RT, Sobel RA, Solomon AJ, Treaba CA, Wuerfel J, Zivadinov R, Sicotte NL, Pelletier D, Reich DS; NAIMS Cooperative. The central vein sign and its clinical evaluation for the diagnosis of multiple sclerosis: a consensus statement from the North American Imaging in Multiple Sclerosis Cooperative. Nat Rev Neurol. 2016 Dec;12(12):714-722. doi: 10.1038/nrneurol.2016.166. Epub 2016 Nov 11. PMID: 27834394.

Scalfari A, Romualdi C, Nicholas RS, Mattoscio M, Magliozzi R, Morra A, Monaco S, Muraro PA, Calabrese M. The cortical damage, early relapses, and onset of the progressive phase in multiple sclerosis. Neurology. 2018 Jun 12;90(24):e2107-e2118. doi: 10.1212/WNL.0000000000005685. Epub 2018 May 16. PMID: 29769373.

Schlaeger R, Papinutto N, Zhu AH, Lobach IV, Bevan CJ, Bucci M, Castellano A, Gelfand JM, Graves JS, Green AJ, Jordan KM, Keshavan A, Panara V, Stern WA, von Büdingen HC, Waubant E, Goodin DS, Cree BA, Hauser SL, Henry RG. Association Between Thoracic Spinal Cord Gray Matter Atrophy and Disability in Multiple Sclerosis. JAMA Neurol. 2015 Aug;72(8):897-904. doi: 10.1001/jamaneurol.2015.0993. PMID: 26053119; PMCID: PMC6002864.

Schrempf W, Ziemssen T. Glatiramer acetate: mechanisms of action in multiple sclerosis. Autoimmun Rev. 2007 Aug;6(7):469-75. doi: 10.1016/j.autrev.2007.02.003. Epub 2007 Mar 6. PMID: 17643935.

Scott LJ. Siponimod: A Review in Secondary Progressive Multiple Sclerosis. CNS Drugs. 2020 Nov;34(11):1191-1200. doi: 10.1007/s40263-020-00771-z. Epub 2020 Oct 27. Erratum in: CNS Drugs. 2021 Jan;35(1):133. PMID: 33108633; PMCID: PMC7773609.

Sellebjerg F, Börnsen L, Khademi M, Krakauer M, Olsson T, Frederiksen JL, Sørensen PS. Increased cerebrospinal fluid concentrations of the chemokine CXCL13 in active MS. Neurology. 2009 Dec 8;73(23):2003-10. doi: 10.1212/WNL.0b013e3181c5b457. PMID: 19996075.

Smith CI, Baskin B, Humire-Greiff P, Zhou JN, Olsson PG, Maniar HS, Kjellén P, Lambris JD, Christensson B, Hammarström L, et al. Expression of Bruton's agammaglobulinemia tyrosine kinase gene, BTK, is selectively down-regulated in T lymphocytes and plasma cells. J Immunol. 1994 Jan 15;152(2):557-65. PMID: 8283037.

Solomon AJ, Watts R, Ontaneda D, Absinta M, Sati P, Reich DS. Diagnostic performance of central vein sign for multiple sclerosis with a simplified three-lesion algorithm. Mult Scler. 2018 May;24(6):750-757. doi: 10.1177/1352458517726383. Epub 2017 Aug 18. PMID: 28820013; PMCID: PMC5794670.

Sørensen TL, Trebst C, Kivisäkk P, Klaege KL, Majmudar A, Ravid R, Lassmann H, Olsen DB, Strieter RM, Ransohoff RM, Sellebjerg F. Multiple sclerosis: a study of CXCL10 and CXCR3 co-localization in the inflamed central nervous system. J Neuroimmunol. 2002 Jun;127(1-2):59-68. doi: 10.1016/s0165-5728(02)00097-8. PMID: 12044976.

Sospedra M, Martin R. Immunology of Multiple Sclerosis. Semin Neurol. 2016 Apr;36(2):115-27. doi: 10.1055/s-0036-1579739. Epub 2016 Apr 26. PMID: 27116718.

Spelman T, Kalincik T, Zhang A, Pellegrini F, Wiendl H, Kappos L, Tsvetkova L, Belachew S, Hyde R, Verheul F, Grand-Maison F, Izquierdo G, Grammond P, Duquette P, Lugaresi A, Lechner-Scott J, Oreja-Guevara C, Hupperts R, Petersen T, Barnett M, Trojano M, Butzkueven H. Comparative efficacy of switching to natalizumab in active multiple sclerosis. Ann Clin Transl Neurol. 2015 Apr;2(4):373-87. doi: 10.1002/acn3.180. Epub 2015 Feb 27. PMID: 25909083; PMCID: PMC4402083.

Storoni M, Verbeek MM, Illes Z, Marignier R, Teunissen CE, Grabowska M, Confavreux C, Plant GT, Petzold A. Serum GFAP levels in optic neuropathies. J Neurol Sci. 2012 Jun 15;317(1-2):117-22. doi: 10.1016/j.jns.2012.02.012. Epub 2012 Mar 10. PMID: 22410258.

Stüve O, Cravens PD, Frohman EM, Phillips JT, Remington GM, von Geldern G, Cepok S, Singh MP, Tervaert JW, De Baets M, MacManus D, Miller DH, Radü EW, Cameron EM, Monson NL, Zhang S, Kim R, Hemmer B, Racke MK. Immunologic, clinical, and radiologic status 14 months after cessation of natalizumab therapy. Neurology. 2009 Feb 3;72(5):396-401. doi: 10.1212/01.wnl.0000327341.89587.76. Epub 2008 Nov 5. PMID: 18987352; PMCID: PMC2677530.

Sun M, Liu N, Xie Q, Li X, Sun J, Wang H, Wang M. A candidate biomarker of glial fibrillary acidic protein in CSF and blood in differentiating multiple sclerosis and its subtypes: A systematic review and meta-analysis. Mult Scler Relat Disord. 2021 Jun;51:102870. doi: 10.1016/j.msard.2021.102870. Epub 2021 Feb 25. PMID: 33819724.

Suthiphosuwan S, Sati P, Guenette M, Montalban X, Reich DS, Bharatha A, Oh J. The Central Vein Sign in Radiologically Isolated Syndrome. AJNR Am J Neuroradiol. 2019 May;40(5):776-783. doi: 10.3174/ajnr.A6045. Epub 2019 Apr 18. PMID: 31000526; PMCID: PMC6786901.

Suthiphosuwan S, Sati P, Absinta M, Guenette M, Reich DS, Bharatha A, Oh J. Paramagnetic Rim Sign in Radiologically Isolated Syndrome. JAMA Neurol. 2020 May 1;77(5):653-655. doi: 10.1001/jamaneurol.2020.0124. PMID: 32150224; PMCID: PMC7063543.

Tallantyre EC, Dixon JE, Donaldson I, Owens T, Morgan PS, Morris PG, Evangelou N. Ultra-high-field imaging distinguishes MS lesions from asymptomatic white matter lesions. Neurology. 2011 Feb 8;76(6):534-9. doi: 10.1212/WNL.0b013e31820b7630. PMID: 21300968; PMCID: PMC3053180.

Teleshova N, Pashenkov M, Huang YM, Söderström M, Kivisäkk P, Kostulas V, Haglund M, Link H. Multiple sclerosis and optic neuritis: CCR5 and CXCR3 expressing T cells are augmented in blood and cerebrospinal fluid. J Neurol. 2002 Jun;249(6):723-9. doi: 10.1007/s00415-002-0699-z. PMID: 12111306.

Thebault S, Abdoli M, Fereshtehnejad SM, Tessier D, Tabard-Cossa V, Freedman MS. Serum neurofilament light chain predicts long term clinical outcomes in multiple sclerosis. Sci Rep. 2020 Jun 25;10(1):10381. doi: 10.1038/s41598-020-67504-6. PMID: 32587320; PMCID: PMC7316736.

Thebault S, Reaume M, Marrie RA, Marriott JJ, Furlan R, Laroni A, Booth RA, Uccelli A, Freedman MS. High or increasing serum NfL is predictive of impending multiple sclerosis relapses. Mult Scler Relat Disord. 2022 Mar;59:103535. doi: 10.1016/j.msard.2022.103535. Epub 2022 Jan 19. PMID: 35078125.

Thompson AJ, Banwell BL, Barkhof F, Carroll WM, Coetzee T, Comi G, Correale J, Fazekas F, Filippi M, Freedman MS, Fujihara K, Galetta SL, Hartung HP, Kappos L, Lublin FD, Marrie RA, Miller AE, Miller DH, Montalban X, Mowry EM, Sorensen PS, Tintoré M, Traboulsee AL, Trojano M, Uitdehaag BMJ, Vukusic S, Waubant E, Weinshenker BG, Reingold SC, Cohen JA. Diagnosis of multiple sclerosis: 2017 revisions of the McDonald criteria. Lancet Neurol. 2018 Feb;17(2):162-173. doi: 10.1016/S1474-4422(17)30470-2. Epub 2017 Dec 21. PMID: 29275977.

Ufer M, Shakeri-Nejad K, Gardin A, Su Z, Paule I, Marbury TC, Legangneux E. Impact of siponimod on vaccination response in a randomized, placebo-controlled study. Neurol Neuroimmunol Neuroinflamm. 2017 Sep 13;4(6):e398. doi: 10.1212/NXI.0000000000000398. PMID: 28955715; PMCID: PMC5608565.

University of Colorado. April 20, 2017 - August 31, 2022). Discontinuation of Disease Modifying Therapies (DMTs) in Multiple Sclerosis (MS) (DISCOMS). Retrieved 31 March 2023 from: https://clinicaltrials.gov/ct2/show/NCT03073603).

van Langelaar J, Rijvers L, Janssen M, Wierenga-Wolf AF, Melief MJ, Siepman TA, de Vries HE, Unger PA, van Ham SM, Hintzen RQ, van Luijn MM. Induction of brain-infiltrating T-bet-expressing B cells in multiple sclerosis. Ann Neurol. 2019 Aug;86(2):264-278. doi: 10.1002/ana.25508. Epub 2019 Jun 19. PMID: 31136008; PMCID: PMC6771938.

Varhaug KN, Barro C, Bjørnevik K, Myhr KM, Torkildsen Ø, Wergeland S, Bindoff LA, Kuhle J, Vedeler C. Neurofilament light chain predicts disease activity in relapsing-remitting MS. Neurol Neuroimmunol Neuroinflamm. 2017 Nov 28;5(1):e422. doi: 10.1212/NXI.0000000000000422. PMID: 29209636; PMCID: PMC5707445.

Varhaug KN, Barro C, Bjørnevik K, Myhr KM, Torkildsen Ø, Wergeland S, Bindoff LA, Kuhle J, Vedeler C. Neurofilament light chain predicts disease activity in relapsing-remitting MS. Neurol Neuroimmunol Neuroinflamm. 2017 Nov 28;5(1):e422. doi: 10.1212/NXI.0000000000000422. PMID: 29209636; PMCID: PMC5707445.

Varhaug KN, Torkildsen Ø, Myhr KM, Vedeler CA. Neurofilament Light Chain as a Biomarker in Multiple Sclerosis. Front Neurol. 2019 Apr 5;10:338. doi: 10.3389/fneur.2019.00338. PMID: 31024432; PMCID: PMC6460359.

Villar LM, Costa-Frossard L, Masterman T, Fernandez O, Montalban X, Casanova B, Izquierdo G, Coret F, Tumani H, Saiz A, Arroyo R, Fink K, Leyva L, Espejo C, Simó-Castelló M, García-

Sánchez MI, Lauda F, Llufriú S, Álvarez-Lafuente R, Olascoaga J, Prada A, Oterino A, de Andrés C, Tintoré M, Ramió-Torrentà L, Rodríguez-Martín E, Picón C, Comabella M, Quintana E, Agüera E, Díaz S, Fernandez-Bolaños R, García-Merino JA, Landete L, Menéndez-González M, Navarro L, Pérez D, Sánchez-López F, Serrano-Castro PJ, Tuñón A, Espiño M, Muriel A, Bar-Or A, Álvarez-Cermeño JC. Lipid-specific immunoglobulin M bands in cerebrospinal fluid are associated with a reduced risk of developing progressive multifocal leukoencephalopathy during treatment with natalizumab. Ann Neurol. 2015 Mar;77(3):447-57. doi: 10.1002/ana.24345. Epub 2015 Jan 30. PMID: 25581547.

von Hehn C, Howard J, Liu S, Meka V, Pultz J, Mehta D, Prada C, Ray S, Edwards MR, Sheikh SI. Immune response to vaccines is maintained in patients treated with dimethyl fumarate. Neurol Neuroimmunol Neuroinflamm. 2017 Nov 15;5(1):e409. doi: 10.1212/NXI.0000000000000409. PMID: 29159204; PMCID: PMC5688262.

Walo-Delgado PE, Sainz de la Maza S, Villarrubia N, Monreal E, Medina S, Espiño M, Fernández-Velasco JI, Rodríguez-Martín E, Roldán E, Lourido D, Muriel A, Masjuan-Vallejo J, Costa-Frossard L, Villar LM. Low serum neurofilament light chain values identify optimal responders to dimethyl fumarate in multiple sclerosis treatment. Sci Rep. 2021 Apr 29;11(1):9299. doi: 10.1038/s41598-021-88624-7. PMID: 33927255; PMCID: PMC8085019.

Wootla, Bharath & Denic, Aleksandar & Keegan, B & Winters, Jeffrey & Astapenko, David & Warrington, Arthur & Bieber, Allan & Rodriguez, Moses. (2011). Evidence for the Role of B Cells and Immunoglobulins in the Pathogenesis of Multiple Sclerosis. Neurology research international. 2011. 780712. 10.1155/2011/780712.

Yang Y, Shi J, Gu Z, Salama ME, Das S, Wendlandt E, Xu H, Huang J, Tao Y, Hao M, Franqui R, Levasseur D, Janz S, Tricot G, Zhan F. Bruton tyrosine kinase is a therapeutic target in stem-like cells from multiple myeloma. Cancer Res. 2015 Feb 1;75(3):594-604. doi: 10.1158/0008-5472.CAN-14-2362. Epub 2015 Jan 14. PMID: 25589346; PMCID: PMC4384656.

Yano H, Gonzalez C, Healy BC, Glanz BI, Weiner HL, Chitnis T. Discontinuation of disease-modifying therapy for patients with relapsing-remitting multiple sclerosis: Effect on clinical and MRI outcomes. Mult Scler Relat Disord. 2019 Oct;35:119-127. doi: 10.1016/j.msard.2019.07.021. Epub 2019 Jul 25. PMID: 31374460.

APPENDIX A: Multiple Sclerosis Disease Modifying Therapy Classification

Moderately-Efficacious	Highly Efficacious
Injectable Medications (Subcutaneous): ● Avonex (interferon beta-1a) ● Betaseron (interferon beta-1b) ● Extavia (interferon beta-1b) ● Glatect (glatiramer acetate) ● Plegridy (peginterferon beta-1a) ● Rebif (interferon beta-1a)	***Injectable Medications (Subcutaneous):*** ● Kesimpta (ofatumumab)
Oral Medications: ● Aubagio (teriflunomide) ● Tecfidera (dimethyl fumarate)	***Oral Medications:*** ● Gilenya (fingolimod) ● Mavenvclad (cladribine) ● Mayzent (siponimod) ● Ponvory (ponesimod) ● Zeposia (ozanimod)
Intravenous Medications: ● None	***Intravenous Medications:*** ● Tysabri (natalizumab) ● Ocrevus (ocrelizumab) ● Lemtrada (alemtuzumab) ● Mitoxantrone

*****This is the full list of DMT currently approved by Health Canada for patients with RRMS

Appendix B: Revised (2017) McDonald Criteria

Requires elimination of more likely diagnoses *Requires demonstration of dissemination of lesions in the central nervous system in space and time*	
Clinical Presentation	**Additional Criteria to Make MS Diagnosis**
In a person who has experienced a typical attack/clinically isolated syndrome at onset	
● 2 or more attacks and clinical evidence of 2 or more lesions; OR ● 2 or more attacks and clinical evidence of 1 lesion with clear historical evidence of prior attack involving lesion in different location	No additional criteria as DIS and DIT have been met.
● 2 or more attacks and clinical evidence of 1 lesion	DIS shown by one of these criteria: ● Additional clinical attack implicating different CNS site ● 1 or more MS-typical T2 lesions in 2 or more areas of CNS: periventricular, cortical, juxtacortical, infratentorial or spinal cord
● 1 attack and clinical evidence of 2 or more lesions.	DIT shown by one of these criteria: ● Additional clinical attack ● Simultaneous presence of both enhancing and non-enhancing MS-typical MRI lesions, or new T2 or enhancing MRI lesion compared to

	baseline scan (without regard to timing of baseline scan) - CSF oligoclonal bands
• 1 attack and clinical evidence of 1 lesion	DIS shown by one of these criteria: • Additional attack implicating different CNS site • 1 or more MS-typical T2 lesions in 2 or more areas of CNS: periventricular, cortical, juxtacortical, infratentorial or spinal cord **AND** DIT shown by one of these criteria: • Additional clinical attack • Simultaneous presence of both enhancing and non-enhancing MS-typical MRI lesions, or new T2 or enhancing MRI lesion compared to baseline scan (without regard to timing of baseline scan) • CSF oligoclonal bands
In a person who has steady progression of disease since onset	
• 1 year of disease progression (retrospective or prospective)	DIS shown by at least two of these criteria: • 1 or more MS-typical T2 lesions (periventricular, cortical, juxtacortical or infratentorial) • 2 or more T2 spinal cord lesions • CSF oligoclonal bands

DIT: Dissemination in time **DIS:** Dissemination in space

Appendix C: Expanded Disability Status Scale

Score	Description
0	Normal neurological exam, no disability in any functional system (FS).
1.0	No disability, minimal signs in one FS.
1.5	No disability, minimal signs in more than one FS.
2.0	Minimal disability in one FS.
2.5	Mild disability in one FS or minimal disability in two FS.
3.0	Moderate disability in one FS, or mild disability in three or four FS. No impairment to walking.
3.5	Moderate disability in one FS and more than minimal disability in several others. No impairment to walking.
4.0	Significant disability but self-sufficient and up and about some 12 hours a day. Able to walk without aid or rest for 500 meters.
4.5	Significant disability but up and about much of the day, able to work a full day, may otherwise have some limitation of full activity or require minimal assistance. Able to walk without aid or rest for 300 meters.
5.0	Disability severe enough to impair full daily activities and ability to work a full day without special provisions. Able to walk without aid or rest for 200 meters.

5.5	Disability severe enough to preclude full daily activities. Able to walk without aid or rest for 100 meters.
6.0	Requires a walking aid (cane, crutch, etc.) to walk about 100 meters with or without resting.
6.5	Requires two walking aids to walk about 20 meters without resting.
7.0	Unable to walk beyond approximately 5 meters even with aid. Essentially restricted to wheelchair though wheels self in standard wheelchair and transfers alone. Up and about in a wheelchair some 12 hours a day.
7.5	Unable to take more than a few steps. Restricted to wheelchair and may need aid in transferring. Can wheel self but cannot carry on in standard wheelchair for a full day and may require a motorized wheelchair.
8.0	Essentially restricted to bed or chair or pushed in a wheelchair. May be out of the bed much of the day. Retains many self-care functions. Generally has effective use of arms.
8.5	Essentially restricted to bed much of the day. Has some effective use of arms and retains some self-care functions.
9.0	Confined to bed. Can still communicate and eat.
9.5	Confined to bed and totally dependent. Unable to communicate effectively or eat/swallow.
10.0	Death due to MS.

Appendix D: Eligibility Criteria and Study Design

<table>
<tr><td rowspan="2">Population</td><td colspan="2">Adults aged 18 years and older in NL, Canada, with clinically definite RRMS, as defined by the revised 2017 McDonald diagnostic criteria (Appendix B).</td></tr>
<tr><td>Inclusion criteria:
EDSS score of 0-5.5 at screening
A diagnosis of RRMS in accordance with the revised 2017 McDonald Criteria (*See note in sampling plan and recruitment section)
Ability to complete the 9-Hole Peg Test (9-HPT) for each hand in < 240 seconds
Ability to perform the Timed 25-Foot Walk Test (T25FWT)</td><td>Exclusion criteria:
A diagnosis of PPMS or SPMS
HIV, hepatitis B/C, active or latent tuberculosis, or progressive multifocal leukoencephalopathy
Severe renal or hepatic disease
Significantly impaired bone marrow function or significant anemia, leukopenia, neutropenia or thrombocytopenia
Any comorbid disease requiring chronic treatment with systemic corticosteroids/immunosuppressants during study
Any previous treatment with immunosuppressive medication without an appropriate washout period</td></tr>
</table>

Intervention	Treatment of RRMS patients with the highly efficacious DMTs.
Control	Treatment of RRMS patients with the moderately efficacious DMTs.
Outcomes	**Primary:** 1. Plasma NfL and GFAP concentrations (measured in pg/mL) **Secondary:** 1. CXCL13 and changes in plasma immune cell subsets
Design	Combined retrospective and prospective, longitudinal, cohort, comparative design.

APPENDIX E: Summary of Findings

Outcome	Statistical Test	Mean±SEM (pg/mL) or R-value	P-value
Plasma NfL demonstrates significant correlation with CSF NfL			
CSF NfL Pre-DMT Between Groups	Mann-Whitney U test	Mod Eff (723.6±249.9) High Eff (1385±267.8)	P=0.0227
Plasma NfL Pre-DMT Between Groups	Mann-Whitney U test	Mod Eff (8.89±1.241) High Eff (13.67±1.972)	P=0.0693
CSF and Plasma NfL Pre-DMT	Spearman correlation	R=0.800	P<0.0001
Plasma GFAP and CXCL13 are not significantly correlated with plasma NfL			
Plasma GFAP Pre-DMT Between Groups	Mann-Whitney U test	Mod Eff = (58.59±8.748) High Eff = (71.43±7.512)	P=0.1930
Plasma CXCL13 Pre-DMT Between Groups	Mann-Whitney U test	Mod Eff = (84.67±12.98) High Eff = (102.0 ±10.09)	P=0.2947
Plasma GFAP and NfL Pre-DMT Correlation	Spearman correlation	R=0.3221	P= 0.1545
Plasma CXCL13 and NfL Pre-DMT Correlation	Spearman correlation	R=-0.2361	P=0.3163
Plasma NfL demonstrates correlation with plasma CD14+ immune cells			
Plasma NfL and CD45+ Immune Cells Pre-DMT	Spearman correlation	R=0.3941	P=0.1320
Plasma NfL and CD3+ Immune Cells Pre-DMT	Spearman correlation	R=-0.1947	P=0.4686
Plasma NfL and CD4+ Immune Cells Pre-DMT	Spearman correlation	R=-0.0427	P=0.8759
Plasma NfL and CD8+ Immune Cells Pre-DMT	Spearman correlation	R=-0.4618	P=0.0738
Plasma NfL and CD14+ Immune Cells Pre-DMT	Spearman correlation	R = 0.6093	P=0.0139
Plasma NfL and CD19+ Immune Cells Pre-DMT	Spearman correlation	R=0.1074	P=0.6096

Plasma NfL and CD56+ Immune Cells Pre-DMT	Spearman correlation	R=-0.0633	P=0.8158
Plasma NfL and CD4+CXCR3+ Immune Cells Pre-DMT	Spearman correlation	R=-0.3647	P=0.1654
Plasma NfL and CD8+CXCR3+ Immune Cells Pre-DMT	Spearman correlation	R=-0.4209	P=0.1053
Plasma NfL and CD14+CXCR3+ Immune Cells Pre-DMT	Spearman correlation	R=-0.0957	P=0.7229
Plasma NfL and CD19+CXCR3+ Immune Cells Pre-DMT	Spearman correlation	R=-0.2971	P=0.2631
Plasma NfL and CD56+CXCR3+ Immune Cells Pre-DMT	Spearman correlation	R=-0.2134	P=0.4246
Plasma GFAP is not significantly correlated with plasma immune cells			
Plasma GFAP and CD45+ Immune Cells Pre-DMT	Spearman correlation	R=0.0000	P>0.9999
Plasma GFAP and CD3+ Immune Cells Pre-DMT	Spearman correlation	R=-0.2507	P=0.3477
Plasma GFAP and CD4+ Immune Cells Pre-DMT	Spearman correlation	R=-0.1133	P=0.6744
Plasma GFAP and CD8+ Immune Cells Pre-DMT	Spearman correlation	R=-0.3412	P=0.1960
Plasma GFAP and CD14+ Immune Cells Pre-DMT	Spearman correlation	R=0.4857	P=0.0582
Plasma GFAP and CD19+ Immune Cells Pre-DMT	Spearman correlation	R=-0.0883	P=0.7438
Plasma GFAP and CD56+ Immune Cells Pre-DMT	Spearman correlation	R=-0.1074	P=0.6906
Plasma GFAP and CD4+CXCR3+ Immune Cells Pre-DMT	Spearman correlation	R=0.1357	P=0.6297
Plasma GFAP and CD8+CXCR3+ Immune Cells Pre-DMT	Spearman correlation	R=0.3664	P=0.1787
Plasma GFAP and CD14+CXCR3+ Immune Cells Pre-DMT	Spearman correlation	R=0.0107	P=0.9718
Plasma GFAP and CD19+CXCR3+ Immune Cells Pre-DMT	Spearman correlation	R=-0.0500	P=0.8626
Plasma GFAP and CD56+CXCR3+ Immune Cells Pre-DMT	Spearman correlation	R=0.2091	P=0.4515
Plasma CXCL13 is not significantly correlated with plasma immune cells			
Plasma CXCL13 and CD45+ Immune Cells Pre-DMT	Spearman correlation	R=-0.2071	P=0.4578
Plasma CXCL13 and CD3+ Immune Cells Pre-DMT	Spearman correlation	R=0.0538	P=0.8520
Plasma CXCL13 and CD4+ Immune Cells Pre-DMT	Spearman correlation	R=-0.1269	P=0.6504
Plasma CXCL13 and CD8+ Immune Cells Pre-DMT	Spearman correlation	R=0.2071	P=0.4578
Plasma CXCL13 and CD14+ Immune Cells Pre-DMT	Spearman correlation	R=-0.1841	P=0.5085
Plasma CXCL13 and CD19+ Immune Cells Pre-DMT	Spearman correlation	R=-0.3789	P=0.1684
Plasma CXCL13 and CD56+ Immune Cells Pre-DMT	Spearman correlation	R=-0.0322	P=0.9105
Plasma CXCL13 and CD4+CXCR3+ Immune Cells Pre-DMT	Spearman correlation	R=0.0725	P=0.8083
Plasma CXCL13 and CD8+CXCR3+ Immune Cells Pre-DMT	Spearman correlation	R=0.2178	P=0.4512
Plasma CXCL13 and CD14+CXCR3+ Immune Cells Pre-DMT	Spearman correlation	R=0.1828	P=0.5286
Plasma CXCL13 and CD19+CXCR3+ Immune Cells Pre-DMT	Spearman correlation	R=0.0813	P=0.7849

Plasma CXCL13 and CD56+CXCR3+ Immune Cells Pre-DMT	Spearman correlation	R=0.2882	P=0.3150
Time from last clinical relapse is not associated with plasma biomarker concentrations			
Time from Last Clinical Relapse and CSF NfL Pre-DMT	Spearman correlation	R=-0.4183	P=0.0747
Time from Last Clinical Relapse and Plasma NfL Pre-DMT	Spearman correlation	R=-0.3359	P=0.1598
Time from Last Clinical Relapse and Plasma GFAP Pre-DMT	Spearman correlation	R=0.1701	P=0.4862
Time from Last Clinical Relapse and Plasma CXCL13 Pre-DMT	Spearman correlation	R=-0.0532	P=0.8338
Time from last clinical relapse was correlated with CD3+, CD4+ and CD19+ plasma immune cells			
Time from Last Clinical Relapse and CD45+ Immune Cells Pre-DMT	Spearman correlation	R=0.3132	P=0.2739
Time from Last Clinical Relapse and CD3+ Immune Cells Pre-DMT	Spearman correlation	R=0.6585	P=0.0123
Time from Last Clinical Relapse and CD4+ Immune Cells Pre-DMT	Spearman correlation	R=0.7477	P=0.0029
Time from Last Clinical Relapse and CD8+ Immune Cells Pre-DMT	Spearman correlation	R=-0.0293	P=0.9228
Time from Last Clinical Relapse and CD14+ Immune Cells Pre-DMT	Spearman correlation	R=-0.4691	P=0.0918
Time from Last Clinical Relapse and CD19+ Immune Cells Pre-DMT	Spearman correlation	R=0.6428	P=0.0150
Time from Last Clinical Relapse and CD56+ Immune Cells Pre-DMT	Spearman correlation	R=-0.3199	P=0.2632
Time from Last Clinical Relapse and CD4+CXCR3+ Immune Cells Pre-DMT	Spearman correlation	R=-0.0198	P=0.9516
Time from Last Clinical Relapse and CD8+CXCR3+ Immune Cells Pre-DMT	Spearman correlation	R=-0.0114	P=0.9722
Time from Last Clinical Relapse and CD14+CXCR3+ Immune Cells Pre-DMT	Spearman correlation	R=-0.2316	P=0.4425
Time from Last Clinical Relapse and CD19+CXCR3+ Immune Cells Pre-DMT	Spearman correlation	R=-0.0510	P=0.8703
Time from Last Clinical Relapse and CD56+CXCR3+ Immune Cells Pre-DMT	Spearman correlation	R=-0.4053	P=0.1697
High efficacy DMT significantly reduces plasma NfL			
Moderate Efficacy DMT Effect on Plasma NfL	Wilcoxon matched pairs rank test	0.2878±0.8752	P=0.9102
Moderate Efficacy DMT Effect on Plasma GFAP	Wilcoxon matched pairs rank test	18.31±9.691	P=0.0742
Moderate Efficacy DMT Effect on Plasma CXCL13	Wilcoxon matched pairs rank test	20.11±17.78	P=0.3008
High Efficacy DMT Effect on Plasma NfL	Wilcoxon matched pairs rank test	-4.786±2.042	P=0.0068
High Efficacy DMT Effect on Plasma GFAP	Wilcoxon matched pairs rank test	12.15±8.837	P=0.1514
High Efficacy DMT Effect on Plasma CXCL13	Wilcoxon matched pairs rank test	-5.039±12.71	P=0.2402
Moderate efficacy DMT reduces plasma CD45+, CD8+, and CD19+CXCR3+ immune cells			
Moderate Efficacy DMT Effect on CD45+ Immune Cells	Wilcoxon matched pairs rank test	-30504±12180 (#cells)	P=0.0391
Moderate Efficacy DMT Effect on CD3+ Immune Cells	Wilcoxon matched pairs rank test	-6.213±3.753	P=0.1953
Moderate Efficacy DMT Effect on CD4+ Immune Cells	Wilcoxon matched pairs rank test	-2.913±2.669	P=0.3828
Moderate Efficacy DMT Effect on CD8+ Immune Cells	Wilcoxon matched pairs rank test	-2.700±1.181	P=0.0156
Moderate Efficacy DMT Effect on CD14+ Immune Cells	Wilcoxon matched pairs rank test	6.738±2.565	P=0.0781

Moderate Efficacy DMT Effect on CD19+ Immune Cells	Wilcoxon matched pairs rank test	-1.065±0.5315	P=0.1094
Moderate Efficacy DMT Effect on CD56+ Immune Cells	Wilcoxon matched pairs rank test	1.325±1.535	P=0.6406
Moderate Efficacy DMT Effect on CD4+CXCR3+ Immune Cells	Wilcoxon matched pairs rank test	-1.868±1.185	P=0.1953
Moderate Efficacy DMT Effect on CD8+CXCR3+ Immune Cells	Wilcoxon matched pairs rank test	-0.8075±0.5012	P=0.1953
Moderate Efficacy DMT Effect on CD14+CXCR3+ Immune Cells	Wilcoxon matched pairs rank test	-0.1225±0.1550	P=0.5234
Moderate Efficacy DMT Effect on CD19+CXCR3+ Immune Cells	Wilcoxon matched pairs rank test	-0.4125±0.1951	P=0.0078
Moderate Efficacy DMT Effect on CD56+CXCR3+ Immune Cells	Wilcoxon matched pairs rank test	-0.0025±0.0999	P=0.9453
High efficacy DMT reduces plasma CD19+ and CD19+CXCR3+ immune cells			
High Efficacy DMT Effect on CD45+ Immune Cells	Wilcoxon matched pairs rank test	-7932±7097 (# cells)	P=0.2969
High Efficacy DMT Effect on CD3+ Immune Cells	Wilcoxon matched pairs rank test	-7.229±7.482	P=0.9375
High Efficacy DMT Effect on CD4+ Immune Cells	Wilcoxon matched pairs rank test	-5.986±6.080	P=0.8125
High Efficacy DMT Effect on CD8+ Immune Cells	Wilcoxon matched pairs rank test	-0.7143±1.301	P=0.5781
High Efficacy DMT Effect on CD14+ Immune Cells	Wilcoxon matched pairs rank test	9.571±6.307	P=0.1562
High Efficacy DMT Effect on CD19+ Immune Cells	Wilcoxon matched pairs rank test	-5.339±0.9799	P=0.0156
High Efficacy DMT Effect on CD56+ Immune Cells	Wilcoxon matched pairs rank test	1.657±1.179	P=0.1719
High Efficacy DMT Effect on CD4+CXCR3+ Immune Cells	Wilcoxon matched pairs rank test	-2.709±1.584	P=0.1562
High Efficacy DMT Effect on CD8+CXCR3+ Immune Cells	Wilcoxon matched pairs rank test	-0.6043±0.3112	P=0.1562
High Efficacy DMT Effect on CD14+CXCR3+ Immune Cells	Wilcoxon matched pairs rank test	-0.1614±0.2364	P=0.7812
High Efficacy DMT Effect on CD19+CXCR3+ Immune Cells	Wilcoxon matched pairs rank test	-1.059±0.2126	P=0.0156
High Efficacy DMT Effect on CD56+CXCR3+ Immune Cells	Wilcoxon matched pairs rank test	-0.1743±0.0943	P=0.1094
High efficacy DMT results in a greater decline in CD19+ and CD19+CXCR3+ plasma immune cells than moderate efficacy DMT			
High vs Moderate Efficacy DMT Effect on CD45+ Immune Cells	Mann-Whitney U test	High Eff (1196±11004) (#cells) Mod Eff (-30504±12180) (#cells)	P=0.1049
High vs Moderate Efficacy DMT Effect on CD3+ Immune Cells	Mann-Whitney U test	High Eff (-7.229±7.482) Mod Eff (-6.213±3.767)	P=0.8665
High vs Moderate Efficacy DMT Effect on CD4+ Immune Cells	Mann-Whitney U test	High Eff (-5.971±6.062) Mod Eff (-2.913±2.668)	P=0.8920
High vs Moderate Efficacy DMT Effect on CD8+ Immune Cells	Mann-Whitney U test	High Eff (-0.7143±1.301) Mod Eff (-2.700±1.165)	P=0.1997
High vs Moderate Efficacy DMT Effect on CD14+ Immune Cells	Mann-Whitney U test	High Eff (9.586±6.304) Mod Eff (6.725±2.568)	P=0.8665
High vs Moderate Efficacy DMT Effect on CD19+ Immune Cells	Mann-Whitney U test	High Eff (-5.377±0.9805) Mod Eff (-1.065±0.5325)	P=0.0093
High vs Moderate Efficacy DMT Effect on CD56+ Immune Cells	Mann-Whitney U test	High Eff (1.643±1185) Mod Eff (1.325±1.535)	P=0.6339
High vs Moderate Efficacy DMT Effect on CD4+CXCR3+ Immune Cells	Mann-Whitney U test	High Eff (-0.1743±0.0940) Mod Eff (-0.0013±0.1000)	P=0.1789
High vs Moderate Efficacy DMT Effect on CD8+CXCR3+ Immune Cells	Mann-Whitney U test	High Eff (-0.6043±0.3112) Mod Eff (-0.8063±0.5016)	P=0.6943
High vs Moderate Efficacy DMT Effect on CD14+CXCR3+ Immune Cells	Mann-Whitney U test	High Eff (-0.1614±0.2364) Mod Eff (-0.0050±0.3253)	P=0.5170

High vs Moderate Efficacy DMT Effect on CD19+CXCR3+ Immune Cells	Mann-Whitney U test	High Eff (-1.060±-0.0688) Mod Eff (0.2129±0.2390)	P=0.0093
High vs Moderate Efficacy DMT Effect on CD56+CXCR3+ Immune Cells	Mann-Whitney U test	High Eff (-0.1743±0.0094) Mod Eff (0.0850±0.1985)	P=0.2931
High efficacy DMT results in a significantly greater decline in plasma NfL than moderate efficacy DMT			
High vs Moderate Efficacy DMT Effect on ΔpNfL	Mann-Whitney U test	High Eff (-4.786±2.042) Mod Eff (0.2878±0.8752)	P=0.0200
High vs Moderate Efficacy DMT Effect on ΔpGFAP	Mann-Whitney U test	High Eff (11.25±9.630) Mod Eff (18.31±9.691)	P=0.7103
High vs Moderate Efficacy DMT Effect on ΔpCXCL13	Mann-Whitney U test	High Eff (-2.517±13.77) Mod Eff (20.11±17.78)	P=0.6038
Moderate-Efficacy DMT results in a decline in plasma NfL that is correlated with a decline in CD19+CXCR3+ immune cells and a concomitant increase in CD3+, CD4+, CD8+, and CD4+CXCR3+ immune cells			
Moderate Efficacy DMT Effect on the Relationship Between ΔpNfL and ΔCD45+ Immune Cells	Spearman correlation	R=0.5238	P=0.1966
Moderate Efficacy DMT Effect on the Relationship Between ΔpNfL and ΔCD3+ Immune Cells	Spearman correlation	R=-0.7857	P=0.0279
Moderate Efficacy DMT Effect on the Relationship Between ΔpNfL and ΔCD4+ Immune Cells	Spearman correlation	R=-0.7857	P=0.0279
Moderate Efficacy DMT Effect on the Relationship Between ΔpNfL and ΔCD8+ Immune Cells	Spearman correlation	R=-0.7381	P=0.0458
Moderate Efficacy DMT Effect on the Relationship Between ΔpNfL and ΔCD14+ Immune Cells	Spearman correlation	R=0.6667	P=0.0831
Moderate Efficacy DMT Effect on the Relationship Between ΔpNfL and ΔCD19+ Immune Cells	Spearman correlation	R=-0.4762	P=0.2461
Moderate Efficacy DMT Effect on the Relationship Between ΔpNfL and ΔCD56+ Immune Cells	Spearman correlation	R=0.4524	P=0.2675
Moderate Efficacy DMT Effect on the Relationship Between ΔpNfL and ΔCD4+CXCR3+ Immune Cells	Spearman correlation	R=-0.8571	P=0.0107
Moderate Efficacy DMT Effect on the Relationship Between ΔpNfL and ΔCD8+CXCR3+ Immune Cells	Spearman correlation	R=-0.7143	P=0.0576
Moderate Efficacy DMT Effect on the Relationship Between ΔpNfL and ΔCD14+CXCR3+ Immune Cells	Spearman correlation	R=0.6707	P=0.0762
Moderate Efficacy DMT Effect on the Relationship Between ΔpNfL and ΔCD19+CXCR3+ Immune Cells	Spearman correlation	R=0.7857	P=0.0279
Moderate Efficacy DMT Effect on the Relationship Between ΔpNfL and ΔCD56+CXCR3+ Immune Cells	Spearman correlation	R=0.3333	P=0.4279
High-Efficacy DMT results in a decline in plasma NfL that is correlated with a decline in CD45+ and CD14+ immune cells and a concomitant increase in CD4+ immune cells			
High Efficacy DMT Effect on Relationship Between ΔpNfL and ΔCD45+ Immune Cells	Spearman correlation	R=0.7857	P=0.0480
High Efficacy DMT Effect on Relationship Between ΔpNfL and ΔCD3+ Immune Cells	Spearman correlation	R=-0.6429	P=0.1389
High Efficacy DMT Effect on Relationship Between ΔpNfL and ΔCD4+ Immune Cells	Spearman correlation	R=-0.8571	P=0.0238

High Efficacy DMT Effect on Relationship Between ΔpNfL and ΔCD8+ Immune Cells	Spearman correlation	R=-0.4286	P=0.3536
High Efficacy DMT Effect on Relationship Between ΔpNfL and ΔCD14+ Immune Cells	Spearman correlation	R=0.8214	P=0.0341
High Efficacy DMT Effect on Relationship Between ΔpNfL and ΔCD19+ Immune Cells	Spearman correlation	R=0.4286	P=0.3536
High Efficacy DMT Effect on Relationship Between ΔpNfL and ΔCD56+ Immune Cells	Spearman correlation	R=0.2500	P=0.5948
High Efficacy DMT Effect on Relationship Between ΔpNfL and ΔCD4+CXCR3+ Immune Cells	Spearman correlation	R=0.0180	P=0.9889
High Efficacy DMT Effect on Relationship Between ΔpNfL and ΔCD8+CXCR3+ Immune Cells	Spearman correlation	R=-0.4636	P=0.3024
High Efficacy DMT Effect on Relationship Between ΔpNfL and ΔCD14+CXCR3+ Immune Cells	Spearman correlation	R=0.1982	P=0.6698
High Efficacy DMT Effect on Relationship Between ΔpNfL and ΔCD19+CXCR3+ Immune Cells	Spearman correlation	R=-0.1786	P=0.7131
High Efficacy DMT Effect on Relationship Between ΔpNfL and ΔCD56+CXCR3+ Immune Cells	Spearman correlation	R=0.0180	P=0.9889
Moderate-Efficacy DMT does not result in any significant change in plasma GFAP or concomitant increase or decrease in immune cells			
Moderate Efficacy DMT Effect on the Relationship Between ΔpGFAP and ΔCD45+ Immune Cells	Spearman correlation	R=0.1429	P=0.7520
Moderate Efficacy DMT Effect on the Relationship Between ΔpGFAP and ΔCD3+ Immune Cells	Spearman correlation	R=0.0476	P=0.9349
Moderate Efficacy DMT Effect on the Relationship Between ΔpGFAP and ΔCD4+ Immune Cells	Spearman correlation	R=0.0476	P=0.9349
Moderate Efficacy DMT Effect on the Relationship Between ΔpGFAP and ΔCD8+ Immune Cells	Spearman correlation	R=0.0476	P=0.9349
Moderate Efficacy DMT Effect on the Relationship Between ΔpGFAP and ΔCD14+ Immune Cells	Spearman correlation	R=-0.2143	P=0.6191
Moderate Efficacy DMT Effect on the Relationship Between ΔpGFAP and ΔCD19+ Immune Cells	Spearman correlation	R=-0.3333	P=0.4279
Moderate Efficacy DMT Effect on the Relationship Between ΔpGFAP and ΔCD56+ Immune Cells	Spearman correlation	R=0.2143	P=0.6191
Moderate Efficacy DMT Effect on the Relationship Between ΔpGFAP and ΔCD4+CXCR3+ Immune Cells	Spearman correlation	R=0.4524	P=0.2675
Moderate Efficacy DMT Effect on the Relationship Between ΔpGFAP and ΔCD8+CXCR3+ Immune Cells	Spearman correlation	R=0.0000	P>0.9999
Moderate Efficacy DMT Effect on the Relationship Between ΔpGFAP and ΔCD14+CXCR3+ Immune Cells	Spearman correlation	R=0.3114	P=0.4496

Moderate Efficacy DMT Effect on the Relationship Between ΔpGFAP and ΔCD19+CXCR3+ Immune Cells	Spearman correlation	R=0.3571	P=0.3894
Moderate Efficacy DMT Effect on the Relationship Between ΔpGFAP and ΔCD56+CXCR3+ Immune Cells	Spearman correlation	R=0.6667	P=0.0831
High-Efficacy DMT results in a decline in plasma GFAP that is correlated with a decline in CD8+ immune cells			
High Efficacy DMT Effect on the Relationship Between ΔpGFAP and ΔCD45+ Immune Cells	Spearman correlation	R=0.3929	P=0.3956
High Efficacy DMT Effect on the Relationship Between ΔpGFAP and ΔCD3+ Immune Cells	Spearman correlation	R=-0.7500	P=0.0633
High Efficacy DMT Effect on the Relationship Between ΔpGFAP and ΔCD4+ Immune Cells	Spearman correlation	R=-0.6071	P=0.1667
High Efficacy DMT Effect on Relationship Between ΔpGFAP and ΔCD8+ Immune Cells	Spearman correlation	R=-0.8214	P=0.0341
High Efficacy DMT Effect on the Relationship Between ΔpGFAP and ΔCD14+ Immune Cells	Spearman correlation	R=0.6429	P=0.1389
High Efficacy DMT Effect on the Relationship Between ΔpGFAP and ΔCD19+ Immune Cells	Spearman correlation	R=0.6071	P=0.1667
High Efficacy DMT Effect on the Relationship Between ΔpGFAP and ΔCD56+ Immune Cells	Spearman correlation	R=0.5000	P=0.2667
High Efficacy DMT Effect on the Relationship Between ΔpGFAP and ΔCD4+CXCR3+ Immune Cells	Spearman correlation	R=-0.3063	P=0.5119
High Efficacy DMT Effect on the Relationship Between ΔpGFAP and ΔCD8+CXCR3+ Immune Cells	Spearman correlation	R=-0.7500	P=0.0633
High Efficacy DMT Effect on the Relationship Between ΔpGFAP and ΔCD14+CXCR3+ Immune Cells	Spearman correlation	R=0.0541	P=0.9167
High Efficacy DMT Effect on the Relationship Between ΔpGFAP and ΔCD19+CXCR3+ Immune Cells	Spearman correlation	R=-0.4643	P=0.3024
High Efficacy DMT Effect on the Relationship Between ΔpGFAP and ΔCD56+CXCR3+ Immune Cells	Spearman correlation	R=-0.3063	P=0.5119
Moderate-Efficacy DMT results in an increase in plasma CXCL13 is correlated with an increase in plasma CD56+CXCR3+ immune cells			
Moderate Efficacy DMT Effect on Relationship Between ΔpCXCL13 and ΔCD45 + Immune Cells	Spearman correlation	R=-0.0476	P=0.9349
Moderate Efficacy DMT Effect on Relationship Between ΔpCXCL13 and ΔCD3 + Immune Cells	Spearman correlation	R=-0.3810	P=0.3599
Moderate Efficacy DMT Effect on Relationship Between ΔpCXCL13 and ΔCD4 + Immune Cells	Spearman correlation	R=-0.3810	P=0.3599
Moderate Efficacy DMT Effect on Relationship Between ΔpCXCL13 and ΔCD8 + Immune Cells	Spearman correlation	R=-0.3095	P=0.4618
Moderate Efficacy DMT Effect on Relationship Between ΔpCXCL13 and ΔCD14 + Immune Cells	Spearman correlation	R=0.1667	P=0.7033

Moderate Efficacy DMT Effect on Relationship Between ΔpCXCL13 and ΔCD19 + Immune Cells	Spearman correlation	R=-0.0476	P=0.9349
Moderate Efficacy DMT Effect on Relationship Between ΔpCXCL13 and ΔCD56 + Immune Cells	Spearman correlation	R=0.6905	P=0.0694
Moderate Efficacy DMT Effect on Relationship Between ΔpCXCL13 and ΔCD4+CXCR3+ Immune Cells	Spearman correlation	R=-0.0238	P=0.9768
Moderate Efficacy DMT Effect on Relationship Between ΔpCXCL13 and ΔCD8+CXCR3+ Immune Cells	Spearman correlation	R=-0.4048	P=0.3268
Moderate Efficacy DMT Effect on Relationship Between ΔpCXCL13 and ΔCD14+CXCR3+ Immune Cells	Spearman correlation	R=0.7066	P=0.0586
Moderate Efficacy DMT Effect on Relationship Between ΔpCXCL13 and ΔCD19+CXCR3+ Immune Cells	Spearman correlation	R=0.3095	P=0.4618
Moderate Efficacy DMT Effect on Relationship Between ΔpCXCL13 and ΔCD56+CXCR3+ Immune Cells	Spearman correlation	R=0.8333	P=0.0154
High-Efficacy DMT did not result in any significant change in plasma CXCL13 or concomitant change in immune cells			
High Efficacy DMT Effect on the Relationship Between ΔpCXCL13 and ΔCD45+ Immune Cells	Spearman correlation	R=0.0357	P=0.9635
High Efficacy DMT Effect on the Relationship Between ΔpCXCL13 and ΔCD3+ Immune Cells	Spearman correlation	R=-0.5429	P=0.2972
High Efficacy DMT Effect on the Relationship Between ΔpCXCL13 and ΔCD4+ Immune Cells	Spearman correlation	R=-0.7714	P=0.1028
High Efficacy DMT Effect on the Relationship Between ΔpCXCL13 and ΔCD8+ Immune Cells	Spearman correlation	R=-0.3143	P=0.5639
High Efficacy DMT Effect on the Relationship Between ΔpCXCL13 and ΔCD14+ Immune Cells	Spearman correlation	R=0.5429	P=0.2972
High Efficacy DMT Effect on the Relationship Between ΔpCXCL13 and ΔCD19+ Immune Cells	Spearman correlation	R=0.4857	P=0.3556
High Efficacy DMT Effect on the Relationship Between ΔpCXCL13 and ΔCD56+ Immune Cells	Spearman correlation	R=0.4857	P=0.3556
High Efficacy DMT Effect on the Relationship Between ΔpCXCL13 and ΔCD4+CXCR3+ Immune Cells	Spearman correlation	R=0.2609	P=0.6167
High Efficacy DMT Effect on the Relationship Between ΔpCXCL13 and ΔCD8+CXCR3+ Immune Cells	Spearman correlation	R=0.4286	P=0.4194
High Efficacy DMT Effect on the Relationship Between ΔpCXCL13 and ΔCD14+CXCR3+ Immune Cells	Spearman correlation	R=0.3143	P=0.5639
High Efficacy DMT Effect on the Relationship Between ΔpCXCL13 and ΔCD19+CXCR3+ Immune Cells	Spearman correlation	R=0.3714	P=0.4972
High Efficacy DMT Effect on the Relationship Between ΔpCXCL13 and ΔCD56+CXCR3+ Immune Cells	Spearman correlation	R=0.2609	P=0.6167
High efficacy DMT results in a greater effect on the relationship between plasma NfL and CD19+, CD4CXCR3+, CD8+CXCR3+, CD14+CXCR3+, and CD19+CXCR3+ immune cells than moderate efficacy DMT			

High Efficacy Versus Moderate Efficacy DMT Effect on Relationship Between ΔpNfL and ΔCD45+ Immune Cells	ANCOVA	N/A	P_s=0.3627 P_e=0.0649
High Efficacy Versus Moderate Efficacy DMT Effect on Relationship Between ΔpNfL and ΔCD3+ Immune Cells	ANCOVA	N/A	P_s=0.4911 P_e=0.2032
High Efficacy Versus Moderate Efficacy DMT Effect on Relationship Between ΔpNfL and ΔCD4+ Immune Cells	ANCOVA	N/A	P_s=0.5947 P_e=0.0925
High Efficacy Versus Moderate Efficacy DMT Effect on Relationship Between ΔpNfL and ΔCD8+ Immune Cells	ANCOVA	N/A	P_s=0.2215 P_e=0.6406
High Efficacy Versus Moderate Efficacy DMT Effect on Relationship Between ΔpNfL and ΔCD14+ Immune Cells	ANCOVA	N/A	P_s=0.8809 P_e=0.0534
High Efficacy Versus Moderate Efficacy DMT Effect on Relationship Between ΔpNfL and ΔCD19+ Immune Cells	ANCOVA	N/A	P_s=0.2584 P_e=0.0062
High Efficacy Versus Moderate Efficacy DMT Effect on Relationship Between ΔpNfL and ΔCD56+ Immune Cells	ANCOVA	N/A	P_s=0.1450 P_e=0.5631
High Efficacy Versus Moderate Efficacy DMT Effect on Relationship Between ΔpNfL and ΔCD4+CXCR3+ Immune Cells	ANCOVA	N/A	*P_s=0.0172
High Efficacy Versus Moderate Efficacy DMT Effect on Relationship Between ΔpNfL and ΔCD8+CXCR3+ Immune Cells	ANCOVA	N/A	*P_s=0.0148
High Efficacy Versus Moderate Efficacy DMT Effect on Relationship Between ΔpNfL and ΔCD14+CXCR3+ Immune Cells	ANCOVA	N/A	*P_s=0.0416
High Efficacy Versus Moderate Efficacy DMT Effect on Relationship Between ΔpNfL and ΔCD19+CXCR3+ Immune Cells	ANCOVA	N/A	*P_s=0.0151
High Efficacy Versus Moderate Efficacy DMT Effect on Relationship Between ΔpNfL and ΔCD56+CXCR3+ Immune Cells	ANCOVA	N/A	P_s=0.0805 P_e=0.4690
High efficacy DMT results in a greater effect on the relationship between plasma GFAP and CD14+, CD19+, and CD19+CXCR3+ immune cells than moderate efficacy DMT			
High Efficacy Versus Moderate Efficacy DMT Effect on Relationship Between ΔpGFAP and ΔCD45+ Immune Cells	ANCOVA	N/A	P_s=0.7813 P_e=0.0760
High Efficacy Versus Moderate Efficacy DMT Effect on Relationship Between ΔpGFAP and ΔCD3+ Immune Cells	ANCOVA	N/A	*P_s=0.0373
High Efficacy Versus Moderate Efficacy DMT Effect on Relationship Between ΔpGFAP and ΔCD4+ Immune Cells	ANCOVA	N/A	*P_s=0.0417
High Efficacy Versus Moderate Efficacy DMT Effect on Relationship Between ΔpGFAP and ΔCD8+ Immune Cells	ANCOVA	N/A	P_s=0.1669 P_e=0.4885
High Efficacy Versus Moderate Efficacy DMT Effect on Relationship Between ΔpGFAP and ΔCD14+ Immune Cells	ANCOVA	N/A	*P_s=0.0129
High Efficacy Versus Moderate Efficacy DMT Effect on Relationship Between ΔpGFAP and ΔCD19+ Immune Cells	ANCOVA	N/A	P_s=0.0808 P_e=0.0051

High Efficacy Versus Moderate Efficacy DMT Effect on Relationship Between ΔpGFAP and ΔCD56+ Immune Cells	ANCOVA	N/A	P_s=0.5669 P_e=0.6889
High Efficacy Versus Moderate Efficacy DMT Effect on Relationship Between ΔpGFAP and ΔCD4+CXCR3+ Immune Cells	ANCOVA	N/A	P_s=0.4128 P_e=0.3802
High Efficacy Versus Moderate Efficacy DMT Effect on Relationship Between ΔpGFAP and ΔCD8+CXCR3+ Immune Cells	ANCOVA	N/A	P_s=0.3864 P_e=0.9046
High Efficacy Versus Moderate Efficacy DMT Effect on Relationship Between ΔpGFAP and ΔCD14+CXCR3+ Immune Cells	ANCOVA	N/A	P_s=0.6503 P_e=0.8103
High Efficacy Versus Moderate Efficacy DMT Effect on Relationship Between ΔpGFAP and ΔCD19+CXCR3+ Immune Cells	ANCOVA	N/A	P_s=0.3458 P_e=0.0151
High Efficacy Versus Moderate Efficacy DMT Effect on Relationship Between ΔpGFAP and ΔCD56+CXCR3+ Immune Cells	ANCOVA	N/A	P_s=0.2597 P_e=0.5241
High efficacy DMT results in greater effect on the relationship between plasma CXCL13 CD4+, CD19+, and CD19+CXCR3+ immune cells than moderate efficacy DMT			
High Efficacy Versus Moderate Efficacy DMT Effect on Relationship Between ΔpCXCL13 and ΔCD45+ Immune Cells	ANCOVA	N/A	P_s=0.7668 P_e=0.2122
High Efficacy Versus Moderate Efficacy DMT Effect on Relationship Between ΔpCXCL13 and ΔCD3+ Immune Cells	ANCOVA	N/A	P_s=0.1127 P_e=0.1950
High Efficacy Versus Moderate Efficacy DMT Effect on Relationship Between ΔpCXCL13 and ΔCD4+ Immune Cells	ANCOVA	N/A	P_s=0.0448
High Efficacy Versus Moderate Efficacy DMT Effect on Relationship Between ΔpCXCL13 and ΔCD8+ Immune Cells	ANCOVA	N/A	P_s=0.7501 P_e=0.6480
High Efficacy Versus Moderate Efficacy DMT Effect on Relationship Between ΔpCXCL13 and ΔCD14+ Immune Cells	ANCOVA	N/A	P_s=0.0670 P_e=0.0914
High Efficacy Versus Moderate Efficacy DMT Effect on Relationship Between ΔpCXCL13 and ΔCD19+ Immune Cells	ANCOVA	N/A	P_s=0.1953 P_e=0.0090
High Efficacy Versus Moderate Efficacy DMT Effect on Relationship Between ΔpCXCL13 and ΔCD56+ Immune Cells	ANCOVA	N/A	P_s=0.9348 P_e=0.2665
High Efficacy Versus Moderate Efficacy DMT Effect on Relationship Between ΔpCXCL13 and ΔCD4+CXCR3+ Immune Cells	ANCOVA	N/A	P_s=0.2717 P_e=0.3950
High Efficacy Versus Moderate Efficacy DMT Effect on Relationship Between ΔpCXCL13 and ΔCD8+CXCR3+ Immune Cells	ANCOVA	N/A	P_s=0.5816 P_e=0.9796
High Efficacy Versus Moderate Efficacy DMT Effect on Relationship Between ΔpCXCL13 and ΔCD14+CXCR3+ Immune Cells	ANCOVA	N/A	P_s=0.1986 P_e=0.7215
High Efficacy Versus Moderate Efficacy DMT Effect on Relationship Between	ANCOVA	N/A	P_s=0.4705 P_e=0.0380

ΔpCXCL13 and ΔCD19+CXCR3+ Immune Cells			
High Efficacy Versus Moderate Efficacy DMT Effect on Relationship Between ΔpCXCL13 and ΔCD56+CXCR3+ Immune Cells	ANCOVA	N/A	P_s=0.2549 P_e=0.6870

SEM = Standard Error of the Mean; Mod Eff =Moderate Efficacy DMT; High Eff = High Efficacy DMT; Δ = Delta; ΔpNfL = Delta Plasma NfL; ΔpGFAP = Delta Plasma GFAP; ΔpCXCL13 = Delta Plasma CXCL13; ANCOVA = Analysis of Covariance; P_s= P-value of the difference in slopes; P_e= P-value of the difference in elevations or intercepts

*When P_s is significant, the slopes differ so much it is not possible to test whether the intercepts differ significantly, and no P_e can be given.

APPENDIX F: Ethics Approval

Ethics Office
Suite 200, Eastern Trust Building
95 Bonaventure Avenue
St. John's, NL
A1B 2X5

September 16, 2014

Dr Craig Moore
Division of BioMedical Sciences
Faculty of Medicine

Dear Dr Moore:

Reference #14.181

RE: **Innate and Adaptive Immune Cell mechanisms in Multiple Sclerosis**

This will acknowledge receipt of your correspondence.

This correspondence has been reviewed by the Chair under the direction of the Board. ***Full board approval*** of this research study is granted for one year effective **September 8, 2014.**

This is to confirm that the Health Research Ethics Board reviewed and approved or acknowledged the following documents (as indicated):

- Application, approved
- Revised consent form, dated September 16, 2014, approved
- Data extraction form, approved
- Revised telephone script, approved

MARK THE DATE

This approval will lapse on September 8, 2015. **It is your responsibility to ensure that the Ethics Renewal form is forwarded to the HREB office prior to the renewal date; you may not receive a reminder, therefore the ultimate responsibility is with you as the Principle Investigator.** *The information provided in this form must be **current to the time of submission** and submitted to HREB **not less than 30 nor more than 45 days** of the anniversary of your approval date.* The Ethics Renewal form can be downloaded from the HREB website http://www.hrea.ca.

The Health Research Ethics Board advises THAT IF YOU DO NOT return the completed Ethics Renewal form prior to date of renewal:

- *Your ethics approval will lapse*
- *You will be required to stop research activity immediately*

email: info@hrea.ca Phone: 777-6974 FAX: 777-8776

- *You may not be permitted to restart the study until you reapply for and receive approval to undertake the study again*

Lapse in ethics approval may result in interruption or termination of funding

It is **your responsibility to seek the necessary approval from the Regional Health Authority or other organization as appropriate. You are also solely responsible for providing a copy of this letter, along with your application form, to the Office of Research Services should your research depend on funding administered through that office.**

Modifications of the protocol/consent are not permitted without prior approval from the Health Research Ethics Board. Implementing changes in the protocol/consent without HREB approval may result in the approval of your research study being revoked, necessitating cessation of all related research activity. Request for modification to the protocol/consent must be outlined on an amendment form (available on the HREB website) and submitted to the HREB for review.

This research ethics board (the HREB) has reviewed and approved the research protocol and documentation as noted above for the study which is to be conducted by you as the qualified investigator named above at the specified site. This approval and the views of this Research Ethics Board have been documented in writing. In addition, please be advised that the Health Research Ethics Board currently operates according to *ICH Guidance E6: Good Clinical Practice* and applicable laws and regulations. The membership of this research ethics board is constituted in compliance with the membership requirements for research ethics boards as defined by *Health Canada Food and Drug Regulations Division 5; Part C.*

Notwithstanding the approval of the HREB, the primary responsibility for the ethical conduct of the investigation remains with you.

We wish you every success with your study.

Sincerely,

Dr Fern Brunger, PhD (Chair Non-Clinical Trials)
Ms. Patricia Grainger, (Vice-Chair Non-Clinical Trials)
Health Research Ethics Board

For office use only: **September 18, 2014**

Researcher Portal File #: 20160977 Dear Dr. Craig Moore:

This e-mail serves as notification that your ethics renewal for study HREB # 2014.181 – Innate and Adaptive Immune Cell Mechanisms in Multiple Sclerosis – has been **approved**. Please log in to the Researcher Portal to view the approved event.

Ethics approval for this project has been granted for a period of twelve months effective from September 8, 2023 to September 8, 2024.

Please note, it is the responsibility of the Principal Investigator (PI) to ensure that the Ethics Renewal form is submitted prior to the renewal date each year. Though the Research Ethics Office makes every effort to remind the PI of this responsibility, the PI may not receive a reminder. The Ethics Renewal form can be found on the Researcher Portal as an “Event”.

The ethics renewal [will be reported] to the Health Research Ethics Board at their meeting dated Sept 7, 2023.

Thank you,

Research Ethics Office
Health Research Ethics Authority 760 Topsail Road
Mount Pearl, NL A1N 3J5
(e) info@hrea.ca
(t) 709-864-8871
(f) 709-864-8870
(w) www.hrea.ca